8-2001

The influence of fiber swelling on paper wetting

Sedef Akinli-Kocak

THE INFLUENCE OF FIBER SWELLING ON PAPER WETTING

By

Sedef Akınlı-Koçak

B.S. Ankara University, 1997

A THESIS

Submitted in Partial Fulfillment of the

Requirements for the Degree of

Master of Science

(in Chemical Engineering)

The Graduate School

The University of Maine

August, 2001

Advisory Committee:

Adriaan Van Heiningen, Ober Chair and Professor of Chemical Engineering,

Co-Advisor

Douglas W. Bousfield, Professor of Chemical Engineering, Co-Advisor

Yang Xiang, Research Engineer in Chemical Engineering

THE INFLUENCE OF FIBER SWELLING

ON PAPER WETTING

By Sedef Akınlı-Koçak

Thesis Co-Advisors: Dr. Adriaan Van Heiningen

Dr. Douglas W. Bousfield

An Abstract of the Thesis Presented
in Partial Fulfillment of the Requirements for the
Degree of Master of Science
(in Chemical Engineering)
August 2001

The water uptake behavior of fibers, especially those at the surface of paper, influences printing, and coating operations. The dynamic water uptake behavior of the surface fibers may determine the initial consolidation of the coating at the surface and the penetration of coating into the paper, but clear studies on this topic have not been reported in the literature.

Four different fiber types and seven different paper sheets were investigated in the present study. The three different fiber types were prepared by carboxymethylation of softwood kraft pulp thereby producing pulps with different water uptake values.

The fiber length and water retention value (WRV) were measured for the different fibers and sheets. The contact angle, liquid absorption time, porosity, sheet formation and roughness of all sheets were determined.

Kaolin clay coatings with and without a soluble polymer carboxymethylcellulose (CMC) were applied by a lab draw down and high speed laboratory coater. The roughness of the paper side of the coating was measured after dissolution of paper fibers.

Carboxymethylation increases the water retention value and swelling of the fibers. It was founded that the effect of the carboxymethylation on the fiber length is small. Carboxymethylated fiber sheets have a higher initial contact angle and faster absorption times than the original softwood kraft for non-swelling fluids. However, the most swellable carboxymethylated fiber handsheet had a slower absorption rate than that of the original fiber. This indicates that swelling of the carboxymethylated surface fibers may lead to closure of the surface pores. The commercial sheets have higher initial contact angle than original softwood and three different carboxymethylated sheets. The carboxymethylated sheet give the better formation based on the original softwood sheet. Carboxymethylation also increases the pore diameter and the pore volume of the original sheets by the formation of pinholes.

Although carboxymethylated sheets have a larger pore volume, and roughnesses than the original sheets, the roughness of the backside of the coating layer was smaller. This result indicates less coating penetration with swellable fibers. This trend is seen with the commercial samples.

The mercury porosimetry test results show more coating penetration into the treated fibers than the original softwood sheets, but paper volume changes during coating may explain this result. Based on the roughness results, it can be concluded that fiber swelling decreases the coating penetration. It was also shown that blade pressure increases the coating dive-in, and that CMC addition reduces the coating penetration into the sheets.

ACKNOWLEDGEMENTS

I would like to express my deepest gratitude to my advisors Dr. Adriaan VanHeiningen and Dr. Douglas W. Bousfield for their excellent and constant guidance, patience, generous support, and valuable advice.

Thanks to Dr. Yang Xiang for accepting to spend some time and energy for the benefit of my thesis.

I would like to thank the sponsors of the Paper Surface Science Program for their support and discussions throughout this research. I would like to thank all the graduate students as well as the staff of the Chemical Engineering department and Pilot Plant for being so helpful and so nice. I really appreciate your contribution to that project.

I dedicate a special thank you to Basant Dimetry and Saybil Nuray Ercan for being very close friends, sharing good and bad moments, their support and encouragement, and for making these last two years in Maine such an interesting and valuable experience in my life. I wish them all good luck in their future work.

I am deeply obligated to my husband Akin Koçak for his continuing support, understanding and patient. I would not have been able to complete this thesis without his love, respect and trust.

Finally, I would like to dedicate this thesis to my family. This work would not have been possible without the patience and everlasting support of my family whom I owe everything.

TABLE OF CONTENTS

LIST OF TABLES

LIST OF FIGURES

CHAPTER 1: INTRODUCTION

The interaction between water and base paper in various converting processes is important, giving rise to several studies focused on the mechanism of water transport in paper. This interaction forms the basis for the manufacture of paper and ultimately controls the functional properties in post-processing and the properties of the final paper product.

This interaction is also significant in coating processes. In paper coating, a water-based pigmented coating is applied to the base paper to enhance the optical and topographical properties of the printing surface. During coating, some of the water contained in the coating (35-50% of the wet coating volume) is absorbed by the hydrophilic cellulosic fibers. Therefore, the water uptake behavior of fibers, especially those at the surface of paper subjected to coating, is important for coating "hold-out" and other coating properties. Specifically, the dynamic water uptake behavior of the surface fibers is partly responsible for the dewatering of the coating solution, and thus for the initial consolidation of the coating at the surface. In other words, the faster the water uptake by the surface fibers, the less is the penetration of the coating as a whole into the inter-fiber porous structure of the basestock.

Paper is not merely a network of fibers but is more strictly **an** aerogel. The network of fibers embraces and creates a network of pores, and paper is thus a two-phase system in which the pores inside the fibers and the voids between the fibers are **an** important part of the paper structure. Thus, the sorptivity of paper is not associated solely with the fact that

it is the pores between the fibers can take up liquid, but also that the fibers themselves take up liquid, provided that the liquid has the ability to cause the fiber components to swell.

1.1. Objective of This Research

The initial coating cake formation is thought to be affected by water uptake of surface fibers and particle bridging in the inter-fiber porous structure. In Figure 1.1(a), a coating is formed on paper consisting of non-swellable fibers by bridging of the coating particles while part of the coating travels through the pores of the paper. However if the fibers are swellable the coating dewaters and the coating particles may not penetrate into the pores (Figure 1.lb).

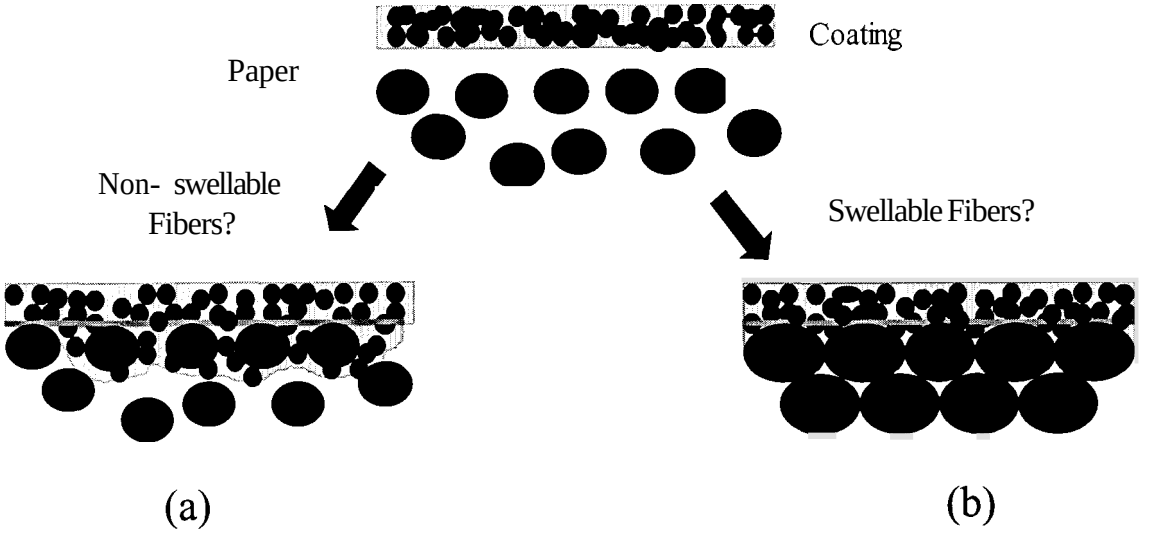

Figure 1.1: Schematic description of the coating process on paper made from a) non-swellable and b) swellable behaviors when coating formed on the paper

Several treatments have been studied which reduce the binder and pigment particles migration into the base paper including that of pretreating paper surface with latex (LePoutre et. al. 1986), hydrophobic sizing (Adams, 1983; Krishnagopolan and Simard 1972), calendering, and increasing the solid contents of coating colors (LePoutre, 1978), etc.

It is known (Talwar 1958; Grignon and Scallan, 1980; Racz and Borsa, 1995) that the carboxymethylation of fibers increases the fiber swellability. Therefore carboxymethylation of fibers may be a treatment to prevent migration of coating particles, and a more uniform coating cake may be formed, due to the increased fluid uptake be these fibers.

Similarly, the water uptake is different for different types of fibers, such as hardwood and softwood kraft fibers, etc. Thus the objective of this research is to clarify the role of the fiber liquid uptake on the fluid uptake and coating "dive-in" of base paper made of these fibers.

1.2. Description of Thesis

The organization of this thesis is described briefly below. Chapter 2 is a literature review including how the fiber properties affect the paper properties; as well as fiber-water interactions such as absorption, swelling, and wetting; and a description of carboxymethylation and the chemistry of the reaction. Chapter 3 provides a detailed description of the equipment, instruments, and the experimental techniques used in the study. Chapter **4** presents results and discussions of the influence of the water retention value (WRV) and fiber type on base sheet properties, and the effect of WRV and fiber

type on coating dive-in. General conclusions and recommendations for future work are presented in Chapter 5.

CHAPTER 2: LITERATURE REVIEW

2.1. Effect of Fiber Properties on Paper Properties

Fiber properties can be used as control variables in papermaking, thereby offering an opportunity to improve simultaneously both optical and strength properties of paper. The information presented in this part is based on the paper by Retulainen (1996) and Retulainen and Nieminen (1996). The effect of fiber properties on paper properties has been demonstrated quantitatively in several experimental studies. There are also mathematical models, but the accurate prediction of paper properties based on the properties of component fibers is still far from perfect. The properties of fibers are not usually considered a control variable. However, treating fiber properties as a control variable provides a powerful and precise tool for adjusting paper properties. The following key fiber properties can be used as control variables:

- Fiber strength
- Fiber length, width and diameter
- Specific bond stress
- Fiber coarseness
- Fiber formation
- Light absorption coefficient

There are several theories for modeling the strength properties of paper. One important semi-quantitative model has been presented by Shallhorn and Karnis (Karnis and

Shallhorn, 1979). Their model gives relatively simple and clear equations for both tensile and tear strength. The parameters used in the model are based on the basic fiber properties listed above.

The Shallhorn–Karnisequations for tensile strength, T, is:

$$\text{For } \tau < \tau_c$$
$$T = N\pi r\tau\frac{\ell}{2} \tag{2.1}$$

$$\text{For } \tau > \tau_c$$
$$T = N\sigma\pi r^2\left[1-(\frac{\sigma r}{2\tau\ell})\right] \tag{2.2}$$

while the Shallhorn-Karnis equation for tear strength, W, is:

$$\text{For } \tau < \tau_c$$
$$W = N\,\pi\,r\,\tau\frac{\ell^2}{12} \tag{2.3}$$

$$\text{For } \tau > \tau_c$$
$$W = \frac{N\,\sigma^3\pi\,r^4}{12\,\ell\,\tau^2} \tag{2.4}$$

where N is the number of fibers per unit cross sectional area of crack, ℓ is length of fibers, r is radius of fibers, σ is strength of fibers (force per unit area), τ is bond shear strength (force per unit area of fiber)

It is interesting to look at the relationship between tensile strength and relative bond area. Page (1969) developed a theory for the mechanism of the tensile failure of paper in terms of the relative importance of fiber strength and bond strength. Equation 2.5 is his derived

formula for the tensile strength of paper in terms of a few basic fiber and paper properties:

$$\frac{1}{T} = \frac{9}{8Z} + \frac{12A\rho g}{bP\ell(R.B.A.)} \qquad (2.5)$$

where T is the finite-span tensile strength of paper, Z is the zero-span tensile strength of paper, a measure of the fiber strength, **A** is a mean fiber cross-sectional area, ρ is the density of the fibrous material, g is the acceleration due to gravity, b is the shear strength per unit area of the fiber-to fiber bonds, P is the perimeter of the average fiber cross section, ℓ is the mean fiber length, and R.B.A. is the fraction of fiber surface that is bonded in the sheet. Quantitatively, this equation states that the strength of weakly bonded paper is controlled by factors associated with bonding strength, but for well bounded paper the paper strength, is dominated by the fiber strength.

Properties affecting tensile strength can be classified into two groups; those that affect the tensile strength area vs relative bonded area (RBA) and the fiber strength. Fiber strength becomes important at higher RBA. Several other fiber properties have an identical effect at 20-40% RBA. For example, increasing fiber length by 20% has the same effect as increasing the fiber width or specific bond strength by 20% or as reducing fiber coarseness by 20%.

The tear strength curve (tear strength vs tensile strength Figure 2.1) on the other hand, has a characteristic maximum which location and the height depend on fiber length, specific bond strength and fiber coarseness.

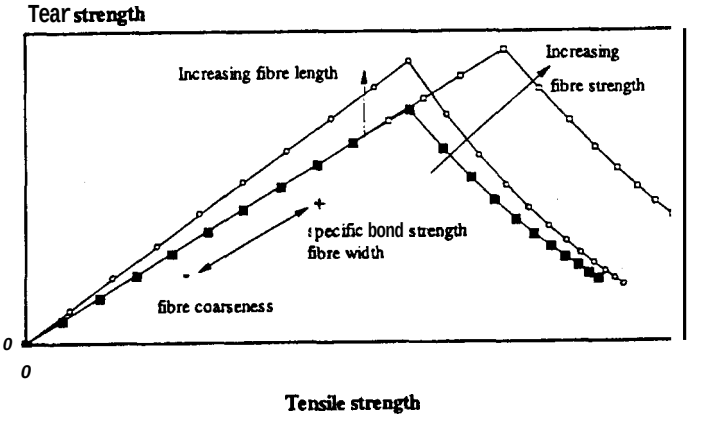

Figure 2.1: The effect of fiber length and strength on the tear strength/tensile strength relationship (Retulainen, 1996)

Regarding the relationship between tear and tensile strength, there is far less scope for improving tear strength at a given tensile strength level. Only two options are available: to increase either fiber length or fiber strength.

2.2. Fiber Modification

Various treatments have been also studied to modify the fibers. It was mensioned in Talwar (1958) that the introductions of acetyl (Bletzinger, 1943), butyryl (Harisson, 1944), methyl (Jayme and Froundjian, 1940), and carboxymethyl (Walecka, 1956) groups on cellulosic materials have been considered at some length, as have their effects on fiber and sheet properties. It was found that low substitution on relatively small groups (methyl, carboxymethyl, acetyl and even butyryl to some extent) invariably results in increased sheet strength for the substituted pulp. Beyond a certain degree of substitution, depending on the group introduced, the character of the substituent group begins to influence pulp properties. Substitution of hydrophobic groups such as acetylated fibers resulted in decreased swelling of the fibers in water and impaired sheet strength for the

pulp. Walecka (1956) and Talwar (1958) studied the strength of paper made from low-substituted carboxymethylcellulose pulps. They found that all of the sheet strength improvement due to sodium carboxymethylation of the rag pulp could be lost if the carboxymethylated cellulose was converted to the free acid or aluminum salt form, showing that the fiber swelling due to carboxymethylation is responsible for the increase in paper strength.

Fiber dimensions have a causal relationship with the optical properties of the sheet. The theory of Kubelka and Munk has been extremely helpful in understanding the optical properties of paper (Casey, 1952). The theory is based on the definition of two fundamental optical constants: the specific scattering coefficient **(S)** and the specific absorption coefficient (K). These coefficients are characteristic of any diffuse material, such as paper, and are defined as follows: K is the limiting value of the absorption of light energy per unit thickness as the thickness becomes very small; **S** is the limiting value of energy scattered backwards per unit of the thickness as the thickness becomes very small. The light scattering coefficient is a linear function of the area of fiber-air interfaces. The actual interfaces in a sheet represent only a fraction of the surface area of wet fibers in the pulp. During papermaking, much of the surface area is lost due to intra- and interfiber bonding and collapse of fiber lumens. The surface area of fibers is known to be a function of fiber coarseness. Therefore reducing fiber coarseness by half doubles the potential light scattering values. Also much of the potential light scattering is due to the fiber lumens, which may collapse during papermaking.

The Kubelka and Munk equation is expressed as follows for diffuse light:

$$R, \quad = 1 + \left(\frac{K}{S}\right) - \left[\left(\frac{K}{S}\right)^2 + 2\left(\frac{K}{S}\right)\right]^{0.5} \tag{2.6}$$

where R_∞ is the reflectance of a pad thick enough to be opaque. If measured at the proper wavelength, the R_∞ value is the paper brightness. Steele and Judd derived a formula which is more workable than Equation 2.6.

$$\frac{K}{S} = \frac{[1 - R_\infty]^2}{2R_\infty} \tag{2.7}$$

With the use of this formula, a single brightness reading (R_∞) will serve to give the K/S value for any paper.

Fiber properties such as fiber length and fiber strength affect the strength properties of paper but not their optical properties. These two parameters are special because they affect the whole relationship between tensile strength and tear strength. Fiber coarseness (and fiber width), on the other hand, has also a strong effect on optical properties. Interfiber bonding and lumen bonding have a pronounced adverse effect on the optical properties of paper.

2.3. Water Transport Mechanism

The interaction between water and base paper in various converting processes are important, giving rise to several studies focusing on the mechanism of water transport in paper. This interaction forms the basis for the manufacture of paper and ultimately

controls the functional properties in post-processing and the properties of the final paper product. The theory of water transport into paper and the role of the fundamental variables that affect the water transport mechanism in paper have been discussed for many years in many publications (Hoyland, 1976a, 1976b, 1976c, 1976d, 1977; Scallan, 1978; Stannet and Williams, 1978; Schuchard and Berg, 1991; Salminen, 1988).

The water transport mechanism is also important for the coating process, especially for understanding the coating water loss and particle migration problems. It has a specific importance in blade coating operations. The coating under pressure tends to move as a plug flow into the porous basestock. It likely will first penetrate the larger pores, such as "pin holes", and then the tighter porous paper medium. Conceivably, water and some binders will migrate into the paper medium while the bulk of the pigments and other solids are retained on the surface. A high solids filter cake may eventually be formed near interface, which progressively grows in thickness as the coating continues to lose water (Baumeister and Kraft, 1981). Several approaches to control the particle migration in this regard have been proposed in the literature (Clark *et. al.,* 1969; Windle *et. al.,* 1970, Baumeister and Kraft, 1981; Gene *et. al.,* 1992). According to these approaches, the capillary migration may be slowed by increasing the water viscosity with addition of water soluble polymeric thickeners or co-binders, and sometimes by a change in the binder surfactant which would reduce paper wetting and reduce the driving force-blade pressure. The volume of water or coating color taken up is also a function of paper roughness. The effect of roughness on the water sorption ability of paper was described by Skowronski and LePoutre (1985). Recently, Young *et. al.* (1993) reported on the effect of thickener-clay interaction on cake formation and water retention under high

speed coating conditions. They found that thickeners adsorbing on clay gave a higher degree of solids flocculation and a lower immobilization solids content, as well as better coating coverage, smoothness and rotogravure printability than thickeners with low affinity for clay.

A good literature review of the water transport mechanism is given by Hoyland and Field (1976a, 1976b, 1976c, 1976d, 1977), and Salminen (1988), and Weise (1997). The information presented in this part is based on these review papers.

The penetration of water into paper covers three areas of interest. These are water-fiber interaction, description of the porous structure of a paper web, and the flow of water through the web.

Water-fiber interaction is an area of much interest. The reaction of cellulose with water produces swelling of the fibers and a structural change. The ability to hold water (Water Retention Value), dimensional changes and strength changes upon wetting are some of the fiber properties of importance. These properties are described in some studies (Nelson and Kalkipsakis, 1964a, 1964b; Walecka, 1956; Racz and Borsa, 1995, 1997; LePoutre *et.al.*, 1973; Marchhessault ***et.*** *al.*, 1978; Bristow, 1971).

The definition of a porous structure is a general scientific problem. Porous structures occur in a great variety of forms and usually they are far too irregular and complicated to allow a rigorous geometric description. Some mathematical models have been developed to describe different geometric regions of the pore structure and require the determination of certain experimental parameters to compare different samples using the same model. These models have some use for porous media also.

Paper porosity, the space between the fibers and within the fibers, is difficult to define. Electron microscopy (ESEM), gas absorption, mercury porosimetry, freeze-drying, solvent-exchange technique, air permeability, and solute exclusion technique are the most common methods that have been used for examination of the porous structure and the water-fiber interaction during wetting. The solute exclusion technique was introduced by Stone and Scallan in 1968. This method quantifies the accessibility of the water-swollen wall to solute molecules ranging in molecular weight from 180 to 2×10^6, and also allows measurement of inaccessible water and accessible water within the porous body if the total amount of water added is known (Stone and Scallan, 1968; Scallan, 1978). Stone and Scallan also developed a structural model for the cell wall of water-swollen wood pulp fibers based on their accessibility to macromolecules.

Fiber rising (DeRoever and Cosper, 1996) is an undesirable change of the sheet surface in which fibers rise above the paper surface upon wetting, detrimental to coating and printed text. Forsberg and LePoutre (1994) made recent ESEM observations on paper, and confirmed that the fiber rising effect originates from ribbon-to-tube dimensional changes of individual fibers, introduced by swelling. In applications of coatings to paper and also offset and water-based gravure printing, interactions between water and paper cause fiber rising, and the associated roughening of the sheet surface produces less smooth coatings.

Forced air permeability measurement can also be done to characterize the pore structure of a sample. **A** standard method is described in the TAPPI test methods (1992-93) where the flow through a sample is determined by collecting a gas that passes through the pores of the paper sample into a sealed container. Flow is then calculated from the rate of pressure increase in the sealed container over time. This technique determines the bulk

permeability of the sample. The bulk permeability can be related to porosity using certain assumptions. Water flow in a paper web is another example of the enormous range of practical situations involving fluid flow in porous media (Hoylan and Field, 1976a).

2.3.1. Water-Fiber Interaction

The interaction of water with fiber components is of prime technological importance. In the water-swollen state, water is the major component of the pulp fiber cell wall - its amount often exceeding that of the sum of the other solid components. In the wall of the wood fiber, water is held in a micro-porous gel of hemicelluloses and lignin which is distributed as fine platelets within a cellulose skeleton consisting of much distorted lamellae. **As** the lignin and hemicelluloses are removed by pulping, the amount of water in the wall increases as water fully occupies the space previously shared with these components (Scallan, 1978).

There are three basic phenomena occurring during water-fiber interaction: absorption, swelling and wetting.

2.3.2. Absorption

In the context of water-fiber interaction absorption, refers to the process where water is taken up by the fibers from the external liquid phase. Various mechanisms have been suggested for the absorption process.

Three types of water have been defined for water contained inside a fiber: water of constitution, imbibed water, and free water.

Water of constitution is that which remains at zero relative vapor pressure. It is water held by fairly strong valence bonds, probably hydrogen bonds. This water forms a monolayer on the cellulose surface. Imbibed water is all the additional water held by the fiber wall when the relative water vapor is increased from zero to 100%. This water accumulates as further layers on top of the basic monolayer. Free water is that held by fiber, after fiber saturation (at 100% relative water vapor pressure) has occurred. This is held by capillary forces and is not bonded in any way.

The amount of water that can eventually be taken up when paper is progressively wetted from zero moisture content upwards is very large. **A** view of the whole process is shown in Figure 2.2, indicating the various water forms. Fibers contained in a humid atmosphere absorb water in the form of water of constitution and imbibed water only. Imbibed water has been further classified by Stone and Scallan (1966). They distinguish between water existing in the wall material itself (the sites on which the water is held are termed microreticular pores) and water existing in the pores of the cell wall (which are termed macroreticular pores).

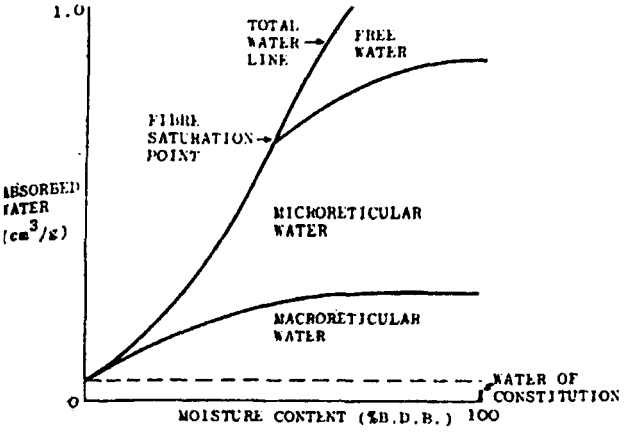

Figure 2.2: Various water forms as a piece of paper progressively wetted (Hoyland, 1976b)

The mechanisms for water absorption by paper have been examined (Hoyland, 1976b, 1977; Verhoeff et. al. 1963; Salminen, 1988), and it has been concluded that penetration under capillary pressure, inter-fiber penetration, and molecular diffusion (swelling) are the predominant processes.

Absorption of Water by Capillary Action

One of the mechanisms for water uptake is capillary pressure. Under this pressure liquid moves into paper. The capillary pressure is positive when the contact angle between the liquid phase and solid phase less than 90". In this case the capillary pressure pulls the liquid phase into the pore system. The penetration of a drop of liquid in a porous substrate is often described as a surface tension driven flow or wicking process. This action was described by Washburn in 1921. In the Lucas-Washburn (L-W) analysis, contact angle, θ , pore radius, R_c, and sheet void fraction, ε, are controlling parameters. The contact angle depends on a multitude of factors including paper moisture content, roughness, heterogeneous composition of the surface, and time. Figure 2.3 represents L-W Absorption Model.

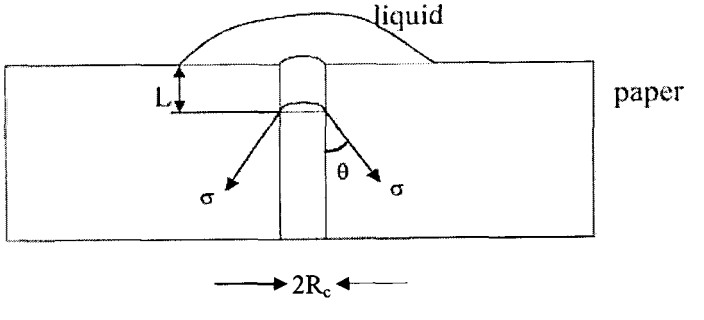

Figure 2.3: Absorption of liquid droplet by capillary action (Agbezuge and Carreira, 1998)

Vertical parallel capillaries form an idealized representation of several randomly distributed voids and capillaries of different size in the paper. After wetting the walls of the capillary, the liquid establishes a contact angle θ. For one capillary the net capillary pressure, AP, is:

$$\Delta P = \frac{2\sigma \cos\theta}{R_c} \tag{2.8}$$

where σ is the surface tension of the liquid, and R_c the radius of the capillary.

If it is assumed that the liquid is Newtonian and the flow is very slow (Re<1), then the average velocity of liquid moving into the capillary is given by Hagen-Poiseuille Law:

$$\frac{dL}{dt} = \frac{\sigma R_c^{\,2} \Delta P}{8\eta L} \tag{2.9}$$

where L is the distance covered by the liquid front during time t, and η is the viscosity.

Combining equation 2.8 and **2.9,** and after integration gives the Lucas-Washburn equation which describes the change in depth of penetration as a function of time and viscosity as:

$$L = \left(\frac{\sigma R_c \cos(\theta_d)}{2\eta} \right)^{1/2} \sqrt{t} \tag{2.10}$$

The Lucas-Washburn equation strictly applies to non-polar liquids in cylindrical capillaries, and does not always apply to penetration of aqueous inks into paper. Fiber swelling and effects due to pore size distribution in paper are not accounted for by this equation.

Hoyland et. al. (1977) put forward a new model for water absorption by fibrous materials and derived the following equation for the liquid penetration depth L, accounting for the swelling of paper in the thickness direction.

$$L = \left(\frac{\sigma R_c \cos\theta}{2\eta} \right)^{1/2} (t - t_w)^{1/2} - K \Delta Z \tag{2.11}$$

where t_w is a surface wetting time, **AZ** is the increase in paper thickness after time t, and K is a constant.

The Lucas-Washburn theory and its range of validity have been reviewed by Kissa (1996) and Middleman (1995).

The penetration of pure liquids and surfactant solutions into fiber networks such as paper strips was investigated by Berg and Hodgson (1988). They found that the liquid penetration distance was proportional to the square root of time, as suggested by Lucas-Washburn equation. They considered a tortuosity factor τ in the equation (Equation 2.12) where τ is the ratio of the real length of the capillary to that of a straight capillary:

$$L = \left(\frac{\sigma R_c \cos(\theta_d)}{2\eta\tau^2} \right)^{1/2} \sqrt{t} = k\& \tag{2.12}$$

Using a model of separate tortuous capillaries, one may express the volume absorbed per unit are a, V', as a function of sheet void fraction ε, and the pore tortuosity factor (Aspler, 1993) as:

$$V' = \frac{\epsilon}{\tau} \sqrt{\frac{R\gamma t \cos\theta}{2\eta}} \tag{2.13}$$

Based on this single capillary model, Middleman (1995) develops a simple dynamic model of a drop, initially sitting on a porous surface, wicking into a porous media below the surface. In the development of this simple model, the wetted diameter of the drop, R_d, or the contact area of the drop is assumed to be independent of time. The interface between the drop and the paper is considered to be the end of a bundle of capillaries, all with individual radii of R_c. The void fraction ε of the surface is given by:

$$\varepsilon = \frac{N_c \pi R_c^2}{\pi R_d^2} \tag{2.14}$$

wher N_c is the number of capillaries that open into the footprint of the drop. The average velocity u of the flow into a single capillary follows from the Lucas-Washburn equation:

$$u = \frac{dL}{dt} = \left(\frac{\sigma R_c \cos(\theta_d)}{8 \eta t} \right)^{\frac{1}{2}} \tag{2.15}$$

If V is the volume of the drop on the surface, the volumetric flow rate is:

$$\frac{dV}{dt} = \pi u \varepsilon R_d^2 \tag{2.16}$$

Assuming that the radius of the drop on the surface is constant, the volume of the liquid remaining at the surface is given by:

$$V(t) = V_d - \pi \varepsilon R_d^2 \left(\frac{\sigma R_c \cos(\theta_d)}{2 \eta} t \right)^{1/2} \tag{2.17}$$

where V_d is the initial volume of liquid.

The penetration time t_p is obtained by stating that V=O at t_p.

$$t_p = \frac{2\eta}{R_c \sigma}\left[\frac{V_d}{\pi R_d^2 \varepsilon(\cos(\theta_d)^{1/2}}\right]^2 \tag{2.18}$$

Another expression for the penetration time t_p can be obtained by considering the porous structure of paper as a packed bed. For laminar flow through a packed bed the Blake-Kozeny equation is valid (Bird ***et.*** *al.*, 1960), i.e.

$$v_0 = \frac{\mathbf{AP}}{H}\frac{D_p^2}{150\eta}\frac{\varepsilon^3}{(1-\varepsilon)^2} \tag{2.19}$$

where v_0 is the superficial velocity, H is the uniform penetration depth of the liquid in the packed bed (or paper) and D_p is the diameter of the packing or particles which make up the packed bed.

If the drop size is large one may assume that most of the penetration or wicking of the liquid occurs in the radial direction of the paper after the nearly "instantaneously" filling of the voids in papers immediately below the contact area of the drop.

For this situation, similar to Equation 2.16, the drop volume balance gives that:

$$-\frac{dV}{dt} = v_0 2\pi R_w h_p \tag{2.20}$$

where R_w is the radius of radial spreading of the liquid in the paper, and h_p is the paper thickness.

Since $H = R_w - R_d$, it follows that:

$$\frac{dV}{dt} = \frac{AP}{H} \frac{D_p^2 \varepsilon^3}{150 \eta (1-\varepsilon)^2} 2 \pi h_p (H + R_d) \tag{2.21}$$

The volume of the drop remaining, V, is given by

$$V = V_d - \pi (H + R_d)^2 \, h, \; \varepsilon \tag{2.22}$$

or

$$dV = -2 \pi h_p \varepsilon (H + R_d) \, dH \tag{2.23}$$

Insertion of Equation 2.21 in 2.23 gives

$$dt = C \, H \, dH \tag{2.24}$$

where

$$C = \frac{150 \eta (1-\varepsilon)^2}{APD,' \varepsilon^2} \tag{2.25}$$

Now at the time of complete disappearance of the drop, i.e. at t,, a mass balance gives that

$$\pi h_p \varepsilon (H + R_d)^2 = V_d \tag{2.26}$$

or

$$H_p = \sqrt{\frac{V_d}{\pi h_p \varepsilon}} - R_d \tag{2.27}$$

where H, is the final distance of radial spreading beyond the initial footprint of the drop.

Integration of Equation 2.24 from t=O to t_p gives

$$t_p = \frac{75\,\eta\,(1-\varepsilon)^2}{\mathbf{AP}\,D_p^{\,2}\,\sigma\cos\theta_d\,\varepsilon^2}\left(\sqrt{\frac{V_d}{\pi\,h_p\,\varepsilon}} - R_d\right)^2 \qquad (2.28)$$

or after insertion of Equation 2.1;

$$t_p = \frac{75\,\eta\,(1-\varepsilon)^2\,R_c}{2\,D_p\;\sigma\cos\theta_d\,\varepsilon^2}\left(\sqrt{\frac{V_d}{\pi\,h_p\,\varepsilon}} - R_d\right)^2 \qquad (2.29)$$

It should be noted that this equation is only valid when the final wetted radius, R_w is comparable to the initial wetted radius of the drop, i.e. R_d. Thus, equation 2.29 represents the situation of the drop test where radial spreading of the droplet in the paper is dominant, while Equation 2.18 describes the vertical wicking into a relatively thick sheet. It should be noted that both Equation 2.18 and 2.29 do not account for any swelling of fibers or any other change of the porous structure of the paper.

Thus, Equation 2.18 is appropriate for situations when the liquid volume is small compared to the void volume in the porous structure immediately below the "footprint" of the deposited fluid (see Bristow Equation below), while Equation 2.29 is applicable when the fluid volume is large compared to the void volume below the deposited fluid on the paper surface.

For industrial situations, fluid absorption during a short period of time is more relevant. During these short contact times the liquid penetration is mainly in the thickness direction of the paper, i.e. the fluid uptake per unit paper surface area is smaller than the paper thickness or caliper.

Bristow (1967) developed a special apparatus to measure absorption contact times between 0.004 and 2.0 sec. Typical results show that the sorption of oils follow a square-root dependence on time, in keeping with the equations for capillary flow. The water measurements show that there is a delay before the water begins to be absorbed. The water absorption obtained by extrapolation to t=O gives a measure of the paper roughness (Bristow, 1967).

Short time penetration into complex porous structures has been studied recently by Bousfield ***et.*** *al.* (2000). They presented a new method to predict the short time absorption into a real pore geometry taking into account fluid properties, surface forces, and complex pore geometry. The porous space is characterized by techniques described in the paper by Toivakka and Nyfors (2000). The Bousfield model calculates the rate of fluid uptake as a function of time.

Molecular Diffusion of Water into the Fiber Cell Wall

Since cellulose and especially hemicelluloses are water-sorbing polymers, water molecules diffuse into the cell wall when a concentration gradient is established. Diffusion of water into cellulose can be very fast. **A** 10mm film of water can be absorbed by cellulose film in less than one second. The diffusion of water into cellulosic materials increases sharply with increasing water content and is slowed down by barriers.

The penetration of water into a fiber is accompanied by swelling. Some studies show that fiber absorption is definitely a property of a particular paper, and not simply related to capillary penetration ability.

The interdependence of swelling and penetration has been investigated by Bristow (1971 and 1972). The uptake of water has been considered the sum of two components. These are flow into the capillaries - termed pore absorption; and penetration into the fibers - termed fiber absorption. The fiber absorption is accounted for as a first approximation by an increase in fiber thickness during penetration. These two types of liquid uptake occur simultaneously; so it can be written:

$$V_{total}=V_{fiber}+V_{pore} \tag{2.30}$$

where V is the volume of liquid per unit area of fiber material and pore space respectively. Bristow showed how pore and fiber absorption terms vary with time in Figure **2.4**

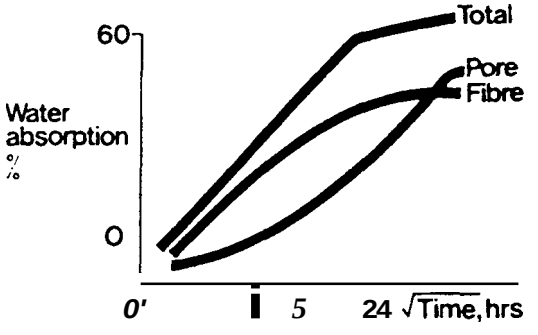

Figure 2.4: Variation of pore and fiber absorption terms with time (Hoyland, 1977)

2.3.3. Swelling

Swelling is one of the important properties of paper and it is one of the mechanisms occurring during water-fiber interaction. The swellability of cellulose fibers is an important property for the paper industry. The water holding capacity (Water Retention

Value) is correlated with the moisture content after the press section, and with the sheet strength after drying. Acidic groups in the carbohydrate fraction influence the degree of swelling. Water molecules diffuse into the amorphous regions of the cellulose matrix and break inter-molecular hydrogen bonds. This allows an increase in the inter-molecular distance of the cellulose chains, which causes swelling. It is believed that swelling occurs as a result of water entering in order to reduce the osmotic pressure. Therefore, there is a swelling equilibrium, where the difference in chemical potential due to concentration differences is balanced by the osmotic pressure.

The degree of swelling of a gel is generally defined as the amount of water (per **gram** of dry substrate) imbibed under specified chemical conditions. This definition of swelling is identical to the concept of the fiber saturation point defined by Tiemann in 1906 as the moisture content when the cell walls are saturated and no moisture remains in capillary voids (Lindstrom 1986). Stone and Scallan (1968) defined a swelling mechanism for the delignified cell wall, which is based on the idea of a displacement of the cellulosic lamellae. They found that most of the inaccessible water (gel water) was located in pores in diameters between ten and a few hundred Å.

Paper swelling is a function of the release of dried-in fiber stress and the bonding stresses between fibers.

Some studies have been done to be able to understand the kinetics of swelling. Bristow (1971) has measured swelling thickness against time for uncoated sized and unsized paper. He also measured the rate of swelling for building boards and he recorded swelling volume against time. In Figure 2.5, water is first absorbed by the interfiber pores and then into the fiber walls (path OAB) for unsized paper. By sizing the paper, sorption along the

interfiber pores is delayed. Once absorption into the sized fiber wall has processed to the liquid-like water stage, interfiber sorption occurs (path OCB).

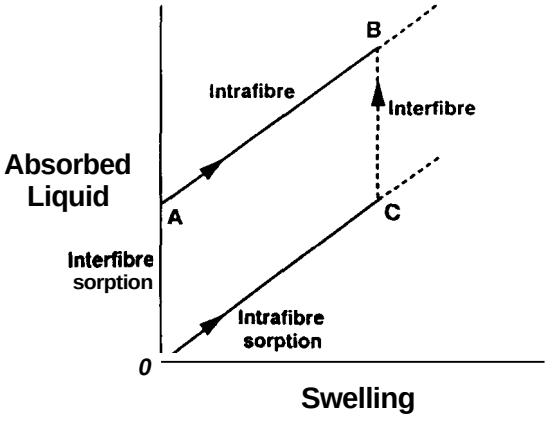

Figure 2.5: Amount of water absorbed by paper compared with fiber swelling (Aspler, 1993, after Bristow, 1971)

There are several methods to determine the cell wall swelling. The more important methods are: the solute exclusion method, centrifugal water retention value (WRV) method and the pressure plate method. The WRV method is the most popular method because of its ease, simplicity, and rapidity. This method has been researched mostly by Jayme and co-workers in between 1948 and 1955. Scallan and Carles (1972) showed that WRV is directly related to the fiber saturation point determined by the solute exclusion technique. The fiber saturation point and WRV results are affected by the pulping process, pulp yield, degree of beating, drying and rewetting and treatments with swelling agents. It was also found that the WRV is a function of a centrifugal force and centrifugation time. From the results it appears that the centrifugal method under conditions of 900 G and 30 minutes centrifugation can be used as a good estimate of the fiber saturation point up to 1.80 g/g.

Treatments, which tend to increase the degree of swelling of a pulp, e.g., beating, and chemical treatment such as sulfonation, carboxymethylation (Nelson and Kalkipsakis, 1964a) and hydrolyzing polyacrylonitrile-grafted cellulose fibers (LePoutre and Hui, 1973), sodium hydroxide addition during recycling (Gurnagul, 1995), increase the strength of the paper made from the pulp. Similarly, factors which tend to reduce the swelling potential, e.g. drying, cross-linking, and hemicellulose removal, impair the strength of the paper made from the pulp (Lindstrom, 1986).

Swelling values for pulps in different chemical environments can be correlated with the tensile strength of the papers made from them (Scallan and Grignon, 1979).

The increased swelling of TMP (Thermo Mechanical Pulp) fibers appears to increase the sheet strength. However, there seems to be no relationship between the level of swelling and sheet strength for kraft pulps (Gurnagul, 1995).

Using carboxymethylation, Schuchardt and Berg (1990) developed a modified capillary model based on individual fiber swelling characteristics, which describes observed deviations from the Lucas-Washburn model. The imbibition of water deviates significantly from Lucas-Washburn kinetics when fibers are carboxymethylated because of the long term swelling of the CMC fibers. The net pore restriction effected by fiber swelling is quantified by a "permeability factor" defined as the ratio of the wicking-equivalent radius in the swollen state to that in the unswollen state. Carboxymethylated fibers are capable of absorbing up to 20 times their weight in water. In the diffusion of liquid into this superabsorbent material the capillary action and diffusion mechanisms are coupled, and it generally reduces the dimensions of the interfiber pore space, decreasing the rate of absorption. In the extreme case, a form of "gel blocking' occurs in which

swelling of the superabsorbent material completely closes the wicking channels, preventing further wicking and limiting liquid transport to a diffusion process. In the Lucas-Washburn equation (2.8), the pore radius R_c describes the effect of the pore structure of fiber networks on the liquid uptake rate. For the situation of the CMC fibers based paper, Schuchardt and Berg plotted the height of advancing liquid as a function of the square root of time. From the slope of this plot, the wicking equivalent radius can be determined if the liquid properties are known and if the advancing contact angle of the liquid on the fibers is known. Any changes in R_c reflect the effect of interfiber debonding, as well as swelling and morphological changes of the fibers themselves. They also found that CMC fibers exhibited a very high rate of swelling for the initial 15-60 seconds of immersion, followed by a slow, roughly linear increase in this parameter for periods ranging from three minutes to over twenty minutes. They defined a permeability factor, P_f (Equation 2.31), as the ratio of the effective pore radius when the fibers are swollen to that, which is measured using a nonswelling reference liquid. This provides a convenient means for assessing the changes in the wicking performance brought about by fiber swelling.

$$P_f = \frac{R_{c,swollen}}{R_{c,referance}} \tag{2.31}$$

The model that Schuchardt and Berg introduced is based on cylindrical capillary tubes. In it, however, the effective capillary radius is a function of time and position for the portion of the structure which has been wet by the liquid. The effects of fiber swelling are thus represented as a progressive constriction of the interfiber pore space with time. Since this constriction takes place only after the fiber walls have been wet by the liquid, the

advancing meniscus constantly sees the initial capillary radius R_o. Neglecting the net flux of liquid into capillary walls, and ignoring any axial diffusion through the walls, the Lucas-Washburn equation is re-derived as follow:

$$\frac{dL}{dt} = \frac{R_h^2}{8\eta}\left[\frac{\Delta p}{L}\right] = \frac{R_h^2}{8\eta}\left[\frac{2\sigma\cos\theta}{R_o L}\right] \tag{2.32}$$

where R_h is the effective hydrodynamic radius behind the advancing liquid front. The approach taken is to approximate R_h as a linear function of time, and to presume that this is an acceptable approximation over the time period of the wicking experiment;

$$R, = R_o - a\,t \tag{2.33}$$

where the constant "a" expresses the rate of constriction. With the introduction of this assumption, the integral form of the modified capillary model is:

$$L = \left[\frac{R_o\,\sigma\cos\theta}{2\eta}\right]^{1/2}\left(t - \frac{a}{R_o}t^2 + \frac{a^2}{3R_o^2}t^3\right)^{1/2} \tag{2.34}$$

2.4. Effect of Substrate Properties on Final Coating Structure

In the paper coating process, a water based pigmented coating is applied to the base sheet to enhance the optical and topographical properties of the printing surface. It is generally believed that basestock absorbency and its spatial variation across the sheet are very important, since these might affect the coat weight pick up and its spatial distribution, as well as the structure and uniformity of the coating layer. Coat weight variation is an

important problem because recent research shows that it is related to print nonuniformity. During coating, some of the water contained in the coating, and also the coating pigments, penetrate the sheet, the latter which defeats the purpose of surface treatment. However there is not much experimental data available in the literature which quantifies penetration of the coating into the base sheet.

Penetration into interfiber capillaries can be described using the Lucas-Washburn approach. If the sheet pore sizes are large, or if the contact angle is low, the solids from the coating suspension might penetrate into the sheet internal pore system. The coating would sink into the sheet, giving poor coating holdout and thus poor coated paper properties. Poor coating holdout is usually inferred from the properties of the coated paper and not directly measured by, for example, microscopic observation of cross sections (Huang and LePoutre, **1998).**

Sandàs and Salminen (1987) studied the water sorption of papers coated with different pigments. For the coated paper, the rate of capillary transport in the fiber network is effected by the coating layer. This layer causes a pressure drop when the water is transported through it to the base paper. The pressure drop is determined by the pore structure and thickness of the layer. Hence, capillary transport in the base paper is determined by the coating layer, molecular absorption, fiber sorption and expansion of the fiber network. The driving potential for water movement under the influence of external pressure is the sum of the capillary forces and the external pressure. When the external pressure is high enough, it is the rate determining factor for water transport. This applies especially for the water movement in the base paper.

Sandàs and Salminen (1987) observed the water sorption of uncoated and paper coated with clay. The measurements were carried out under external pressure (P=0.5 atm), as well as under the influence of capillary forces only (P=0.0 atm). They found that the surface properties of the coating layer influence water uptake only up to the point where the layer is saturated with water. When liquid has passed this layer, the transport rate is determined by the flow losses in the pore structure and the sorption properties of the base paper. At high external pressure the physical structure of the pore system is the rate determining factor for water penetration. External pressure is very important in the industrial sorption processes. If a liquid penetrates in the layer under the influence of high external pressure, the transport rate cannot be effectively regulated by surface chemical means. On the other hand, at low external pressure the water movement and sorption rate in the coating layer can be determined by the capillary forces.

Skowronski and LePoutre (1985) looked at commercial papers of different mechanical pulp contents and water sorption levels which were treated on a laboratory puddle type blade coater with coating color and with water alone. They reported that the volume of water or coating color taken up was a function of paper roughness. On low-water sorption paper, the coating color take up increased linearly with roughness. High water sorption paper took up much more water and also more coating than the low water sorption paper. Water treatment had little effect on the mechanical properties of the papers, but it caused an increase in roughness and thickness and a decrease in air resistance and gloss. The results after blade coating depended on the rate and extent of the destructive action of water absorbed by paper from the coating before and after the application of the coating. If the contact time is long enough, the destructive action of water results in debonding,

internal stress redistribution, and fiber swelling. If these factors act before the passage of the blade, they can increase roughness and thus increase the volume of applied coating. If the action of these factors is delayed until after the blade passage, they can decrease the roughness of coated paper.

LePoutre (1978) also studied the influence of the absorbency of the substrate on the surface structure of clay-latex coatings. The surface of coating applied at 40% solids on an absorbent substrate (milipore filter) exhibited a very disordered arrangement of the kaolin plates and an almost complete absence of latex and clay fines. They examined and observed under the scanning microscope the effect of substrate absorbency, coating weight, color solids, and water retention additives on coating structure. At high solids content of coating, the milipore filter had a considerably lower coating weight and a higher a pigment cake build up than that on an impermeable plastic film, surface of the coating on the milipore filter is slightly rougher than that on the plastic film surface. With increasing the coating weight the differences between milipore and plastic film disappear. At low solids, some flocculation occurred and coating on the plastic film seems to be a little rougher than high solids. The coating on milipore filter is very rough even at the lower magnification. As the coating weight is increased, the milipore coating becomes less rough and contains much more fines and more latex. They concluded that the coatings on publication grade paper set very quickly and had coating weights similar to those on the milipore filter, while on board the coatings set more slowly and had weights comparable to those reached on the plastic substrate.

Huang and LePoutre (1998) presented the effect of base sheet absorbency on coating pickup, mass distribution, and sheet properties. They examined porous handsheets, dense

handsheets (smooth), and rough handsheets which were produced from a 50/50 blend of bleached hardwood and softwood pulp at different refining levels, and commercial LWC. The pigment system they used was a blend of fine clay and ground $CaCO_3$, with average equivalent spherical diameter of 0.5 μm, much smaller then the 6.2 μm pore size of the coarsest sheet. **A** latex binder was also used. The solid content was held constant at 60%. The coating was applied on a CLC blade coater. They also looked at sizing effects. They found that the higher absorbency of the unsized sheets would lead faster dewatering and produced a thicker filter cake of coating. Their results showed that two important contributors to base sheet absorbency- hydrophobic sizing and sheet density/porosity- had very different effects. On dense-smooth papers, hydrophobic sizing led to lower coating pickup. On rough papers, the lack of influence of sizing was explained by the overwhelming effect of roughness on the metering action. Hydrophobic sizing improved coated gloss slightly, particularly on dense sheets but it had no effect on coated roughness, regardless of base sheet density. This is attributed to the surface topography causing a variation in coat weight underneath the surface fibers, where it is shielded from the light. Coating holdout and mass distribution were significantly poorer on all porous sheets.

Some simulation studies of the motion of spherical particles and how the coating structure is affected by different properties were done by Toivakka *et. al.* (1992). They simulated the leveling of coating on a base sheet with a sinusoidal roughness. The surface of the wet coating immediately after passage of the blade is smooth. During the subsequent dewatering, the coating layer shrinks, and a rough surface are formed. They found that a densified layer of particles is formed on the paper surface if the absorption is

the prevailing dewatering mechanism. If extreme drying or a very hydrophobic base paper is used a dense layer of particles if formed at the coating-air interface. The in-plane motion of particles is small under typical drying conditions: contraction of the coating is dominant factor controlling the leveling of coating on a rough substrate. Particle motion into pores is prevented by a bridging mechanism. Coating with low initial volume fraction of solids or a high electrostatic stabilization, result in an increased loss of particles into the base sheet. At high initial volume fraction solids the pore was blocked by a group of particles trying to enter the pore simultaneously. In this case the pore was usually blocked almost immediately with few particles being lost into the pores. The blocking mechanism provides a possible explanation why high solids coatings have good ''coating holdout''. The simulations suggested that the following factors lead to a decreased loss of particles into the substrate and therefore to better properties of the final coated product; high application volume fraction solids, small average pore size of base paper, low electrostatic stabilization and hydrophobic paper (the flux into the pores is minimal).

2.5. Wetting and Contact Angle

When the free surface of a liquid meets a solid, the two intersect at a definite angle 8 which depends on the nature of the liquid and the solid. The angle of contact between a liquid and a solid is the angle between the solid surface and the tangent plane to the liquid surface at the point of intersection. Maximum wetting occurs when $\theta = 0''$, partial wetting when $0^{o} < \theta < 90^{o}$, and no wetting when $\theta \geq 90''$.

To explain the phenomenon of wetting and contact angle the concept of surface energy can be used. As soon as movement of the liquid on the solid surface is considered, hysteresis of the moving contact angle is observed. This is best described by imaging a drop of water running down a plane, as shown in Figure 2.6.

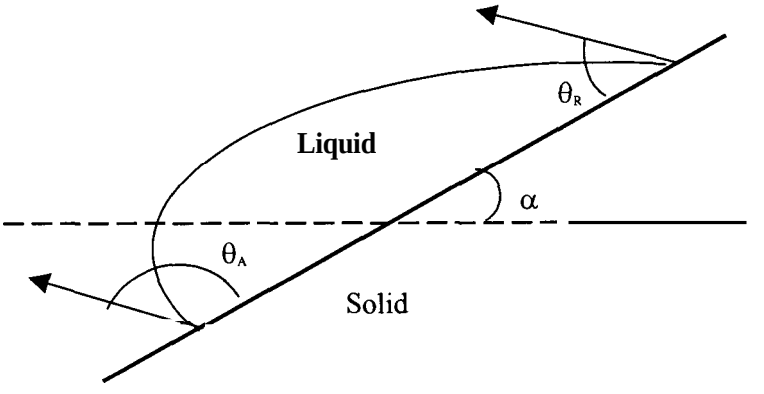

Figure 2.6: Hysteresis of contact angle (Hoyland, 1976b)

Thus the observed contact angle is no longer a characteristic of the system, but also a function of the motion. The larger contact angle is called apparent advancing contact angle θ_A, and the smaller is called apparent receding contact angle θ_R. If we consider a drop spreading on a dry surface, the drop spreads with a contact angle equal to the advancing contact angle θ_A. On the contrary, when the drop recoils, the angle is equal to the receding contact angle θ_R. The difference between θ_A and θ_R leads to a contact angle hysteresis.

The roughness of the surface over which the liquid moves can appreciably affect the apparent contact angle (Figure 2.7). If a roughness factor, R, is defined as the ratio of the actual surface area to the geometric surface area, then the apparent contact angle, θ_{ap}, is related to the real (intrinsic) contact angle, θ_{in}, by (Wenzel, 1939):

$$\mathrm{Cos}(\theta_{ap}) = R\ \mathrm{Cos}(\theta_{in}) \qquad (2.35)$$

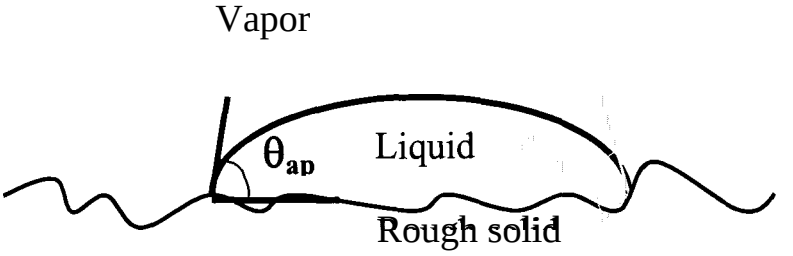

Figure 2.7: Apparent and real contact angle (Bouchon, 2000)

If θ_{in} is smaller than 90 degrees, θ_{ap} decreases as the roughness increases. On the contrary, if θ_{in} is larger than 90 degrees, θ_{ap} increases as the roughness increases.

Thus roughness influences the wetting or non-wetting characteristics of a system. This is experimentally confirmed by Wink and Van den Akker (1957).

The heterogeneous composition of the surface also affects the apparent contact angle. Thus the macroscopically measured angle of the contact of a liquid and a rough surface is probably a mean of a distribution of local contact angles resulting from the surface roughness and heterogeneity (Hoyland, 1976b).

Measuring contact angles on porous substrates presents a difficulty due to absorption and the heterogeneity of the surface. Elftonson and Strom (1995) measured the contact angles of aqueous solutions on model porous and non-porous substrates. They found that the initial contact angle on the porous material is higher than on the non-porous material when the angle is high. For lower contact angles, the initial contact angle is lower on the porous material than on the non-porous material. This is mostly due to the high penetration of the liquid into the pores and a lateral spreading induced by surface

capillaries. Initial penetration and capillary-induced spreading are promoted by low equilibrium contact angles.

It takes time to bring the solid and liquid actually together to the point where the liquid has wetted the solid. This is referred to as a wetting time. For a particular system the wetting time is most influenced by the flow properties of the liquid. Several studies have been done and have found that the wetting time increases with increasing viscosity. Since the wetting process is time dependent, it was found that the contact angle must also be time dependent. It follows then that a roughness effect must also alter the wetting time of the surface. Time dependence of the contact angle then becomes an indication of the rate at which surface wetting will occur.

The wetting and contact angle for cellulose is complicated by the absorption of water into the cellulose fiber. **A** drop of water placed on the surface of a sheet of paper disappears very quickly by capillary and by fiber sorption. Some experiments were done on untreated cellulose surfaces, and the value of the initial contact angle was found to depend upon the moisture content of the sample. The initial contact angle decreases rapidly with time, the rate at which this occurred increasing as the sample moisture content increased (Hoyland, 1976b). The recorded angle being 33" for paper conditioned at 0% relative humidity, and 18° at 100% relative humidity, with a considerable change of the contact angle over time; the contact angle could decrease from the initial value by about 11" after 10 minutes (Hoyland, 1976b).

2.6. Carboxymethylation of Cellulose Fibers

Cellulose etherification is a very important branch of commercial cellulose derivatization that started considerably later than the conversion of the polymer to esters. Preparation of cellulose ether was reported for the first time in 1905 by Suida, who reacted the polymer with dimethylsulfate to give a methylcellulose. Carboxymethylcellulose (CMC) was first prepared in 1918, and was already produced commercially in the early 1920's in Germany (Klemm *et. al.*, 1998). The latest patent to synthese sodium carboxymethyl cellulose was issued by Taguchi *et. al.* in 1985 (US patent & Trademark Office, Patent # 4,525,585). Most of the work discussed in the literature deals with soluble CMC having a high degree of substitution, DS (DS greater than 0.5). On the other hand, low substitution of cellulosic pulps is also important because it changes the hydrophilicity of the fibers. CMC of DS>0.5 is completely soluble in water and finds widespread application (thickener in printing-ink, food, paint, cosmetic industries, anti-deposition agent in detergents, paper sizing etc.). At low **DS** (<0.2) CMC retains its fibrous nature, whereas many of its characteristics differ from those of original fiber. This kind of CMC is much less known than the soluble form.

The hydroxyl groups of cellulose play an important role in the pronounced affinity of cellulose for water and in the bonding of cellulose fibers during the formation of paper. Several investigators (Jayme and Froundjan, 1940; Bletzinger, 1943; Aiken, 1943; and Harrison, 1944) have studied cellulosic pulps in which varying amount of these hydroxyl groups have been substituted with hydrophobic groups such as the methoxyl or ethoxyl groups. It was also found that at low DS the affinity for water of these substituted celluloses was increased, due to an opening up of the cellulosic structure making more

cellulosic hydroxyl groups available or bonding and for the adsorption of water. If hydrophilic groups instead of hydrophobic groups are used for substitution, the resulting products should have properties that differ both from original and hydrophobic substituted pulps. At low DS's the increase in affinity for water of these substituted pulps should be greater and this increase should be retained at higher DS's. The physical properties i.e. strength of handsheets formed from a pulp substituted with hydrophilic groups should also be increased (Walecka, 1956).

Reid and Daul (1947, 1948, and 1949), and Daul *et. al.* (1952) studied CMC products from a DS of 0.015 up to 1.8. They prepared CMC filaments, yarns and cloths, and studied some of their properties of interest to the textile industry. They have observed increased tensile strengths, degrees of swelling, and water absorption in cotton threads and yarns that had been partially carboxymethylated. These are properties that would be of interest in the paper industry. They also conducted a pilot-scale carboxymethylation of cloth, which showed that it is possible to use standard machinery for the process.

Low-DS CMC pulps (DS's from 0.006 to 0.062) were first prepared, retaining the fibrous nature of the pulps, and without excessive degradation in 1956 by Walecka using rag pulps. He also examined the papermaking behavior of these pulps and further determined the physical strength properties of handsheets formed from these pulps. Higher burst and tensile values were obtained for the higher DS sheets. Beating time is also effective on treated pulps. It is also seen that as the DS is increased, the opacity of the CMC sheets decreases. Also, sheets prepared from the CMC pulps were considerably less porous to passage of air than were the control samples. Further, upon drying, it was theorized that the carboxymethyl groups facilitated increased bonding both within and between fibers,

therefore producing the increased physical strength properties observed. Nelson and Kalkipsakis (1964a) carboxymethylated a Eucalypt kraft pulp in nonaqueous medium and reported burst factor and tensile strength changes. They also compared carboxymethylation under aqueous and nonaqueous conditions. For carboxymethylation under aqueous conditions, the unbeaten strengths of the treated pulps were in most cases slightly higher than those of the untreated pulp, but beaten strengths were generally inferior. Using 30% sodium hydroxide gives the most increased strength. On the other hand, under nonaqueous conditions, all treated pulps showed lower freeness and higher unbeaten strengths than untreated pulp. They reached higher DS values using Walecka's method with Eucalypt pulp.

The behavior of salts of a carboxymethylated pulp was also described by Talwar (1958) and Nelson and Kalkipsakis (1964b). The free acid and the aluminum salt forms of carboxymethylated rag pulps have lower strength than the sodium forms (Talwar, 1958). Sodium salt of high DS pulps exhibited a high level of unbeaten strength but showed no increase on beating (Nelson and Kalkipsakis, 1964a). Alkali-metal, ammonium, and substituted ammonium salts showed the highest unbeaten strength at all levels of degree of substitution. For different cases, Na^+ gives the highest burst factor and tensile strength. They also looked at the hydration of the unbeaten pulps using water retention measurement. The free acid form showed the same water retention value as the untreated control at low DS but lower values at higher DS. Na^+ gave higher water retention values with increasing DS than the other salt forms (Nelson and Kalkipsakis, 1964b).

2.6.1. Chemistry of Carboxymethylation Reaction

Carboxymethylation is a well-known etherification reaction. However it deffers from other cellulose etherification reactions in that alkali cellulose does not need be prepared separately in a preceding treatment, although normally it is. The classical process of carboxymethylcellulose preparation under heterogeneous conditions starts from an alkali cellulose obtained by steeping with aqueous NaOH of 20-30 % (by weight) concentration and subsequent pressing. Etherification is then performed by reaction of this alkali cellulose with sodium monochloroacetate or monochloroacetic acid. The carboxymethylation reaction and a side reaction that produces sodium glycolate and NaCl are shown in Figure 2.8.

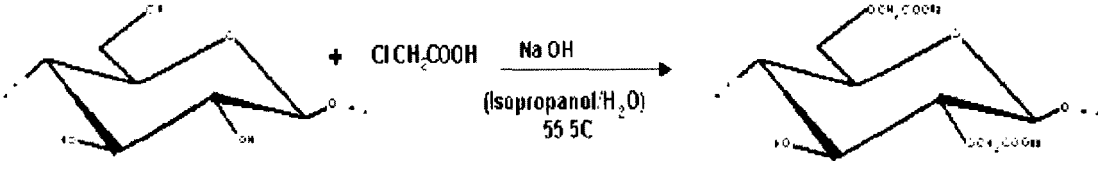

$$R_{cell}(OH), + ClCH_2COONa + NaOH \rightarrow R_{cell}(OH), OCH_2COONa + NaCl + H_2O \quad (1)$$

$$ClCH_2COONa + NaOH \rightarrow HOCH_2COONa + NaCl \quad (2)$$

Figure 2.8: Carboxymethylation reactions; (1) main reaction, (2) side reaction (Klemm *et. al.* 1998; Ott *et. al.,* 1954)

The primary hydroxyl group, at C-6, and the two secondary ones, at C-2 and C-3, are potential sites for the reaction (Figure **2.9).**

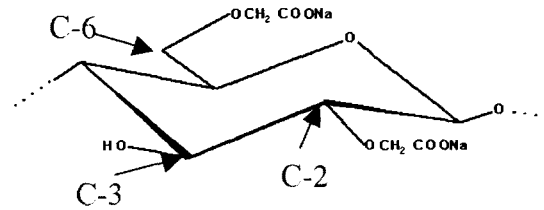

Figure 2.9: Carboxymethylcellulose unit (Klemm *et.al.* 1998)

1 mol or 2 mol of NaOH are consumed in this process per mol of etherifying agent converted to a carboxymethyl group inside the polymer and to sodium glycolate depending respectively on whether alkali cellulose or cellulose is used. At 50-70°C the reaction takes place over several hours as an exothermic process (Ott ***et.*** *al.,* 1954). In carboxymethylation under homogeneous conditions, LiCl/N,N-dimethylacetamine (DMAc) is being used as cellulose solvent (Heinze et. al., 1994).

The extent of reaction is usually characterized by the degree of substitution (DS). DS is the fraction of carboxymethyl functional groups per glucose unit. The usual DS is between 0.6 and 0.9, but the highest reported value in the literature is about 2.8 (McLaughlin and Herbst, 1950a). The water solubility of cellulose can be controlled within wide limits via the DS. The DS is often expressed in 'mmol COOH/g of sample'. The following equation is used for determining the DS from the measurement of the carboxyl group content of the sample (Klemn ***et.*** *al.*, 1998).

$$\mathrm{COOH(mmol/g)} = \frac{\mathrm{DS} \times 1000}{162 + (\mathrm{DS} \times 58)} \qquad (2.36)$$

Several methods are being used to determine the carboxyl group content in carboxymethylcellulose. Unruh and Kenyon in 1942 proposed a calcium acetate method. This method is simple and easy for rayon pulps and other cellulosic materials in which

the carboxyl content is very small, and not easy to determine by any other method. Sobue and Okuba (1956) determined the carboxyl group using the dynamic ion-exchange (potentiometric titration) method. They described this method and also compared it with the calcium acetate method. They found that in the ion-exchange method the effect of carbon dioxide can be entirely ignored, and can be completed in a very short time. The ion-exchange method also does not suffer from undesirable effects due to the high pH in calcium acetate method. The most common method for measuring the carboxyl group content is potentiometric titration with sodium hydroxide in the presence of sodium chloride. The most recent method was introduced by Katz *et. al.* (1984). This method is based on a conductometric titration of sulphonic and carboxylic acid groups within cellulosic fibers. In this method, the carboxylic groups are converted to their hydrogen form, and are then titrated conductometrically with NaOH in the presence of 0.001 M NaCl. The method is rather simple and direct. Scallan *et. al.* (1987) studied the theoretical considerations and confirmed the interpretations made in the experimental method. They also found that ion-exchange resins substituted with either weak or strong acid groups also show titration curves of the predicted shape and with the same dependency on the sodium chloride concentration.

2.6.2. Kinetics of Carboxymetylation and Effect of Reaction Parameters

The kinetics of carboxymethylation and effect of reaction parameters on reaction efficiency were studied in many years. The kinetics of the reaction are dependent on the concentration of NaOH, time, temperature, the ratio of water to cellulose, the ratio of monochloroacetic acid to cellulose, and the manner in which the reagents are added.

McLaughlin and Herbst (1950b) found that the carboxymethylation efficiency was improved by lower reaction temperatures, by decreasing excess sodium hydroxide, and by increasing the pulp shredding time at low water contents. The optimum water to cellulose mole ratio was 1.3 to 1.

Philipp *et. al.* (1980) examined the effect of the reaction medium and the physical structure of cellulose on esterification. From the reagent consumption and the increase in the DS in a heterogeneous system the effective rate constants were derived and the temperature dependence and the effect of the physical structure of cellulose were evaluated.

Heinze *et. al.* (1994) obtained a DS **up** to 1.7 with a sufficiently excess of monochloroacetic acid and powdered NaOH after a reaction time up to 72 h. **A** reactivity ratio of C2/C3/C6 of 3.0:1.0:2.1 was reported in Baar *et. al.* 1994 for samples of DS>1 obtained by a slurry process with isopropanol as solvent. According to Heinze and Pfeiffer (1999), both the highest DS and conversion of monochloroacetic acid are reached using a 15% NaOH solution,

Olaru *et. a/.* (1980) presented a polynomial equation which shows (in a quantitative manner) that the DS is influenced both by alkalization parameters (time, temperature, NaOH/cellulose-molar ratio, and water/cellulose-molar ratio) and esterification parameters (time, monochloroacetic acid/cellulose-molar ratio) using a multiple data regression technique. They found that DS is most influenced by the NaOH/cellulose and water/cellulose molar ratio.

H NMR spectroscopical studies were done by Heinze and Pfeiffer (1999). It was concluded that both the concentration of the alkali hydroxide solution and the reaction

time influence the partial DS at position C-2 and C-6, while position C-3 shows the lowest reactivity, independent of the reaction conditions used. The best DS result was obtained at a NaOH concentration of 15% and 5 h reaction time at 55°C.

Daul *et. al.* (1952) partially carboxymethylated cotton and they found an increased reaction at the same concentration of reagents obtained by increasing the temperature of sodium hydroxide to about 67° – 77°C. Negligible reaction occurs below 10°C; above 80°C substitution is not increased.

2.6.3. Effect of Carboxymethylation on Swelling

The swellability of cellulose fibers is a very important property for the paper industry. The water holding capacity correlates strongly with the volume and structure of the pores in the fiber wall. The acidic groups of cellulose influence the degree of swelling. The most widely used method of introducing acidic groups into cellulose is carboxymethylation. The number of acidic groups was found to play a significant but not determinative role in the level of improvement in swelling caused by carboxymethylation Carboxymethylation has been found to increase the water retention value and improve the papermaking properties of fibers in a proportional way (Nelson and Kalkipsakis, 1964a). According to Scallan and Grignon (1979), the paper made from the pulp is increasingly stronger in order of $Na^{+} > Li^{+} > Ca^{++} > Mg^{++} > H^{+} > Al^{+++}$. It is believed that the stronger the cationic form, the greater is the total number of free ions kept within the cell wall. This causes the entry of additional water into the wall by osmosis, and the accompanying swelling and plasticization increases the ability of fibers to bond extensively. In the most recent study, the swelling of cellulosic fibers having different carboxyl contents over a

wide range achieved by varying the parameters used during carboxymethylation was investigated (Racz and Borsa, 1997). It was found that the concentration of sodium hydroxide has the most significant effect on swellability. The proportion of acidic groups in the H-form has a large but not determinative role in the degree of swelling. **A** linear correlation was found between the degree of swelling and degree of collapse, the structural change in the cell wall (hornification), of non-dried samples.

2.7. Effects of Treatments on Coating Holdout and Penetration

For improving coating holdout several effects, including (a) changes in the pigmentation, (b) addition of water retention agent, (c) destabilization of the coating, or (d) increasing the pigment binder interaction have been studied. However, base paper treatments are also an important factor for improving coating holdout.

It was mentioned as in Adams (1983) it was reported that in unsized paper the liquid phase of the coating readily wets the fibers because of capillary action and penetrates rapidly into the sheet. In sized paper, the penetration was considerably reduced because the walls of the pores resisted wetting.

The effect of size press treatment was studied by Adams (1983). He size press treated the paper and paperboard base stocks with conventional and reactive sizes. The surface treatments were hydroxyethyl, sodium carboxymethylcellulose, a styrene-maleic anhydride copolymer, and ketene dimer reactive size. In order to define base sheet holdout properties, porosity, sizing and contact angle and water retention time of the coating were measured. On absorbent, unsized papers, rapid initial wetting of the fibers is the primary cause of poor coating holdout. Only treatment with the reactive size reduced

coating penetration time. It also showed the greatest increase in the apparent contact angle between the paper surface and water. On sized paperboard, where hydrophobicity is already provided by internal sizing, capillary pore size appears to be the controlling factor. The optimum treatment must involve barrier formation or some other mechanism to cover or fill the pores. In this case CMC contributed the greatest amount of holdout to basestock. In CMC treated board, the CMC rapidly picks up water from the penetrating liquid. This allows the polymer to swell, which increases the extent of pore coverage and adds viscosity to the coating color both of which aids in slowing both capillary and pressure induced migration.

LePoutre *et.al.* (1986) also studied the pretreatment of basestock. They hypothesized that the controlled surface addition of a film-forming, hydrophobic, polystyrene-butadiene latex at the surface of LWC basestock would plug some of the pores and reduce pressure migration, provide a hydrophobic surface that would reduce capillary migration, and reinforce interfiber bonding at the surface to improve pick resistance. They also examined hydrophobic sizing alone by studying the effect of the presence of film-forming polymers in solution in water (CMC) or in a solvent, and the effect of calendering.

Suppressing the migration of coating components into wood-containing basestock by hydrophobic sizing or by applying a film-forming polymer from a solution or an emulsion did not improve unsupercalendered coated paper properties. Pretreatment with filming polymers in aqueous solution or emulsion was ineffective because irreversible changes caused by debonding, swelling, and stress relaxation processes take place as the water applied with the polymer contacts the fibers. In fact, the beneficial effect of

polymer in filling surface voids is more than offset by the adverse destructuring effect of water. Their data also suggest that these structural changes are triggered by diffusion of water molecules into fiber walls and that the diffusion process is rapid.

Calendering was effective. Thus It is possible that the combination of polymer addition and calendering, as a pretreatment would afford improvements in coated properties, at some cost however.

Effects of mechanical and chemical treatments on pore size distribution in wood pulps were examined by Berthold and Salmen (1997). They used inverse size-exclusion chromatography to examined for effect of different treatment on the fiber swelling (pore volume and pore-size distribution). They found that the apparent pore size distribution shifted from mainly small pores with a lower proportion of smaller pores for an unbleached kraft pulp. This trend was even more pronounced for a bleached kraft pulp. Recycling of pulps caused irreversible partial pore collapse.

Recently, the study of precalendering, surface wetting and hydrophobicity treatment was repeated by Forseth and Helle (1998). They found that after water coating of the uncalendered base paper, no change in roughness was observed. When using pre calendered news-print type base paper, wetting of the paper surface raised the roughness significantly, but a considerable part of the smoothening achieved by the precalendering was retained after the water treatment. Water-induced roughening of the precalendered base paper was reduced by increasing the hydrophobicity of the base paper, but the reduction is small compared to the overall moisture-induced roughening. They couldn't observe any effects for uncalendered based paper.

CHAPTER 3: EXPERIMENTAL METHODOLOGY

This chapter describes the carboxymethylation of pulp fibers, the characterization of the produced and original pulps, and the measurements done on the coated and uncoated papers obtained from three pulps and on commercially available papers. Four different fiber types and seven different paper sheets are analyzed. Carboxymethylation was done on only one type of fibers, softwood kraft pulp. Three different carboxymethylated fibers were produced. The original softwood kraft pulps as well as the three different carboxymethylated pulps were used for handsheet making in addition to the **4** types of handsheets, **3** commercial sheets were studied, LWC, woodfree, and TMP.

3.1. Carboxymethylation of Cellulose Fibers

The most widely used method of introducing acidic groups into cellulose is carboxymethylation.

Carboxymethylation produces significant changes in the physical and chemical properties of fibers depending upon the degree of substitution. The aim of the carboxymethylation is to investigate the swelling of cellulosic fibers having different carboxyl contents.

3.1.1. Experimental Procedure

Carboxymethylation in a mixture of isopropanol/water was carried out similarly to the procedures described by Klemm ***et. al*** **(1998)** and by Heinze ***et. al.*** (1**994).**

Materials Used

A bleached softwood kraft pulp used in laboratory experiments was in the form of finely distributed pieces of air dried pulp, and as 20% consistency pulp.

Monochloroacetic acid (MCA), sodium hydroxide, isopropyl alcohol, ethyl alcohol and acetic acid were used as reaction ingredients.

The reactor is a batch type, cylindrical glass reactor equipped with a stirrer, condenser, water bath, and temperature controlling system.

Procedure

Air-dried bleached softwood pulp was disintegrated isopropyl alcohol, and then filtered. The disintegrated pulp was subsequently vigorously stirred in 500 ml of isopropyl alcohol in the cylindrical glass batch reactor. While stirring 15% (w/w) aqueous sodium hydroxide was added dropwise during 15 min. at room temperature. After stirring another one hour, the glass reactor was placed in the water bath and allowed to equilibrate until the temperature inside the reactor reached 55°C. Monochloroacetic acid was then added during a 30 min. period while stirring vigorously. The mixture was stirred for another 2 h at 55°C, and then filtered. The product was washed four times with 70% aqueous ethanol, followed by two washes with distilled water, and then neutralized with weak acetic acid. The product was filtered after being washed.

Three carboxymethylations were performed and the experimental conditions are shown in Table 3.1. In order to estimate the reproducibility of the results we repeated each carboxymethylation two times.

Table 3.1: Experimental conditions for number of trials

REACTION PARAMETERS	Carboxymeth. #1 (Started with air dried pulp)	Carboxymeth. #2 (Started with air dried pulp)	Carboxymeth. #3 (Started with 20% consistency pulp)
NaOH Conct. (%)	15	15	15
Time (hr)	*2*	2	2
Temperature (°C)	*55*	*55*	*55*
Molar Ratio of MCA to NaOH	0.087	0.032	0.087
Molar Ratio of MCA to Pulp	0.154	0.057	0.154

3.1.2. Determination of Carboxyl Content

The carboxyl group content of pulp is determined by the conductometric titration method. The experimental procedure is similar to that used by Katz *et al.* (1984), and measures the conductance *of* a pulp suspension during titration. The conductance of a solution is the sum of the conductance of all the ions present (Scallan *et al.,* 1987).

Materials Used

Three carboxymethylated and original fully bleached softwood kraft pulp were examined. All pulps were washed in deionized water and were examined in a never-dried condition.

0.1 M hydrochloric acid, 0.001 M sodium chloride, and 0.1 M sodium hydroxide solution were used. The conductivity meter was a bench/portable type of VWR. **A** magnetic stirrer was used for stirring the suspension and a micro-burette for titration.

Procedure

The acidic groups in approximately 3 g O.D. of pulp were converted to their hydrogen form by soaking twice in 0.1M hydrochloric acid for 45 min and then washing with deionized water to a constant conductance. The pulp was drained and dispersed in 450 ml of 0.001 M sodium chloride. Titration was carried out with 0.1 M sodium hydroxide dispensed from a micro-burette while the suspension was stirred. The alkali was added at a rate of 0.5 ml every 5 min and the conductance measurement was recorded after the conductance reached equilibrium (Kartz ***et*** *al.,* 1984).

A Typical conductance versus titration volume of 0.1 M sodium hydroxide graph is shown in Figure 3.1.

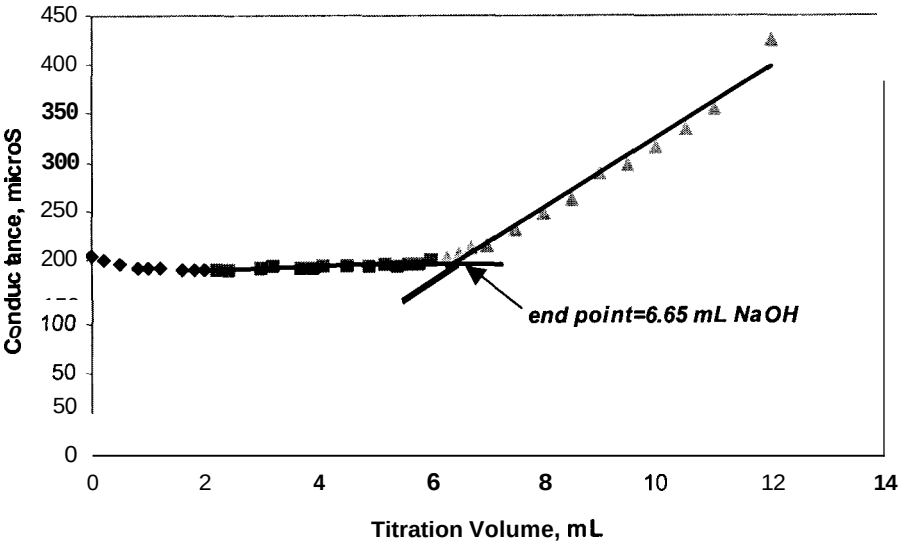

Figure 3.1: Sample conductance graph

Calculation of the Carboxyl Content

Using the titration endpoint (Figure 3.1.), the molarity of the sodium hydroxide, and the *dry* mass of the pulp, the mmol of carboxyl groups per kg of dry pulp is calculated by Equation 3.1.

$$\text{Amount of carboxyl groups}[\text{mmol/kg}] = \frac{\text{M x V x 1000}}{\text{m}} \qquad (3.1)$$

where M is the molarity of sodium hydroxide (moles/L), V is the endpoint volume of sodium hydroxide (mL), and m is the dry mass of the pulp (g).

Using the amount of carboxyl groups, the degree of substitution (DS) can be calculated from Equation 3.2.

$$\text{DS} = \frac{\mathbf{162C}}{1000 - (58\ \text{C})} \qquad (3.2)$$

where C is the amount of carboxyl group (mmol/g) that is calculated from Equation 3.1 (Klemm et *al.*, 1998).

The conductometric titration curves for all three carboxymethylated and original softwood kraft pulp are shown in Figure 3.2.

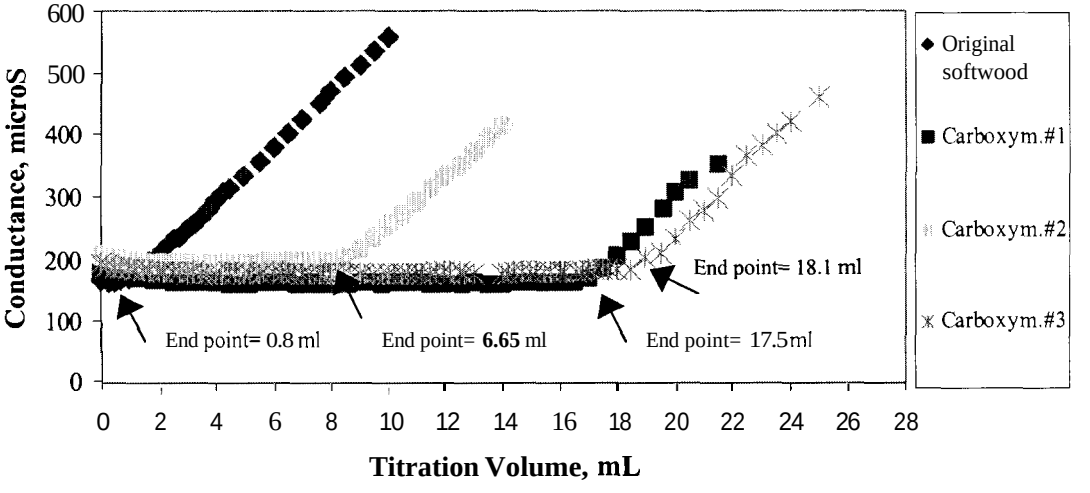

Figure 3.2: Conductometric titration curves

The carboxyl group content and DS for the carboxymethylated and the original softwood kraft pulp are shown in Table 3.2. For the listed DS of the carboxymethylated pulps, the amount of carboxyl groups in softwood pulp was subtracted from that of the carboxymethylated pulps.

Table 3.2: Amount of carboxyl groups and DS

SAMPLE	ORIGINAL SOFTWOOD PULP	Carboxymeth. #1 (Started with air dried pulp)	Carboxymeth. #2 (Started with air dried pulp)	Carboxymeth. #3 (Started with 20% consistency pulp)
Amount of Carboxyl Group (mmol/kg)	26.66	*583.33*	280	603
Degree of Substitution (DS)	0.0043	0.094	0.04	0.096

3.2. Fiber Characterization Tests

The fiber properties, which were measured, are fiber length and water retention value (WRV). The fiber length is measured by the Kajaani Fiber Length Analyzer. The water retention value, which is the dynamic water uptake behavior of the surface fibers, is measured by the centrifugation method.

3.2.1. Fiber Types

Three major categories of pulp were used for the study.

1) Bleached softwood kraft pulp; with the original softwood and the carboxymethylated pulps: #1, #2 and *#3*.

2) Bleached hardwood kraft pulp; in the form of light weight coated (LWC), which is mostly hardwood, and Woodfree pulp.

3) Thermo Mechanical Pulp (TMP).

3.2.2. Fiber Length Analysis

Pulp and paper made from wood consist of fibers and fiber fragments. The length distribution of different fibers in the pulp can contribute to various properties of the final product. Fiber length is a fundamental property of pulp. The fiber length of the pulp samples was determined with the Kajaani FS-100 Optical Fiber Length Analyzer. The measurement method is based on the ability of the fibers to change the direction of light polarization.

The Kajaani FS-100 consists of a measuring unit, a microprocessor-based control unit, a keyboard with alphanumeric display, and a printer and plotter for reporting. The length-measuring unit consists of a glass capillary tube through which fibers pass as a 0.01 % diluted suspension. One side of the capillary tube is a light source; a light-detecting element is on the other side. A magnetic stirrer is used to disperse the wet pulp samples. About 50 ml of the dilute sample are poured into the analyzer funnel. The counting begins by pressing the start key on the keyboard (Piirainen, R, 1985)

Triplicate samples are run. A minimum of 2000 fibers are counted to get a good result. When the counting finishes, the analyzer gives three kinds of reports. The first is a frequency table, the second one is weighted distribution, which gives the percentage of fibers by length in each class as a percentage of the total length of fibers, and the last one is a population distribution which describes the amount of fibers in a certain fiber class as a percentage of the total amount of fibers. This process also gives three kinds of average fiber length. The first one is the arithmetic average fiber length (L_N, mm). This is calculated from the number of measured fibers (n_i) in different length fractions (i=the

total number of fraction) and from the average length of the fraction (l_i) (Equation 3.3) (TAPPI Test Methods, 1992-93b, and Kajaani FS-100 Lab Manual, 2000)

$$L_N = \frac{\sum_i (n_i l_i)}{\sum_i (n_i)} \tag{3.3}$$

The second length is the length-weighted average fiber length (L_L, mm). The arithmetic average fiber length is not always the most meaningful indicator of the fiber length because the effect of short fibers is emphasized. The length-weighted average length is calculated according to the Equation 3.4.

$$L_L = \frac{\sum (n_i l_i^2)}{\sum (n_i l_i)} \tag{3.4}$$

The third length is mass-weighted average length (L_M, mm). This is calculated from Equation 3.5.

$$L_M = \frac{\sum (n_i l_i^3)}{\sum (n_i l_i^2)} \tag{3.5}$$

3.2.3. Water Retention Value

Water retention value (WRV) is a measure of the amount of the water contained in the fiber wall of the pulp fibers. **A** higher swellability of the samples is characterized by a higher WRV.

The WRV test is performed using a centrifuge method. After disintegration of **2** o.d. grams of pulp sample, the pulp suspension is filtered through a tarred filter crucible under moderate vacuum. After that, the weight of crucibles with pulp was adjusted to a weight for the centrifuge (60g generally acceptable). The crucible is covered with parafilm and cotton pads to prevent breaking. The sample was then centrifuged at 900 G's for exactly 30 minutes. The centrifuge has free-swinging heads capable of producing 900 G's (this is equal to 2000 rpms). After centrifugation, the crucible is removed immediately and weighed to the nearest 0.001 grams and recorded. It was then placed in a drying oven at 105°C overnight and weighted again after drying.

Data were obtained on never dried samples and on samples dried at room temperature and rewetted with distilled water. The average of four replicates was calculated for of the each seven pulp types. The WRV is calculated according to Equation 3.6

$$\mathrm{WRV} = \frac{[\text{sample wt. after centrifuge} - \text{sample wt. after drying}]}{[\text{sample wt. after drying}]} \qquad (3.6)$$

where sample wt.(g) is the weight of the pulp sample by subtracting the weight of the crucible (Water Retention Value, Lab Manual, 2000).

Stock temperature, beginning pad moisture content, degree of packing of the moist pad, type of centrifuge and other factors may have an unknown influence on results.

The procedure can easily be adapted to other liquids for determining the so-called liquid retention value (LRV) (TAPPI Useful Methods, 1991).

3.3. Sheet Tests

The sheet properties, which were measured, are contact angle, liquid absorption time, air permeability, porosity, and roughness. Surface analysis and imaging were also performed using optical microscopy. The contact angle is measured by the drop test. The liquid absorption is evaluated by the Bristow Wheel test and using results from contact angle measurements. Pore sizes of the sheets are obtained by mercury porosimetry. The roughnesses of the sheets and the backside of the coatings are measured using the Stylus Profilometer and using the Laser Scanning Confocal Microscope (LSCM).

3.3.1. Sheet Used

Three commercial sheets LWC, Woodfree and TMP, the original softwood kraft pulp sheet, and the three experimental carboxymethylated sheets were tested. Table **3.3** is presents the basic properties of the sheets used for testing. The thickness was measured by TMI Micrometer (Caliper) and the void fraction of the base sheets were measured based on the cumulative volume (ml/g) taken up by Hg-porosimetry shown in Figure **4.23.**

Table 3.3: Basis weight, thickness and void fraction of the sheets tested

SAMPLE	Original Softwood	DS:0.04	DS:0.094	DS:0.096	LWC	Woodfree	TMP
Basis Weight (g/m^2)	71	71	71	70	40	80	45
Thickness (mm)	0.12	0.17	0.16	0.12	0.07	0.12	0.08
Void Fraction	0.61	0.72	0.71	0.61	0.62	0.56	0.61

3.3.2. Contact Angle and Time of Absorption

The contact angles are measured to determine the wettability of the various sheets. Water ethylene glycol, and silicon oil are used for the contact angle measurements. The drops are created with a 10 pl syringe. The drop volume is **4** pl. Drops are released from the syringe on the sheet samples. The entire process is recorded by a video camera and the time measured by a timer. Figure 3.3 shows the experimental set-up.

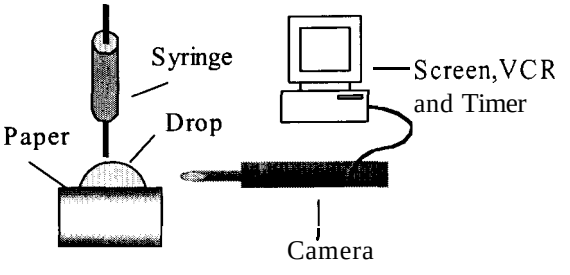

Figure 3.3: Experimental set-up for contact angle determination

The time is considered to be zero at the instant the drop impacts on the substrate. Contact angles are measured at time zero and after very short time intervals. The images were analyzed with Image Pro Plus, an image processing software.

The contact angle is determined by averaging the values obtained with 2 to **4** drops. The method consists of measuring the height and base of the drops directly from the image analysis software as shown in Figure **3.4.**

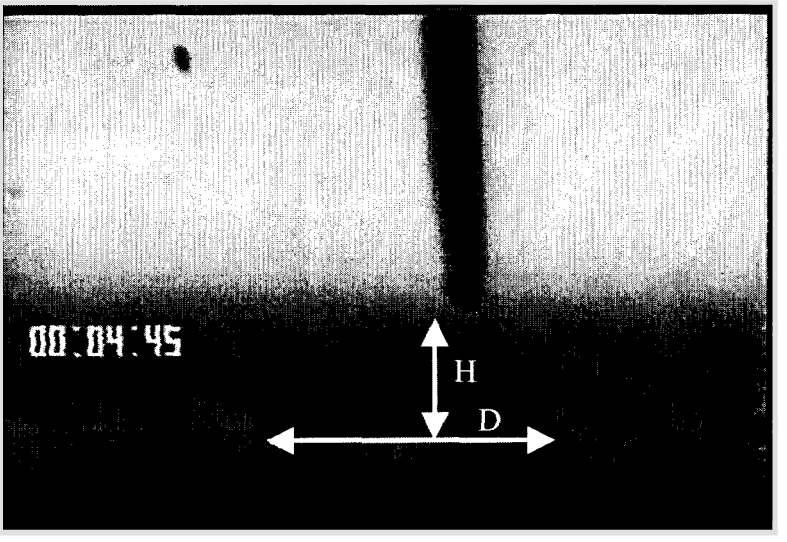

Figure 3.4: Measurement of contact angle

The contact angle is then calculated using Equation 3.7 (Wu, 1982).

$$\tan\left(\frac{\theta}{2}\right) = \frac{2H}{D} \qquad \textbf{(3.7)}$$

where H is the height of the drop and D is a diameter of a drop. The development of the contact angle with time is recorded and plotted.

Time of absorption is measured from the contact angle images as the difference in time when the drop first contacts with paper, and the time when the drop disappears completely. Three model fluids are used which are water, silicon oil, and ethylene glycol. These fluids are chosen because of their different physical properties shown in Table 3.4.

Table 3.4: Physical properties of model fluids

	(mPa.s)	(mN/m)
Water	1	72.8
Silicon Oil	5	35.8
Ethylene Glycol	26	48.4

3.3.3. Bristow Absorption

Liquid absorptivity of a paper during short times of contact with a liquid is evaluated with a socalled Bristow wheel. The instrument has an aluminum wheel, and can rotate at a fixed speed (cm/second). **A** rectangular strip of the sample sheet is attached *to* the wheel. **A** liquid holder placed above the wheel. The liquid holder has **a** slot, which is approximately 1 mm long and 0.5 mm wide. The rate of absorption can be calculated from the area of the liquid trace, the speed of the wheel, and the amount of the liquid used (Bristow, 1967 and Bristow, 1986). Figure 3.5 shows the apparatus.

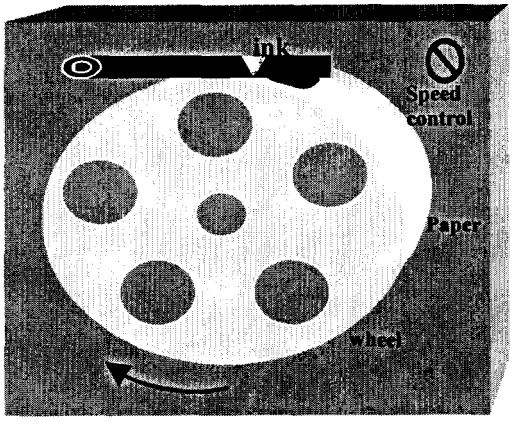

Figure 3.5: Simplified schematic of the Bristow Wheel apparatus

The length of the track is dependent on the surface roughness of the paper and its absorptivity, on the dimensions of the slot and speed of the wheel and on the volume and type of liquid used.

For the experiment, a 1% dye-based ink water solution is used. The liquid volume is fixed for all experiments, which is 10 μL. Three fixed speeds are used for each sample; 1, 3, 5 cm/second. The areas of the ink traces were measured by image processing software due to the non-rectangular shapes of the traces obtained. Three replicates were done for each sheet sample at the three different speeds.

3.3.4. Mercury Porosimetry

The pore size distribution is measured using mercury porosimetry. Mercury porosimetry uses the principle of pressurized capillary penetration by mercury to measure the pore size distribution of a substrate or powders. The instrument used is a Poresizer 9320 manufactured by Micromeritics. The pores shape is assumed to be cylindrical.

The poresizer has two built-in low pressure ports and one high pressure chamber. Data collection, data reduction, and data display are processed by the optional control module. (Poresizer 9320 Manual).

The method involves submerging a porous sheet in mercury and then applying pressure to the mercury (0 to 30,000 psia). When a sufficient pressure is reached, the mercury will enter the pores of the sheet. The size of the intruded pores is related to the pressure causing the intrusion and the volume of the intruded pores is the volume of mercury forced into them. If this process is continued over a range of pressures, the result is a distribution of the pore volume of the sheet with respect to its pores sizes, i.e., a pore size distribution (Winslow, 1969).

After finishing the data collection, the poresizer gives different types of data and curves. The data are cumulative intrusion, incremental intrusion, and differential intrusion, log differential intrusion, cumulative pore area, and incremental pore area. (Poresizer Manual).

From the pressure versus intrusion data, the volume and pore size distribution are generated using the Washburn equation, assuming cylindrical pores.

$$P = \frac{-2\sigma\cos\theta}{R_c} \qquad (3.8)$$

where P is the pressure causing the intrusion, R_c is the radius of the cylindrical pore being intruded, σ is the surface tension of mercury (485 dyne/cm), and θ is the contact angle between the mercury and the pore wall (130^0).

3.3.5. Air Permeability

The permeability of paper may be issue as an indicator of such variables as degree of beating, absorbency (penetration of water), etc. It is influenced by both the internal structure and the surface finishing. Internal structure is controlled by type and length of fiber, degree of hydration, orientation, and compaction.

The air permeability is the property of a sheet that allows the passage of air when pressure difference exists across the boundaries of sample. It is evaluated by obtaining the rate of flow of air through a sample under the experimental conditions (at 70° F and 29.92 in Hg).

Sheffield-type air permeability meter was used. It has Sheffield variable area type consisting of an air flowmeter gouge, a test head, calibration, and clean, dry air at a pressure of 413 to 413 kPa (60 to 125 psi) air flowmeter gouge is the float type, consisting of adjustable pressure regulator, floats in tapered glass columns, and a mercury manometer. The apparatus consists of an air supply, a pressure controller, a pressure measuring device, an air flow measuring device, and a test head assembly, with pneumatic device that clamps the sample between two orifice plates that determine the exposed test area. An air flowmeter have the capability to measure the range of flow of 0 to 400 cubic centimeters/minute.

lcm orifice diameter was used, and a total of 10 reading were done on each sheet (TAPPI Test Methods, 1992-93c).

Calculation of the permeability of the sheets the Darcy's Law was used which is a generalized relationship for flow in porous media. Permeability is the term used of the conductivity of the porous medium with respect to permeation by Newtonian fluid. It

shows the volumetric flow rate is a function of the flow area, elevation, fluid pressure and a proportionality constant. It may be stated in several different forms depending on the flow conditions.

The permeability is defined by Darcy's Law. In sufficiently slow, unidirectional, steady flow:

$$Q = \frac{\kappa A \Delta P}{\eta L} \tag{3.9}$$

where Q is a volumetric flow rate, **A** is the normal cross-sectional area of the sample, **AP** is the pressure gradient, κ is permeability (m^2) and η is the viscosity of the fluid and L the length of the sample in the macroscopic flow direction (Dullien, 1992). This equation is used for the airflow through the orifice. If we arrange the Equation 3.9 according to L, take the derivation with time, and place the Equation 2.8 for **AP,** the relationship would be shown below:

$$t, = \frac{L^2 \eta R_p}{\kappa 4 \cos\theta} \tag{3.10}$$

where t, is the time of absorption, R_p is radius of the pore, and θ is the initial contact angle.

3.3.6. Sheet Formation

A new method for formation characterization was used in which the nonuniformity of formation is partitioned into its components as a function scale of formation. This method

has been developed at McGill University, Canada. In this method, a Fourier transform-based power spectrum analysis partitions the intensity of the nonuniformity of the formation into its components as a function of the scale of formation. It is named that relation the Paper Formation Line. The range of scale of formation over which these components of formation are presently determined is from 0.6mm up to 97mm. For practical use it was found it generally sufficient to define the Paper Formation Line by grouping the complete spectrum of results into 10 components of formation, each components of formation providing a quantitave measure of the nonuniformity of formation at a specific value of scale of formation. This technology describes simply and quantitatively how the formation nonuniformity is distributed across the sheet. The measurements for all carboxymethylated sheets, original softwood sheet, LWC and woodfree were done in the Department of Chemical Engineering, Pulp and Paper Science Centre, McGill University, Montreal (Bernie et. al., 1999,2000).

3.3.7. Surface Roughness Measurements

The characterization of surface roughness of paper is important in many applications, especially printing. Describing the surface topography in measurable, quantitative terms is more difficult. Two common methods are used to characterize the surface texture in terms of roughness. The first one is the very common stylus profilometer method, and the second one is laser scanning confocal microscopy. The roughness measurements on LSCM were done in the Advanced Wood Chemistry Science Department, University of Maine.

3.3.7.1. Stylus Profilometer

The stylus profilometer is used to characterize the sheet surfaces on a macroscopic scale. The instrument used for the tests is an Alpha-Step 200 manufactured by Tencor Instruments. The instrument is a computerized step profiler with programmable X-Y stage, and a 9" video monitor, which plays a magnified view of the sample and stylus during the scan, as well as provides scan profiles and a summary of scan data. The system allows setting, and storing if desired, of a variety of scan parameters, such as scan direction, scan length/sampling rate and vertical units (KA vs pm). Measurement cursors are used for base line correction, to obtain a variety of data, and/or to zoom in on a particular section of a scan profile (Tencor Profilometer, Alpha Step 200 Manual). The technique uses a fine, cone-shaped diamond stylus tip of 12 μm which is applied onto the surface with a given load. Measurement of the vertical movement of the stylus occurs as the material is moved in the horizontal direction.

The available scan lengths are 80, 400, 2000 and 10000 pm, with scan times of 8 and 40 seconds. The highest resolution possible was 0.5nm with the upper limit of measurement being 320 pm, in the vertical direction. The horizontal resolution was 40 nm, with up to 2000 data points sampled on every scan. Stylus force is also controllable, which is the vertically applied force on the sample during measurement. A maximum of 25 mg is available with the Alpha-Step 200.

A scan length of 2000 μm, a scan time of 40 seconds, and a force of 8 mg are used for the measurements. The stylus is easily capable of etching a path on coated paper, and hence a low magnitude of force was used. A lower force entails the risk of the stylus losing contact with the sample during the scan.

The profilometer provides an analysis of four important surface characteristics, such as the average height, the difference between the highest and lowest points, the average roughness, and the cross-sectional area. The arithmetic average roughness (Ra) is determined using the graphical-centerline method. Figure 3.6 shows the principle of measurement;

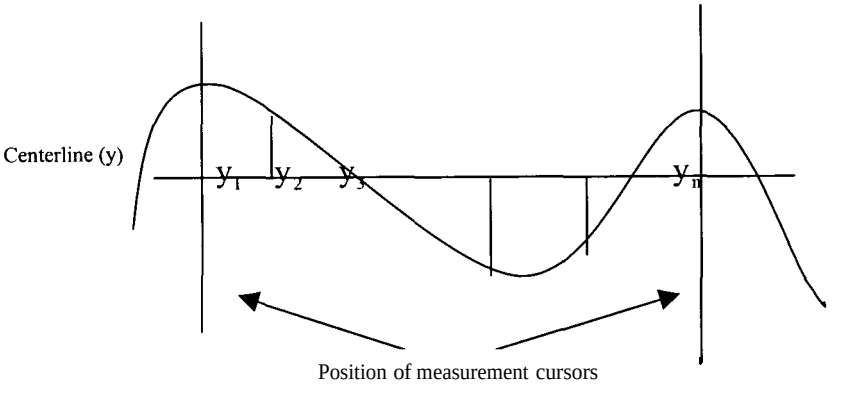

Figure 3.6: Measurement of roughness with the stylus profilometer (Tencor Profilometer, Alpha Step 200 Manual)

Ra is calculated as Equation 310.

$$Ra = \frac{\sum_{i=1}^{n} |y_i|}{n} \qquad (3.10)$$

where n is the number of points between the measurement cursors and the distances are measured from the centerline as shown in Figure 3.6 (Tencor Profilometer, Alpha Step 200 Manual).

Roughness calculation methods

A surface topography, described by height z over an x-y plane, requires a huge amount of information to completely describe it. Therefore, the complex profile information is converted into a single number, which is easy to understand and compare using standard mathematical operations.

The more commonly used roughness parameters are most easily introduced in terms of a one-dimensional profile/surface z(x). The average, mean, or expected value of z(x) over distance L, is defined **as** follows,

$$\bar{z} = \lim_{L\to\infty} \frac{1}{L}\int_0^L z(x)dx \tag{3.11}$$

The surface $z(x) = \bar{z}$ would be considered perfectly smooth. Roughness is defined in terms of deviations from the mean value. The arithmetic average roughness σ_a or R_a is given by equation 3.12.

$$\sigma_a = \lim_{L\to\infty} \frac{1}{L}\int_0^L \left|z(x) - \bar{z}\right| dx \tag{3.12}$$

Another surface-height average is the root-mean square (rms) roughness σ or R_q, which is also defined in terms of surface-height deviations from the mean surface.

$$\sigma = \{\lim_{L\to\infty} \frac{1}{L}\int_0^L [z(x) - \bar{z}]^2 dx\}^{1/2} \tag{3.13}$$

This definition depends upon the existence of the limit, as L approaches infinity, which is satisfied for real surfaces.

For real surfaces, the two representative surface heights, σ and σ_a are usually very similar.

3.3.7.2. Laser Scanning Confocal Microscopy (LCSM)

The laser scanning confocal microscope (LCSM) is a relatively new tool used in pulp and paper studies. In recent years, it has become increasingly evident that this new technique can provide answers in quantitative terms to several questions about the structure and functional properties of paper and fibers. It also is easy to prepare the samples and the LCSM produces crisp images with little effort. Compared to traditional microscopic methods, confocal imaging has an advantage when studying:

- Fiber-water and web-water interactions,
- Surface topography,
- Cross-sectional images without fiber destruction (Weise, 1997).

The basic principle of a confocal microscope is shown in Figure 3.7.

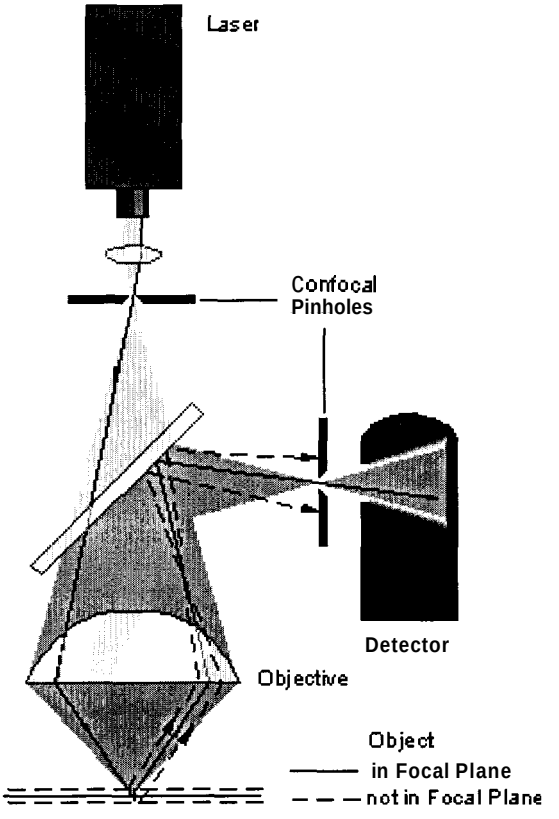

Figure 3.7: The basic principle of a confocal microscope (LEICA, 2000a)

The main elements of the LCSM are a laser which is a light source with almost ideal properties for confocal imaging, because of high degree of monocromaticity at high brightness and at small divergence, because of a high degree of spatial and temporal coherence; illumination pinhole which ensures a point-shaped light source; a scanner which can be performed by one or more galvanometer-driven mirrors or by opto-acoustic elements; and a detector which can be a photomultiplier tube (PMT) or a photo-diode and used to control the brightness of the image.

Confocal Imaging

In the confocal microscope all structures out of focus are suppressed at image formation. This is obtained by an arrangement of diaphragms which, at optically conjugated points of the path of rays, act as a point source and as a point detector respectively. Rays from out-of-focus are suppressed by the detection pinhole.

The depth of the focal plane is, besides the wavelength of light, determined in particular by the numerical aperture of the objective used and the diameter of the diaphragm. At a wider detection pinhole the confocal effect can be reduced. To obtain a full image , the image point is moved across the specimen by mirror scanners. The emitted/reflected light passing through the detector pinhole is transformed into electrical signals by a photomultiplier and displayed on a computer monitor screen.

One of advantages of the confocal microscopy technique is that it combines real 3D and spectroscopic imaging techniques. Optical sectioning provides the basis for confocal 3D imaging. An advantage of this technique is the reduction of the scanned probe volume and in particular the enhanced resolution. The recorded confocal data consist of sets of single planar images forming a volumetric stack. Compared to conventional light microscopy, the images contain more details. However, the problem is that human visual perception has difficulty in recognizing three-dimensional structures from sectioned data (Nickel *et al.*, 2000).

Roughness calculation methods

In LSCM, the roughness measurement function requires that a topographical image has been generated from a series of horizontal sections. The data set z (x,y) is first reduced by

means of the cumulation of identical height values. The result is a histogram with a number of data bars n(z) with identical height values Z which can be used for further evaluation.

The Table 3.5 summarizes the implemented algorithms (LEICA, 2000b):

Table 3.5: LSCM's implemented algorithms

LSCM Roughness	*LSCM Algorithms*
P_a ; Average peak-to-trough height The arithmetic mean of the weighted height values of all profile ordinates in the current work window, after filtering out of form deviation and major ripple components. The values are weighted according to their position in the data field within the range (-127,+127).	$P_a = (\frac{1}{x \cdot y}) \sum_{i=0}^{255} H(i) \cdot (i - 255)$
P_t, P_h, P_d; Maximum peak-to trough height Distance R_t between the level of the maximum peak R_h and valley R_d in the current work window. Valleys and peaks are specified as profile values H(i).	$P_h = \max [H(i)]$ $P_d = \min [H(i)]$ $P_t = P_h - P_d$
P_q ; Square average peak-to-trough height Square root of the arithmetic mean of the second power of the height values of the profile ordinates within the work window.	$P_q = \sqrt{\left(\frac{1}{x \cdot y}\right) \sum_{i=0}^{255} [H(i)]^2}$
S_k ; Bias of the amplitude distribution Unit for the asymmetry of the profile values H(i). The mean of the profile values in the work window is used for calculation.	$\bar{Z} = (\frac{1}{x \cdot y}) \sum_{i=0}^{255} H(i)$ $S_k = (\frac{1}{R_a^3})(\frac{1}{x \cdot y}) \sum_{i=0}^{255} [H(i) - \bar{Z}]^3$

Figure 3.8 shows the surface roughness analysis sample result from LSCM software.

a b

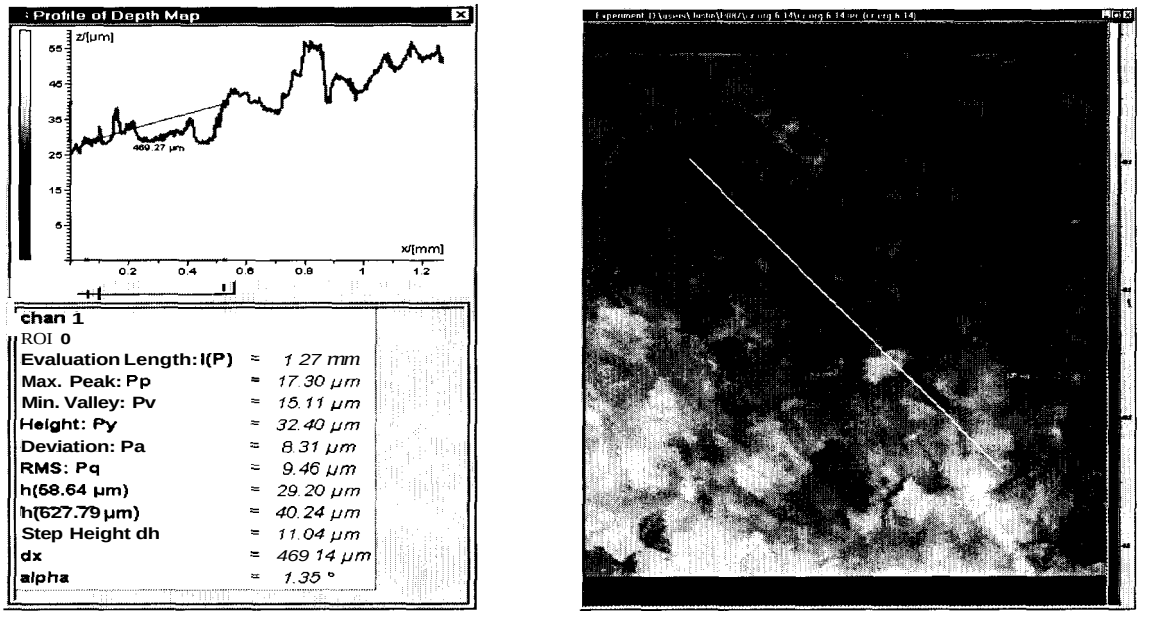

Figure 3.8: **A** sample surface roughness analysis a) statistics of results with profile of depth map b) topographical image with measuring area (sample line) form LSCM software

Statistical table gives the evaluation length which is the line that measurement is done along, deviation which is the surface roughness of the sample and other statistical numbers.

3.3.8. Surface Analysis Using The Standard Optical Microscope

The optical microscopes enable observation of submicron structures, determine their surfaces profiles, and observe selected cross sections of transparent materials without cutting the sample into thin slices. The Nikon Optiphot-2 optical microscope is used for

uncoated and coated paper surfaces, porosity and formation and roughness. Side lightening was used for the surface roughness images.

Principle of Operation

In this instrument, the sample is uniformly illuminated through the objective lens by a filament lamp or other bright incoherent light source such as a mercury vapor lamp. The objective lens forms a real inverted image of the object at the intermediate image plane of the microscope. The distance of the intermediate image plane from the back focal plane of the objective is called the *tube* ***length.***

This image is viewed through the eyepiece which provides additional magnification. The eyepiece forms a virtual image of the object at a comfortable viewing distance from the eye, normally 250 mm for a standard observer. With this arrangement, the total magnification is the product of the objective and eyepiece magnifications, so that high total values, up to 2000X, can be achieved in a small space. Several parameters are used to describe the performance of **an** optical microscope. Among these are the magnification (M) and the numerical aperture **(N.A.).**

The magnification determines the size of the image at the detector. For a simple lens the magnification in the transverse direction is given by the negative ratio of the image distance to the objective distance. Values of eyepiece magnification are 2.5- 10.0X. The magnification of the objective can vary from 1.5 to 200X.

The magnification, by itself, does not determine the resolution of the microscope. To determine the resolution, the numerical aperture of the objective, defined by the relationship as below,

$$\mathbf{N.A.} = n \sin 8, \qquad \textbf{(3.14)}$$

must also be known. In this equation n is the refractive index of the medium between the lens and the sample, and θ_0 is the half angle subtended by the lens at its focus. The larger the angle, the more light that can be collected; hence the numerical aperture is a measure of both the resolution and light gathering ability of the lens.

The simplified schematic of a standard optical microscope is shown in Figure 3.9 (Corle and Kino, 1996).

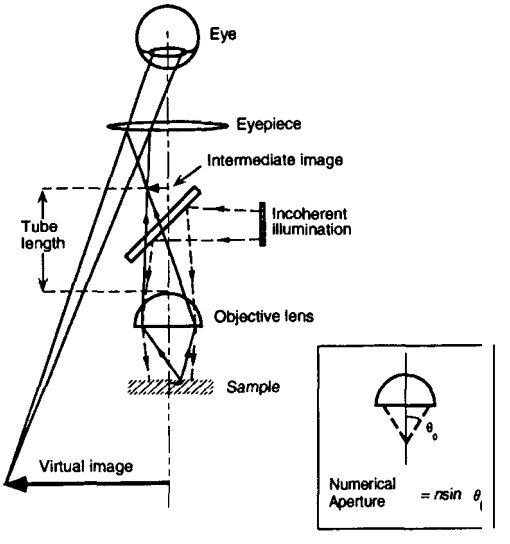

Figure 3.9: Simplified schematic of a standard optical microscope (Corle and Kino, 1996)

3.4. Coating Preparation Techniques

3.4.1. Coating Specifications and Application Methods

One experimental coating is used with no CMC and with CMC addition. The experimental coating ingredients are: kaolin clay (Covergloss, HUBER,

HBR110155171), styrene butadiene latex binder (DOW, CP 620NA) and CMC (HERCULES, 7L). The binder concentration is 10 parts per hundred (pph).

Preparation of Coating Dispersion

The coating colors were prepared in a conventional manner from dry pigment and dispersed pigment solutions. The clay pigment was received in dry form. A slurry was prepared at 60.89 % solids by weight; the pH was adjusted using NaOH.

Binder was subsequently added to the pigment suspensions to generate a range of pigment volume concentration (PVC) levels. The initial solids contents of the coating suspensions containing mineral pigments were adjusted to be between 60 to 65-weight.

CMC was first dissolved in **2** mL methyl alcohol, and the solution is added to water until a total weight of 100g. The mixture was well mixed for about half an hour. Then the CMC solution was added to the coating slurry and mixed.

Coating Application Methods

Experimental coatings were applied on the original softwood kraft paper; the three different DS value papers, LWC, Woodfree, and TMP samples.

Two different application methods were used. The first is a laboratory rod draw down coater. The second one is a blade high speed cylindrical laboratory coater (CLC-6000). The same speed and gap size was used for the two types of coating and all sheets on the drawn down coater. The CLC coater can coat at speeds up to 1905 m/min. The blade is manufactured by Pacific Hoe and Knife. The width of a coated sample is **140** mm for all speeds. **A** second coating can be applied, which is automatically shifted to the right by **2**

to 3 mm relative to the first coating. The CLC-6000 has 36 IR lamps, each 1kW controllable between 15% and 100% output for drying (CLC-6000,2001).

The experimental coating with CMC was applied with the CLC coater on softwood kraft pulp paper, DS:0.096 paper, LWC, woodfree, and TMP samples. The double coating method was used to coat the handsheets.

3.4.2. Dissolution of the Fibers from Coated Paper

In order to study the penetration of the coating in to the porous paper structure the pulp fibers were removed by a chemical and an enzymatic degradation method. Cupriethylenediamine (CED) was used in the chemical method.

3.4.2.1. Chemical Method

A solution of Cupriethylenediamine (CED) solution is commonly used for measuring the degree of cellulose degradation of pulp fibers by dissolving the pulp in the CED solution and subsequent measurement of viscosity of the dissolved fiber solution.

Before dissolution, a piece of backing tape is placed on the coated side of the coated paper sample to provide strength to the separated coating. The coated paper sample is soaked in CED and then shaken for 30-40 minutes. The fibers turn into a blue gel formation. Then the sample is removed, which can be removed from the coating by washing with water. The separated coating is then ready for analysis after drying (Dickson and LePoutre, 1997)

3.4.2.2. Enzymatic Method

The use of enzymes has the potential to reduce the need for strong chemicals. In enzymatic dissolution of paper fibers, Novozyme 342 (NOVO NORDISK, Novozymes) is used. Novozyme 342 is a special cellulase which operates optimally ~50C and pH of 7.0 while most other commercial cellulases tend to work best in acidic conditions. Novozyme 342 is commonly used in deinking of mixed office waste process. It was also used on this study to avoid dissolution of soluble components in the coating color.

Two types of experiments were done on the coated paper samples. In the first one, the undiluted enzyme is used. In the second experiment, the enzyme is mixed with a sodium phosphate buffer solution to maintain the desired pH.

In the first experiment the coated paper samples are obtained with a 1 hole paper puncher and incubated in 2 ml of Novozyme 342 enzyme. The temperature condition is met by placing the enzyme mixture in a 50C oven and using a rocking table to agitate the samples. Each sample incubates in a single well of a multiwell tissue culture dish. The incubation time was set at 24 hrs and the pH was - 5.5 throughout the course of the reaction. Following the digestion, the samples are washed in distilled and placed on glass microscope slides. They were allowed to dry before microscopic observation.

In the second experiment 1.5 mL Novozyme 342 (90 EGU/g), 1.5mL Sodium Phosphate buffer, pH 7.0 [39% NaH2PO4 (0.1 M) and 61% Na2HPO4 (0.1 M)] mixture were used to digestion. This 3 mL reaction mixture was incubated with a paper sample the size of a binder notebook hole punch in an isolated chamber. The reaction time was 48 hours. Following the digestion, the samples were washed in distilled and placed on glass microscope slides and were allowed to dry before observation.

CHAPTER 4: RESULTS AND DISCUSSION

4.1. Influence of WRV and Fiber Type on Base Sheet Properties

The influence of water retention value (WRV) and fiber type on basis sheet properties was investigated.

WRV is a measure of the amount of the water contained in the fiber wall of the pulp fibers. The measurement value is the remaining water content of the pulp after it has been subjected to centrifugation at 900G for 30 minutes to remove the inter-fiber moisture, but not the intra-fiber moisture of the water-swollen fibers.

Table 4.1 shows that for the never dried or as received samples the original bleached soft wood kraft pulp, LWC, Woodfree and DS:0.04 have about the same water retention value of 1.2 ± 0.1 (g/g). However, the two carboxymethylated pulp samples with a relatively high DS, i.e. DS:0.094 and DS:0.096, have a water retention value about two times higher than that of the original bleached softwood kraft. This shows that at a relatively high degree of carboxymethylation the swelling of the fiber wall of the softwood kraft pulp is significantly increased, in agreement with earlier findings by Nelson and Kalkipsakis (1964).

The "as received" TMP sample has a WRV value of 2.0 g/g, i.e. also significantly higher than the original softwood pulp and the two commercial sheets of LWC and Woodfree. The explanation for this behavior is that TMP is a mechanical pulp, and LWC and Woodfree are (almost) solely made from chemical pulp. In the latter two the fibers are mostly ribbon-like with the lumen collapsed. However, for many TMP fibers the lumen is

still uncollapsed, and many may still retain a significant amount of moisture after centrifugation in the WRV test method. Thus although the undelignified TMP fiber walls contain much less moisture when suspended in water than the kraft fibers (LWC and Woodfree are also (mostly) kraft fibers), the rigidity of the TMP fibers leads to the availability of unclasped lumen void space so that the WRV for TMP is larger than that of the chemical fibers. Therefore the WRV of TMP is mostly indicative of the moisture retained in the uncollapsed lumen void space rather than that of the fiber wall.

The water retention values after air drying and rewetting (WRV_2) are significantly smaller than those of never dried-samples (WRV_1). This is related to the irreversible collapse of pores during low temperature drying, i.e. when rewetted these pores do not open again due to strong bonding between the collapsed surfaces. This behavior is called hornification. It is known that the hornification is much more pronounced during air drying (at room temperature) than during high temperature on the papermachine. This effect of drying on the reduction of the WRV was also demonstrated by Racz and Borsa (1997). Since sheet properties are determined on handsheets which have been air-dried for the original samples and the carboxymethylated samples, the WRV_2 results in Table 4.1 are the appropriate values to be used when interpreting sheet properties and coating results. However for the commercial sheets which were used as received, the WRV_1 results for the "as received samples" are the relevant values to be used for data analysis.

Table 4.1: Water retention values for different samples

SAMPLE	WRV_1 (g water/ g dry pulp) (never-dried pulp or as received sample)	WRV_2 (g water/ g dry pulp) (air-dried and rewetted pulp)
Original	1.18	1.01
DS:0.04	1.1	1
DS:0.094	2.45	1.41
DS:0.096	2.26	1.96
LWC	1.2	1.19
Woodfree	1.3	1.12
TMP	2.02	1.22

Fiber length is an important parameter for describing the fiber type. The Kajaani Fiber Length Analyzer was used for these experiments. The results are shown in Table 4.2.

Table 4.2: Fiber length analysis results

SAMPLE	Arithmetic Average Length (mm)	Length-Weighted Average (mm)	Mass-Weighted Average (mm)
Original	1.15	1.99	2.59
DS:0.04	1.05	1.78	2.36
DS:0.094	1.03	1.72	2.19
DS:0.096	1.05	1.96	2.53
LWC	0.45	0.94	1.40
Woodfree	0.43	0.78	1.38
TMP	0.72	1.51	2.1

The length weighted average fiber length (LWAFL) of the carboxymethylated DS:0.096 pulp is the same as that of the original softwood kraft pulp. The LWAFL of the DS:0.04

and DS:0.094 is slightly shorter than that of the original pulp, possibly because of some fiber shortening/cutting when the air-dried original pulp was disintegrated by vigorous stirring before and during carboxymethylation. The Ds:0.096 pulp, on the other hand, was prepared by starting with an already disintegrated 20% consistency pulp (see Table **3.2).** These results show that the effect of the carboxymethylation treatment on the fiber length is small. The LWAFL of TMP is again smaller because of the contribution of fines and cut the softwood fibers. LWC and Woodfree have the smallest LWAFL because these sheets are (mostly) made of shorter hardwood kraft fibers.

4.1.1. Contact Angle

To determine the wettability of the base sheets, the contact angles of sessile drops of different liquids were measured. The theory of wetting and the measurement and calculation of the contact angles have discussed previously in the chapter 2. Drops of approximately 4 μL were deposited on the sheets from a syringe. Water, ethylene glycol, and silicon oil were used as fluids. Figure 4.1 presents the apparent contact angle results (ignoring the sheet surface roughness) for water during the initial wetting process.

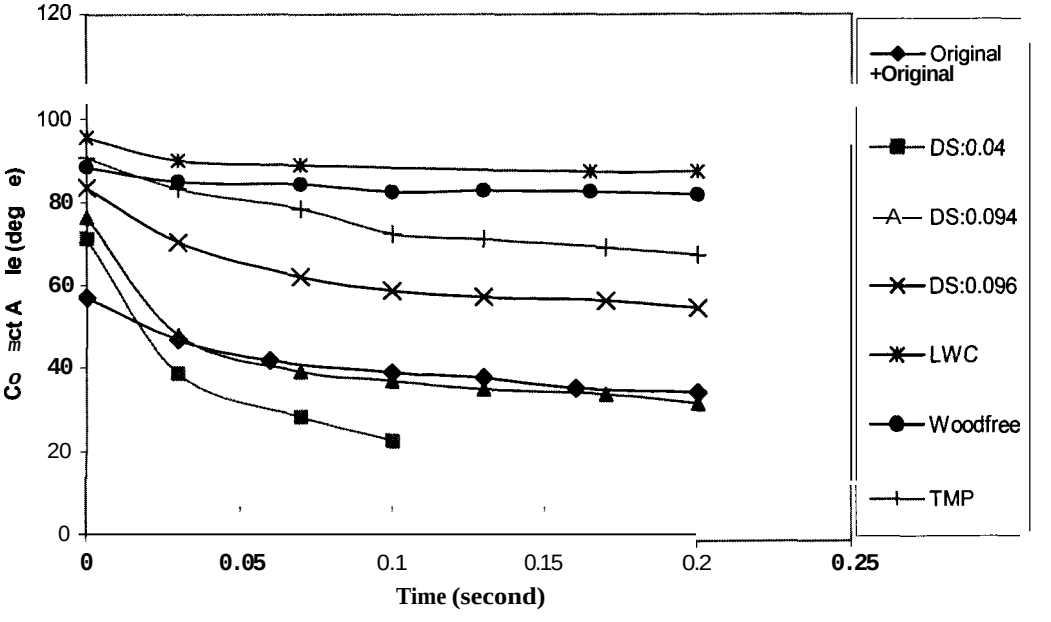

Figure 4.1: Contact angles versus time using water

From this figure, it can be seen that the initial contact angle of the carboxymethylated papers is about 20" bigger then that of the original softwood pulp. Although carboxymethylated sheet are thought to be more hydrophilic than the untreated softwood kraft pulp and three commercial sheets, but they are also more swellable than others. Therefore introduction of carboxymethyl groups makes the fiber structure more accessible to water and this may be responsible for the increase in the initial contact angle of the carboxymethylated fibers compared to that of the original sheet. The DS:0.04 and DS:0.094 pulps started with air-dried pulp and this may have affected the uniformity of the carboxymethylation throughout the fiber walls. The DS:0.04 sheet also feels softer then the other carboxymethylated and the original sheets. The DS:0.04 was produced by decreasing the amount of monochloroacetic acid charge. Thus the surface of the DS:0.04 and DS:0.094 may be more strongly carboxymethylated than the bulk of the fibers which

could explain the increase in the initial contact angle relative to the original sheet. However, this increase disappears at longer contact times, while this is not the case for the DS:0.096 handsheets.

The initial contact angle of the three commercial sheets, LWC, Woodfree and TMP, is about 30-40° higher than that of softwood bleached kraft. This may be caused by the presence/addition of surface active chemicals in the white water during papermaking which changes the surface energy of these sheets, and increases the wetting contact angle with water. Figure 4.2 shows some initial contact angle images of water.

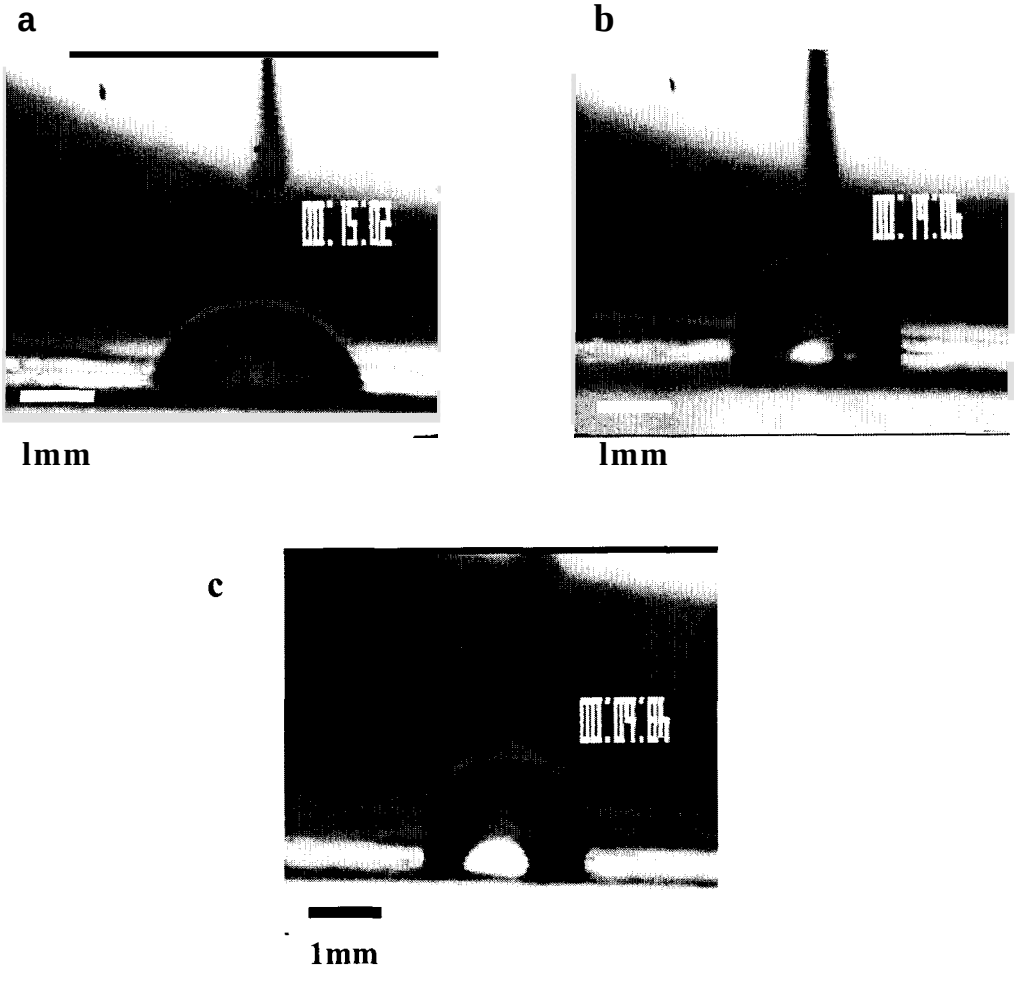

Figure 4.2: Initial contact angle images of water a) original softwood paper b)DS:0.096 and c)LWC paper

The contact angle results with 4μl ethylene glycol drops are shown in Figure **4.3.**

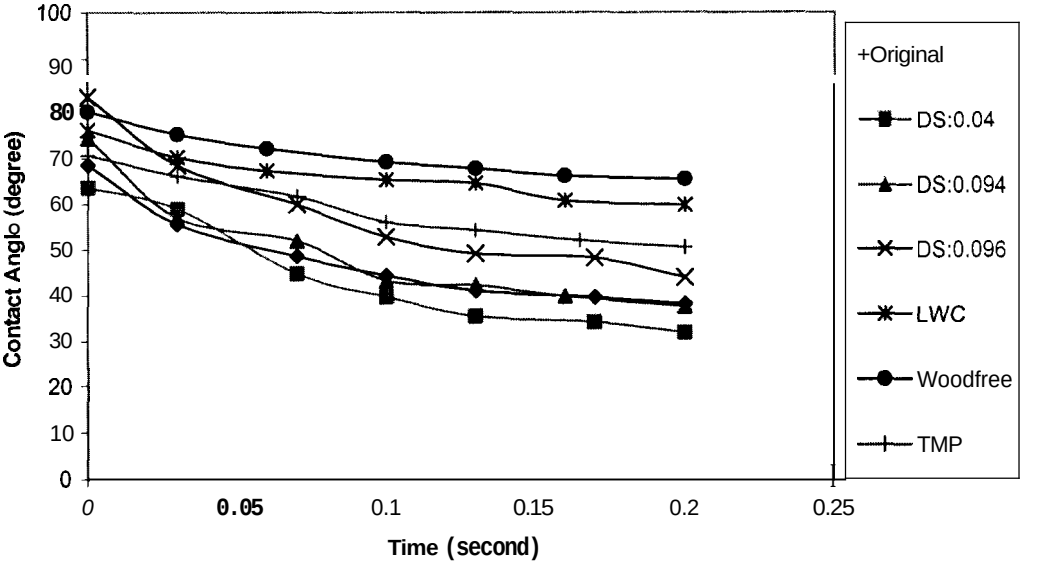

Figure 4.3: Contact angles versus time using ethylene glycol

It shows that the contact angle behavior over time with ethylene glycol for the original haft pulp and carboxymethylated pulps in generally similar to that obtained with water. However, the initial contact angle of the commercial sheets with ethylene glycol are somewhat is smaller than that with water. This is because of the lower surface tension and higher viscosity of ethylene glycol. And the wetting time is longer than when using water. For ethylene glycol, Woodfree has the biggest initial contact angle between the commercial sheets followed by, LWC, and TMP. DS:0.096 has the biggest initial contact angle followed by DS:0.094, original kraft pulp and DS:0.04. For the carboxymethylated pulps the contact angle decreases very rapid because ethylene glycol leads to less swelling of the fibers, so it penetrates the porous sheet structure more by bulk flow rather than by diffusion into the fibenvalls.

Water and ethylene glycol can enter into the fiber walls and at the same time penetrate into the pores between fibers. Silicon oil, on the other hand, only penetrates into the inter-fiber void space. Figure **4.4** represents the contact angle development using silicon oil as fluid.

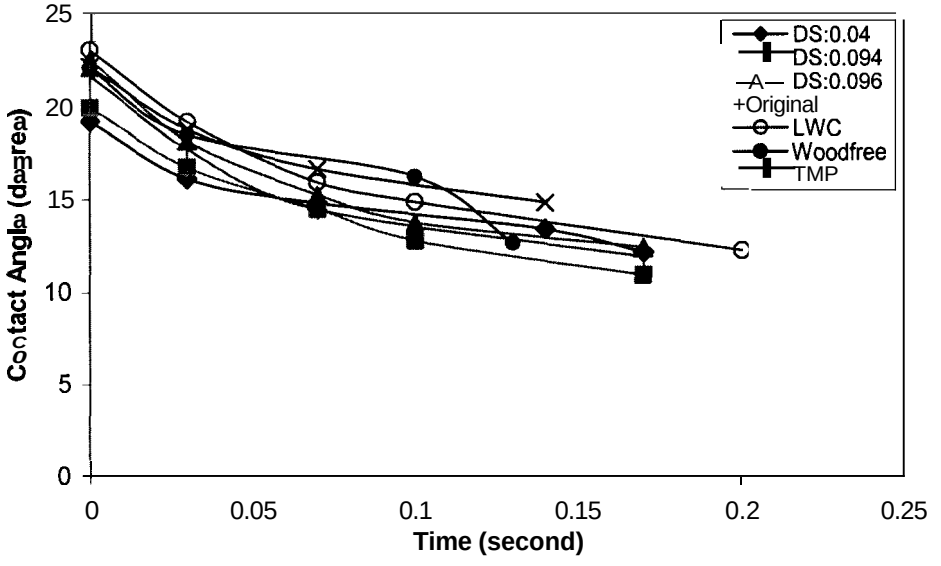

Figure 4.4: Contact angles versus time using silicon oil

It can be seen that for all types of papers the initial contact angles are much smaller than both water and ethylene glycol. It can be seen that there is not much difference between untreated and treated papers. The initial contact angle value varies between **23**" and 19º.

4.1.2. Time of Absorption and Bristow Absorption

Another value obtained from the contact angle image analysis technique is the time for complete absorption of a single drop. The results are reported in Figure **4.5** for water,

ethylene glycol and silicon oil. It can be seen that the absorption time is shorter for the paper made from the DS:0.04 and DS:0.094 carboxymethylated fibers compared to that of the original softwood haft pulp using ethylene glycol and silicon oil. On the other hand, time of water absorption of the DS:0.096 sheet is larger than that of the original softwood haft. The latter result may be interpreted that these uniformly carboxymethylated pulp fibers swell to such a degree that the pores are significantly dosed, so that the water penetrates slower into the pores. It can also be seen that the absorption time for the LWC, Woodfree, and TMP paper is much larger than that of the original bleached softwood haft fibers for water, ethylene glycol and silicon oil.

The absorption results obtained with the three different fluids do not show identical trends as can be seen in Figure 4.5 a, b and c.

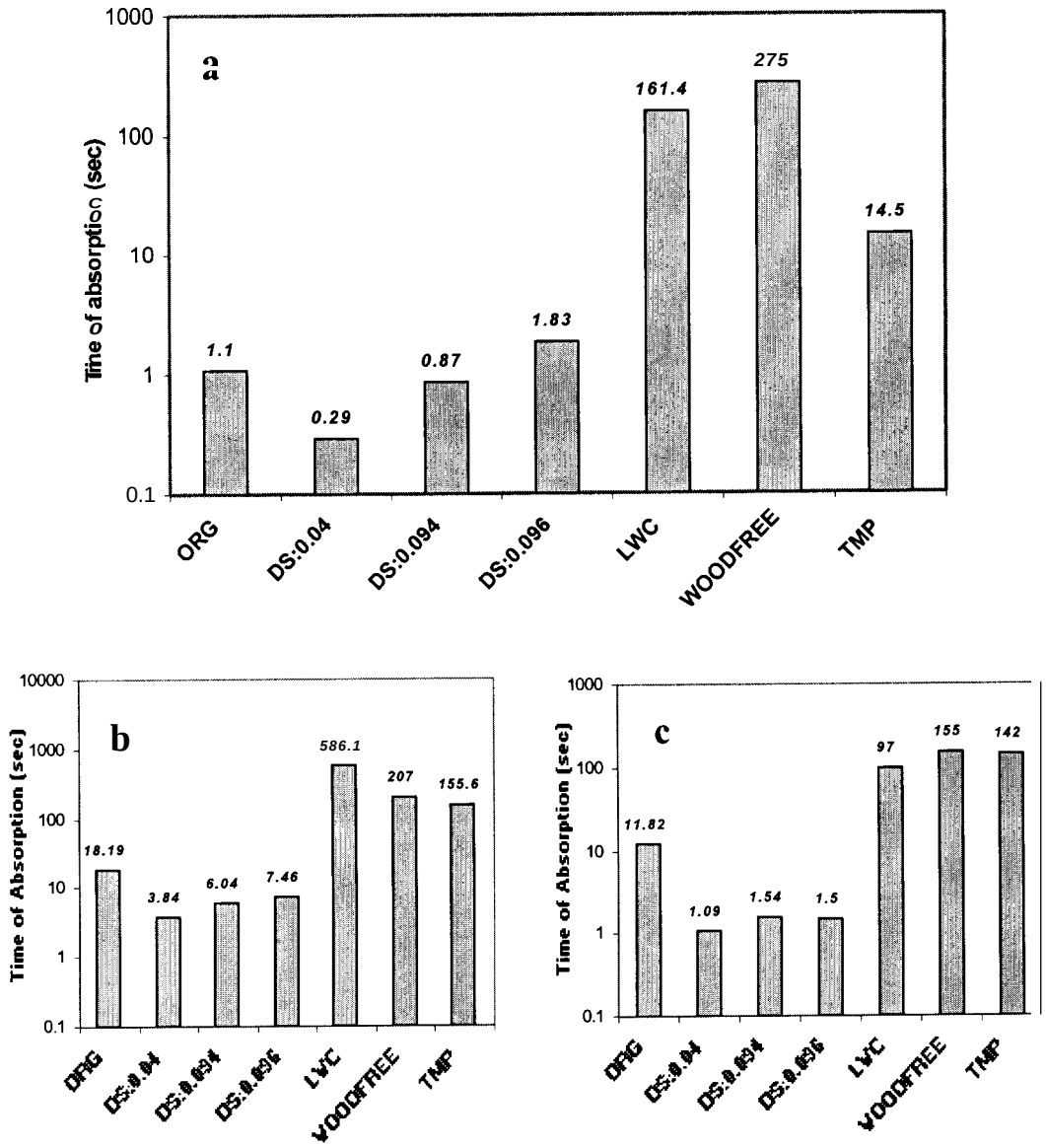

Figure 4.5: Comparison of time of absorption of paper samples for a) water, b) ethylene glycol, and c) silicon oil

These results indicate that water alters the pore structure of treated papers. It is not surprising that the more swellable fibers are able to take up more water and have a shorter absorption time than silicon oil, because silicon oil does not swell the fibers. Absorption times for ethylene glycol are the longest followed by silicon oil and water. Since silicon

oil and ethylene glycol have a lower surface tension and higher viscosity than that of water the water absorption time for all types of paper is much longer than the silicon oil and ethylene glycol absorption time. For water and silicon oil, woodfree has the longest absorption time followed by LWC for water and TMP for silicon oil but for ethylene glycol, this order changes. This could be due to a higher surface roughness of the sheets. The present results also agree with many other studies (Hoyland 1976) which have found that the wetting time increases with increasing viscosity.

Bristow Absorption

The test is performed on Bristow Wheel results are shown in Figure 4.6.

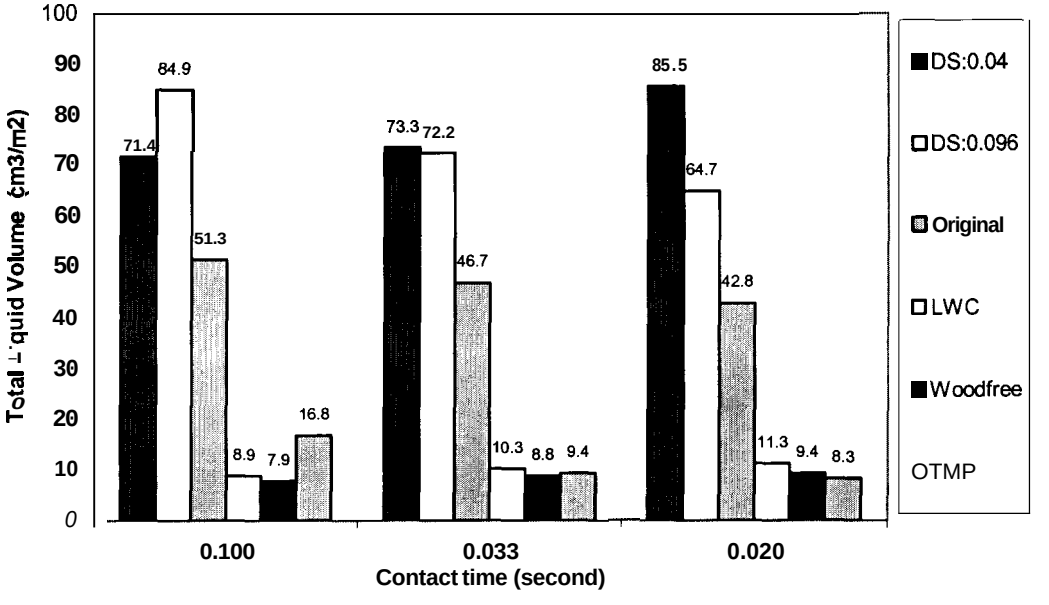

Figure 4.6: Total liquid volume versus contact time

It can be seen that the two sheets made from carboxymethylated fibers have a higher water uptake than the sheet made fi-om the untreated original softwood kraft. This is in agreement with the WRV of the different fibers. For DS:0.096, the volume taken up decreases with increasing contact time. This is the total disagreement with theoretical the Bristow curve which requires a linear increase in total liquid volume with the square root of time.

The explanation for the present behavior of the carboxymethylated sheets and the original sheet may be that for these highly absorbing papers the absorption process is nearly complete already at the shortest contact time.

There is not much difference between in the water uptake by LWC, woodfi-ee and TMP.

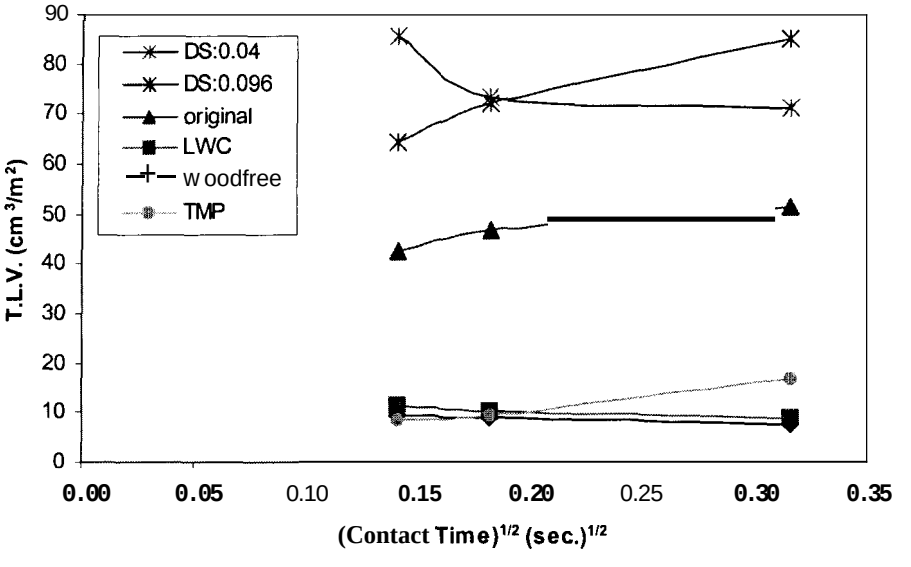

Figure 4.7: Bristow absorption curves with water

The explanation for the relatively low water uptake by these commercial sheets, and the independence of this value with the contact time is that the uptake rate is so slow for

these sheets that even at the largest contact time the water uptake is determines by the roughness of the sheets which is not too much different for these sheets.

4.1.3. Pore Structure

The pore structure of the base sheet is an important parameter for absorption and base sheet properties. The pore size and pore volume are measured by mercury porosimetry. The results of the mercury porosimetry tests are shown in Table 4.3.

Table 4.3: Intrusion data summary of mercury porosimetry

SAMPLE	**Total Intrusion (Pore) Volume, (mLHg/gpaper)**	**Total Pore Area, (m^2/g)**	**Peak in Pore Size Distribution (μm)**
Original	0.60	2.10	9.5
DS:0.04	1.1	1.62	20
DS:0.094	0.74	0.32	20
DS:0.096	0.71	1.23	20
LWC	0.61	4.95	2.95
Woodfree	0.59	3.88	4.05
TMP	0.74	4.18	4

It shows that three untreated papers, i.e. LWC, woodfree and the one made from the bleached softwood kraft fibers, all have also similar pore volume of about 0.6 ml/g paper The carboxymethylated papers and TMP have a higher pore volumes than these untreated papers. The results in Table 4.3 also show that the carboxymethylated fiber sheets have a larger dominant pore size than all the original pulp sheet, while the commercial sheets have the smallest dominant pore size.

The pore size distribution can be seen in Figure **4.8.** All paper samples show a narrow distribution. Dominant pore sizes being 8.5μm for original soft wood, **4pm** for wood free, **3.1μm** for TMP, 2.7μm for LWC, and **20μm** for all the carboxymethylated papers respectively. The large pore size of the carboxymethylated papers may partly explain their faster water uptake rate.

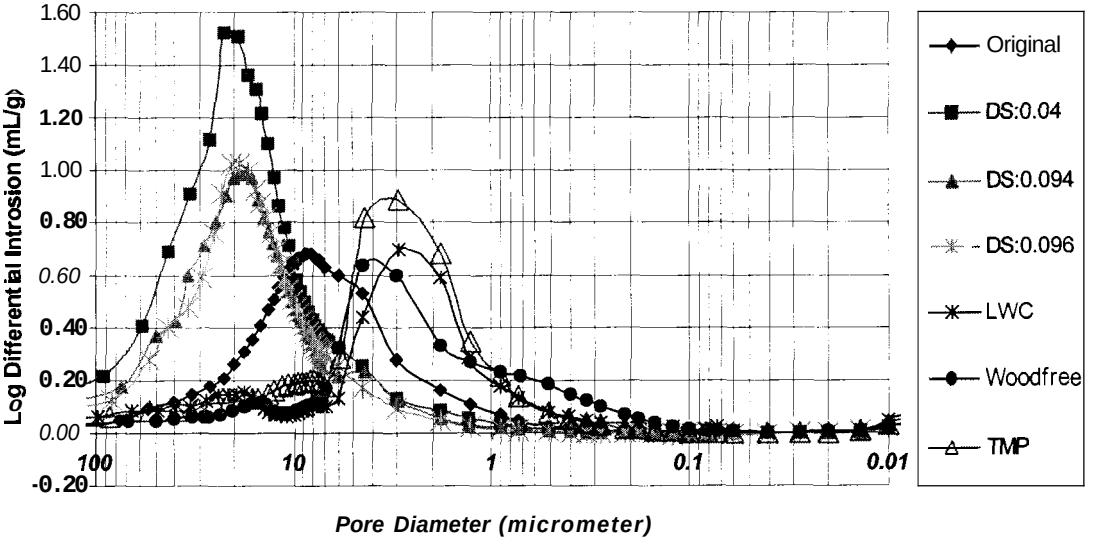

Figure 4.8: Pore size distribution

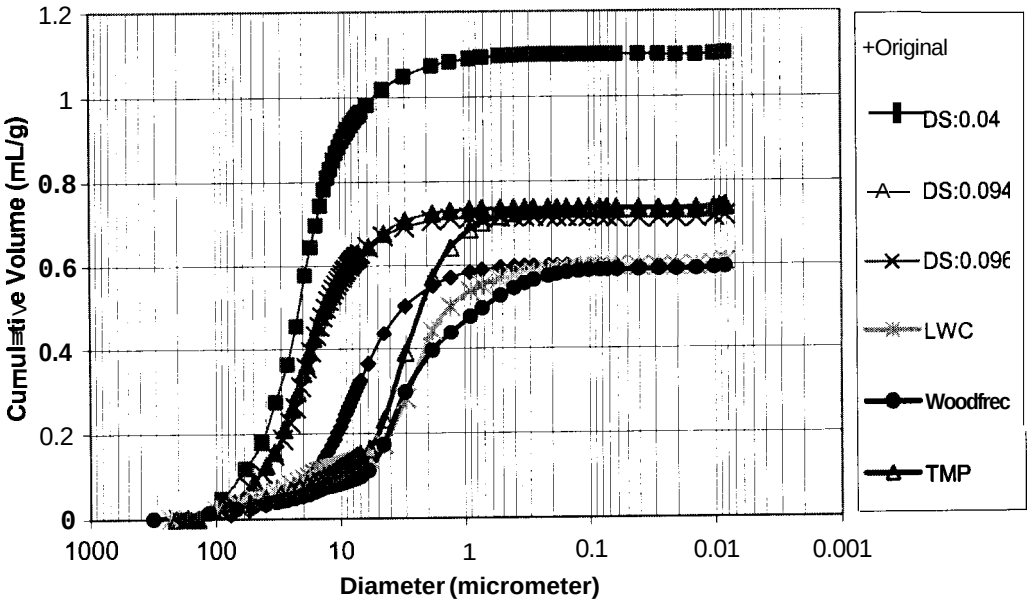

Figure 4.9: Cumulative volume

The cumulative pore volume graph is shown in Figure 4.9. It shows that DS:0.04 has the highest cumulative volume followed by TMP and the other two carboxymethylated fiber sheets. TMP has a higher pore volume than the other untreated papers because the mechanical fibers are stiff and lead to a more porous structure of the sheet.

4.1.4. Air Permeability

Air permeability results were used as an indicator of water absorbency. The air permeability results are shown in Table 4.4. The orifice diameter was 1cm.

Table 4.4: Air permeability results

SAMPLE	Original Softwood	DS:0.04	DS:0.094	DS:0.096	LWC	Woodfree	TMP
Air Permeability (cm^3/min)	269.1	**1600.6**	1563.5	1365.4	21.2	19.3	14.3
Permeability K (m^2)	$1.3x10^{-14}$	$1.1x10^{-13}$	$9.8x10^{-14}$	$6.4x10^{-14}$	$5.8x10^{-16}$	$9x10^{-16}$	$4.2x10^{-16}$

Using Equation 3.10, time for absorption water for original softwood sheet, DS:0.04, DS:0.094 and DS:0.096 and the ratio of time for original and time for treated sheets were calculated. These ratios were compared with the ratios from the time of absorption test results. The comparison is shown in Table 4.5.

Table 4.5: Comparison time of absorption ratio results

Ratio	$t_{org}/t_{DS:0.04}$	$t_{org}/t_{DS:0.094}$	$t_{org}/t_{DS:0.096}$
Calculated	1.93	1.01	0.28
Experimental	3.8	1.26	0.6

These results shows that the experimental ratios *are* higher than calculated from air permeability results for all the DS sheets except DS:0.096. This means that there is a slower absorption than expected. Because, all treated papers have higher porous and air

permeability values than the original paper. Calculated numbers are smaller but the experimental ratios are higher than 1. Calculated ratios should match with experimental if there is only capillary penetration. But if it is higher low then swelling must be change the results we would see treated samples faster water uptake rate.

4.1.5. Surface Roughness

The stylus profilometer is used to obtain roughness of the paper samples. The experiments were done on air-dried papers and wet papers (with water). Results are shown in Table 4.6.

Table 4.6: Roughness data from stylus profilometer

SAMPLE	DRY (μm)	WET (μm)	AFTER DRYING (μm)
Original	3.7	8.1	4.6
DS:0.04	5.8	14.2	10.3
DS:0.094	7.5	17.2	10.6
DS:0.096	3.6	15.7	7.6
LWC	3.9	6.4	4.7
Woodfree	3.3	9.3	**4.8**
TMP	3.9	10.1	6.0

DS:0.094 is the roughest followed by DS:0.04, LWC, TMP, original softwood, and woodfree. It can bee also seen that the untreated papers have similar roughness values. When the papers are being wet carboxymethylated papers have much higher roughness

values than the untreated ones. These results show that carboxymethylated paper fibers are more swellable and absorbent. **A** comparison between carboxymethylated papers shows that DS:0.04 has the lowest value fallowed by DS:0.096 and DS:0.094. When the papers are dried all untreated paper fiber roughness returns to near dry roughness but untreated papers are still much rougher then those untreated fibers.

Roughness measurements are done also by confocal microscopy. Table 4.7 represents the confocal microscope results as a comparison with stylus profilometer results.

Table 4.7: Comparison with Stylus and Confocal Microscope results

SAMPLE	**Stylus Profilometer (μm)**	**Confocal Microscope (μm)**
Original	3.7	4.6
DS:0.04	5.8	6.4
DS:0.094	7.5	4.6
DS:0.096	3.6	4.1
LWC	3.9	8.4
Woodfree	3.3	3.8
TMP	3.9	1.9

The roughness numbers are in the confocal somewhat similar to that seen in stylus results. The comparison between carboxymethylated papers, DS:0.04 is the roughest followed by DS:0.094 and DS:0.096. DS:0.094 and DS:0.096 have the same value as the original. For the commercial sheets, LWC is the roughest followed by Woodfree and TMP. TMP has relatively small roughness numbers than the other commercial sheets in

confocal microscope measurement, but for the stylus measurement, all commercial sheets have about the same roughness numbers.

4.1.6. Sheet Formation

Nikon Optiphot-2 optical microscopy is used to look at the papers surfaces, porosity and formation. Some pictures are shown in Figure 4.10, 4.11, and 4.12.

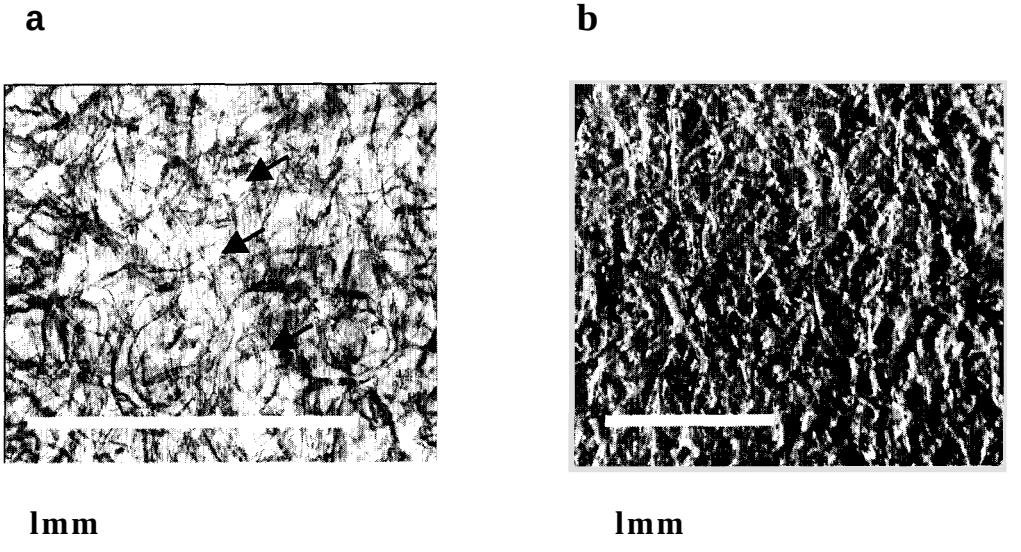

Figure 4.10: DS:0.04 sheet a) formation (10X) and b) surface roughness images (5X)

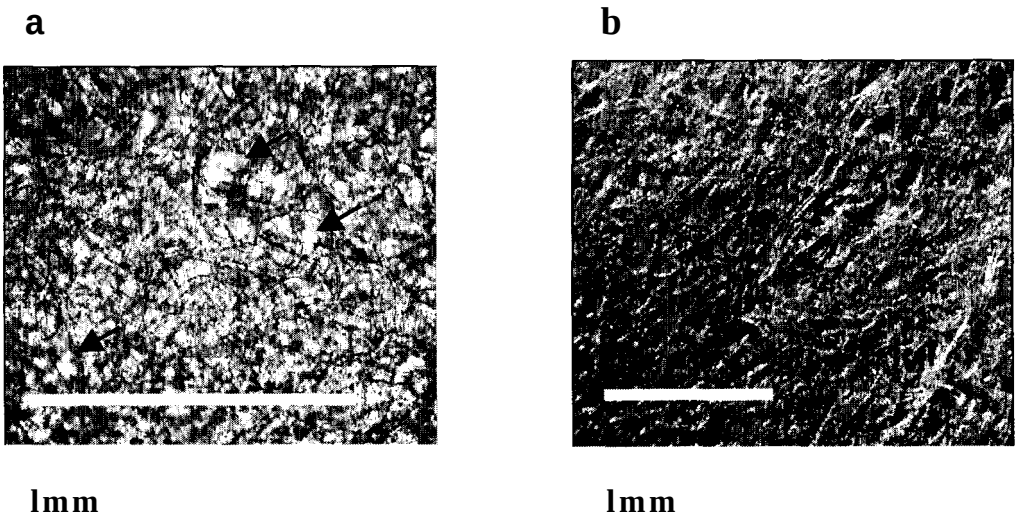

Figure 4.11: DS:0.096 sheet a) formation (10X) and b) surface roughness images (5X)

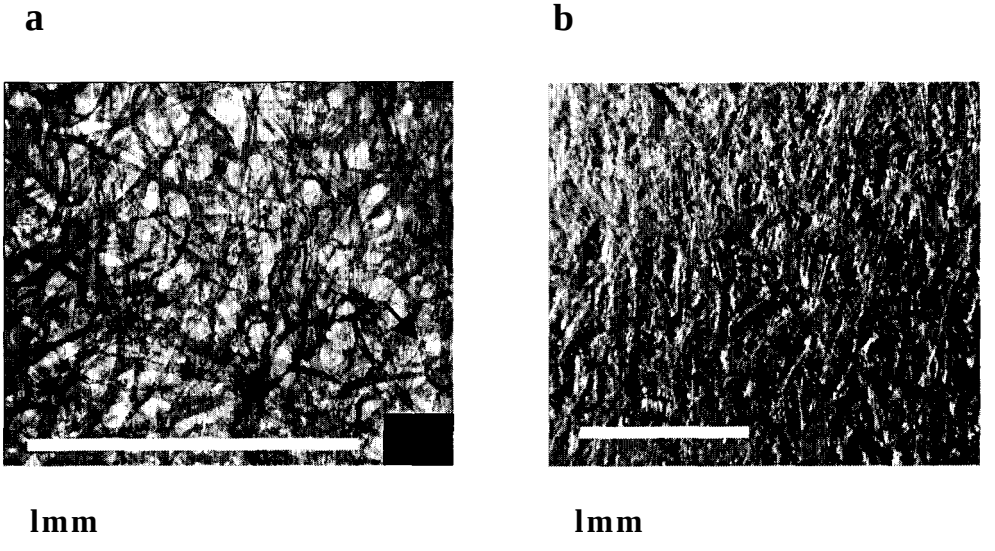

Figure 4.12: Original softwood kraft sheet a) formation (10X) and b) surface roughness (5X) images

From the surface images, carboxymethylated papers look rougher than the original one. Especially DS:0.04 which has a higher roughness value from Stylus then other carboxymethylated, original, and commercial sheets. This result is the same as the profilometer results. On the other hand, in the sheet formation images, there are some

bright areas. Which means that there are very tiny pinholes between fibers. This could be happened during air-drying stage of the handsheet making. The original paper has very few pinholes and less rough. It is also agrees with the mercury porosimetry test results for carboxymethylated sheets. They have very large pore diameter and volume, because of these very tiny pinholes.

Figure **4.13,** 14 and 15 presents the sheet formation and surface roughness of LWC, woodfree and TMP samples.

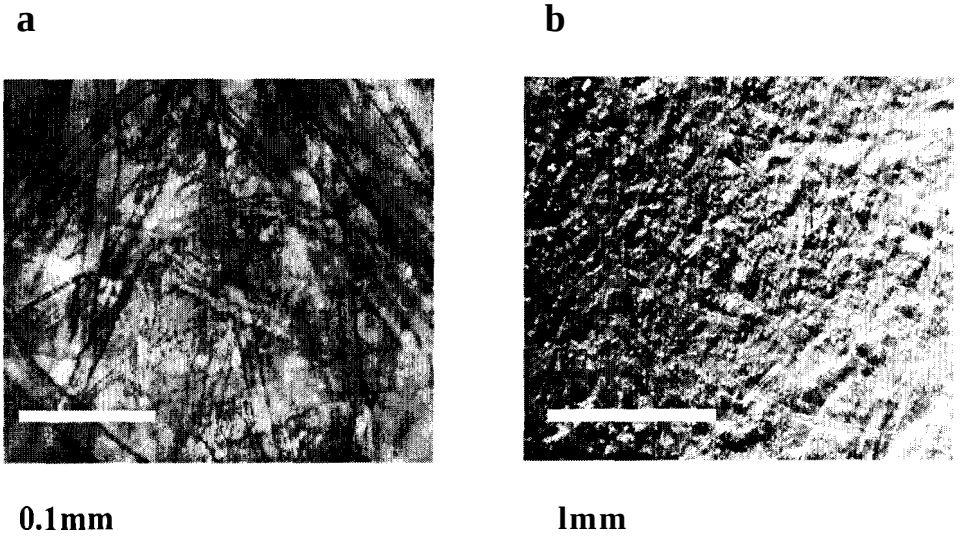

Figure 4.13: LWC sheet a) formation (40X) and b) surface roughness (5X) images

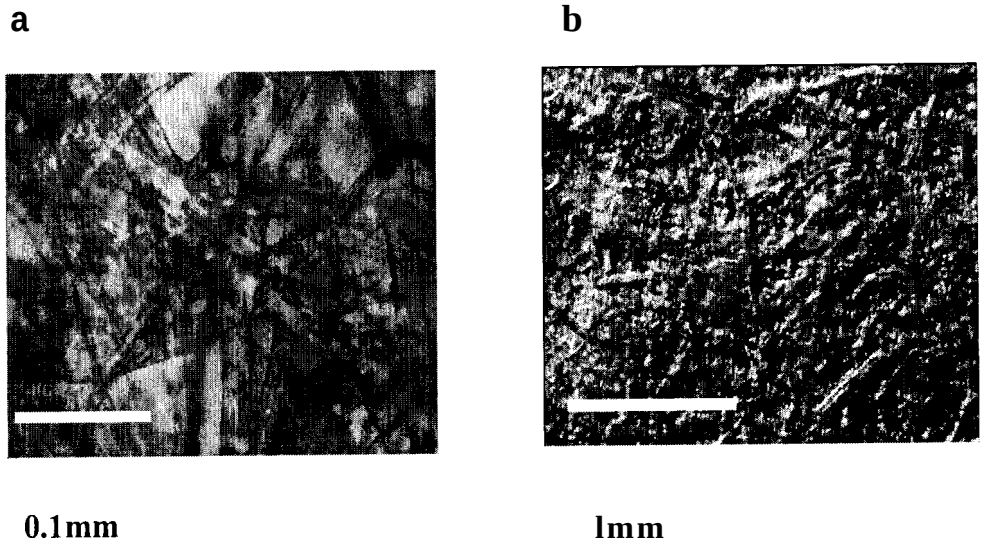

Figure 4.14: Woodfree sheet a) formation (40X) and b) surface roughness (5X) images

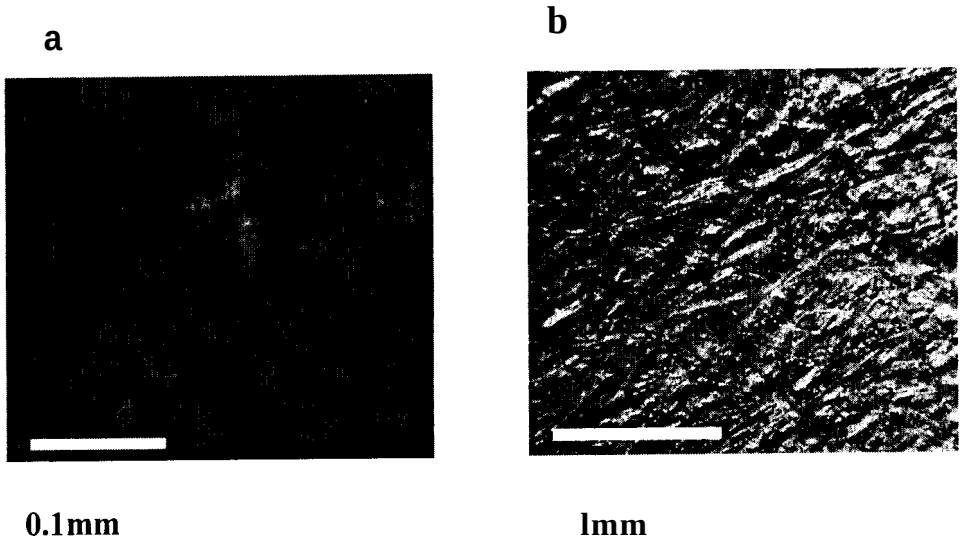

Figure 4.15: TMP sheet a) formation (40X) and b) surface roughness (5X) images

LWC, woodfree and TMP sheet roughness look the same. Therefore, it agrees with the roughness measurements. **A** fiber formation is similar because of the fiber length and surface chemicals.

Paper formation is also examined for all carboxymethylated sheets, original softwood sheet, LWC, and woodfree. Original paper used as a reference sheet. Figure **4.16** shows relative composite of sheet formation.

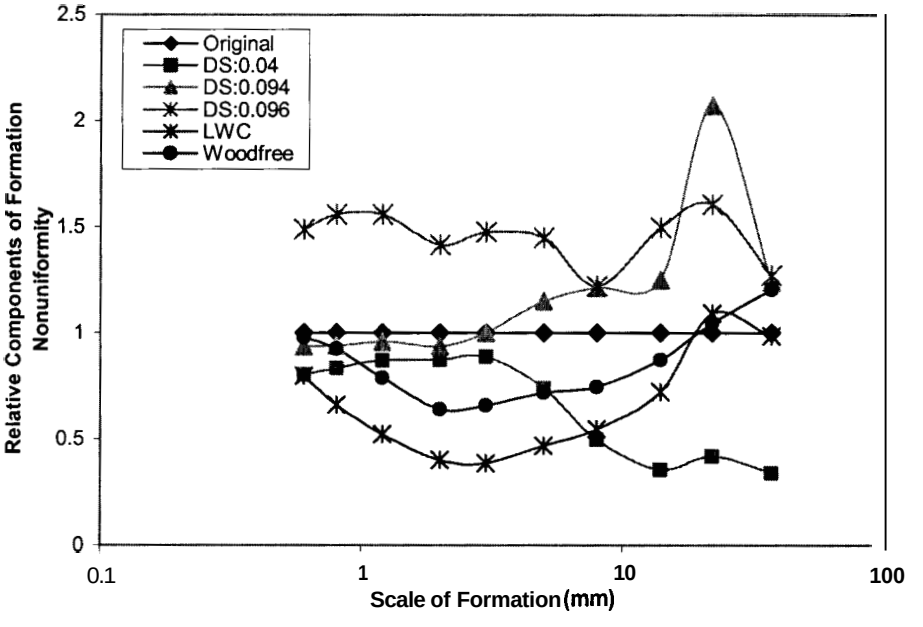

Figure 4.16: Relative paper formation lines, reference sheet original paper

With six sheets, five relative paper formation lines as the original sheet, being taken as the reference, becomes the line at **an** ordinate of 1. On the ordinate, 1.1 means 10% 'better' formation than the reference sheet (10% less in non-uniformity) at the specific scale of formation. ***An*** ordinate of 0.9 means 10% 'worse' formation.

It is seen that DS:0.096 has the best formation of the six sheets, about 50% better than the original sheet over the entire 0.6-37mm range of scale formation. DS:0.094 has 5-10% poorer formation over 0.6-2 mm scale of formation, then 10-20% better formation over 5-37mm scale. DS:0.04 is 10-15% worse formation over small scale of formation, 0.6-3mm, then gets distinctly worse for larger scale, over which it has the worst formation of the six sheet although this is not the case over the 0.6-3mm range scale.

LWC has the worst formation over 0.6-8mm range, but the 22-37mm scale it is right at the average formation of the all sheets. Woodfree has formation components mostly intermediate between the LWC and the original reference sheet. The formation components for these three sheets coverage over the 22-37mm scale of formation range. The pinhole doesn't affect the method. **A** pixel size about 0.25mm in the image grabbing step were used, so a pinhole is an order of magnitude smaller than that.

4.1.7. Summary of the Results

Table 4.8 presents a summary of the fiber and sheet properties studied in this part.

Table 4.8: A summary of fiber and sheet properties

SAMPLE	*Original*	*DS:0.04*	*DS:0.094*	*DS:0.096*	*LWC*	*Woodfree*	*TMP*
WRV_1 (g water/ g dry pulp) (never-dried pulp)	1.18	1.1	2.45	2.26	1.2	1.3	2.02
WRV_1 (g water/ g dry pulp) (never-dried pulp)	1.01	1	1.41	1.96	1.19	1.12	1.22
Arithmetic Average Length (mm)	1.15	1.05	1.03	1.05	0.45	0.43	0.72
Initial Contact Angle, Water (degrees)	57.05	71.27	76.41	83.49	95.66	88.43	90.76
Time of Absorption, Water (second)	1.1	0.29	0.87	1.83	161.4	275	14.5
Peak in Pore Size Distribution (μm)	9.5	20	20	20	2.95	4.05	4
Stylus Roughness (μm)	3.7	5.8	7.5	3.6	3.9	3.3	3.9
Confocal Roughness (pm)	4.1	6.4	4.6	4.1	8.4	3.8	1.9
Air Permeability (cm^2/min)	269.1	1600.6	1563.5	1365.4	21.2	19.3	14.3

4.2. Influence of WRV and Fiber Type on Coating Dive-in

After seeing the water retention, wet paper roughness and time of absorption results we wanted to see how these carboxymethylated fibers behave when the papers are coated. Do they really close the pores when they swell or not? To answer this question we had to look at the roughness of the paper side of the coating after dissolution of all paper fibers.

Two agents are used for dissolving the fibers, CED and Enzyme (NOVOZYME 342). The degradation methods were discussed in chapter 3.

4.2.1. Coating Back Surface Roughness

Kaolin clay and clay-latex-CMC coatings were used. Clay coating was applied by rod draw down coater, coating with CMC was applied both rod draw down coater and blade CLC. Coat weights for the carboxymethylated papers are higher than the original paper. This is expected because of the higher absorbency. The method using CED solution worked better than the enzyme. Therefore, results that are presented in Figure 4.17, 4.18 and 4.19 are obtained from CED method by using Stylus profilometer

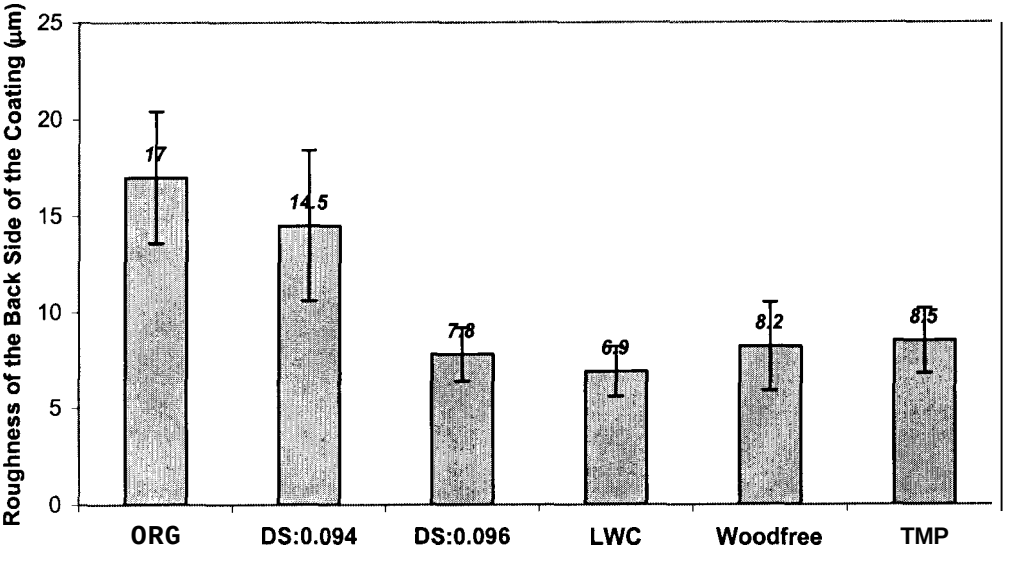

Figure 4.17: Backside of the clay coating applied by rod draw down coater

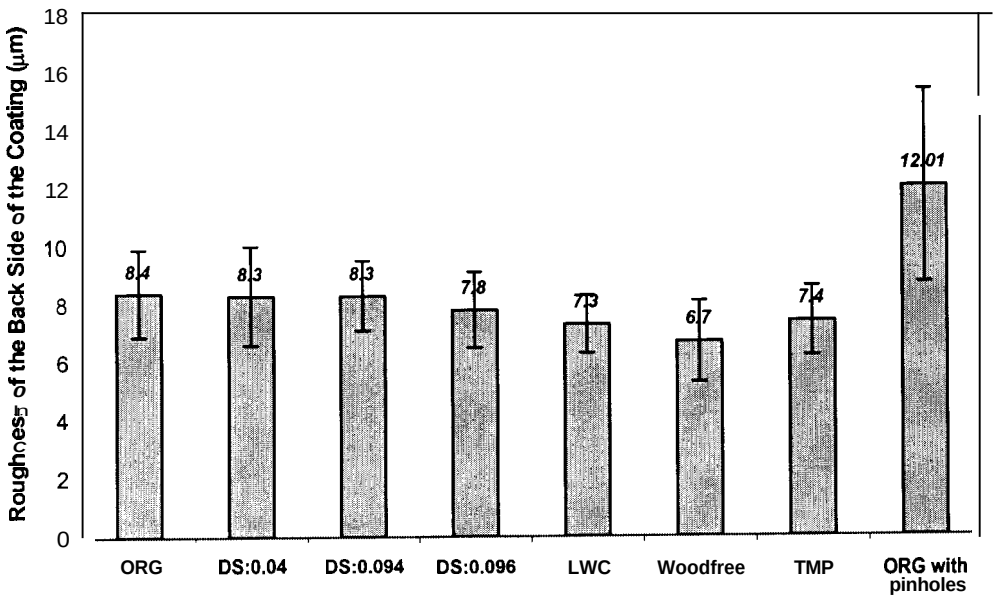

Figure 4.18: Backside of the clay-latex-CMC coating applied by rod draw down coater

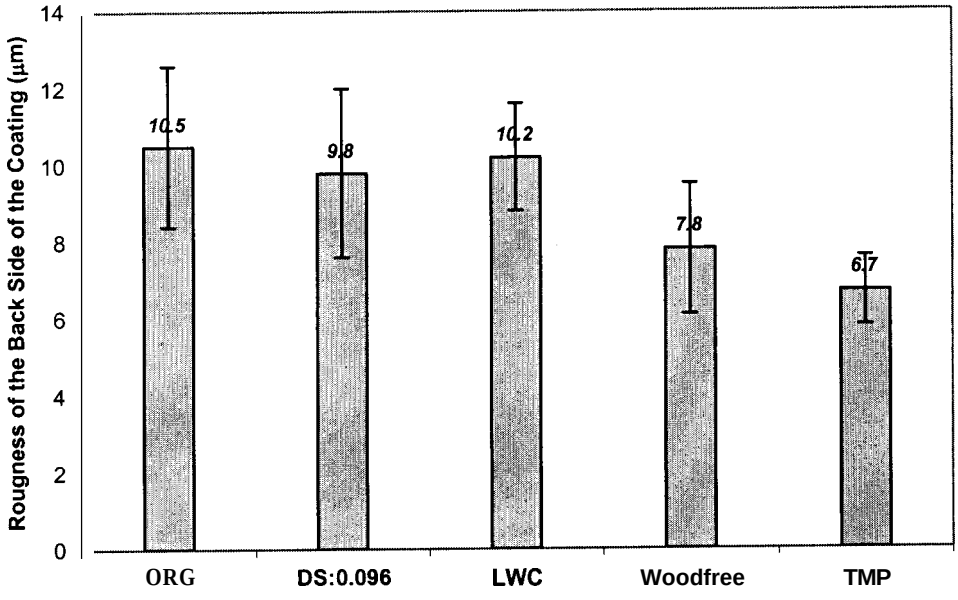

Figure 4.19: Backside of the clay-latex-CMC coating applied by blade CLC

Although the carboxymethylated papers have big pores and pinholes, they did not show a drastic difference in roughness of the backside of the coating. With clay coating on the rod draw down application, carboxymethylated sheets have smaller roughness than the original softwood haft paper. This result is important, especially in view of the larger roughness of the treated samples wet and after drying. CMC addition reduced this difference and decreased the roughness values. It is also seen that other untreated papers have the same values with clay and clay-latex-CMC system. CMC addition does not make any big change for them.

A pinhole has the potential to cause a large roughness if coating penetrates into the hole. To check if a pinhole can increase roughness and change penetration, we made some pinholes randomly on the original softwood haft sheet, coated it with the CMC coating and analyzed the backside roughness of the coating. The pinholes in the original did increase backside roughness as shown in Figure 4.18. Therefore, swelling and water uptake by the fibers in the treated pulps reduced coating penetration.

From Figure 4.19, it is seen that the roughness values are higher than the rod draw down application results. Blade pressure may push the coating into the pores and increase backside roughness. Comparing the two application method there is a correlation between pressure and coating penetration. In CLC application, TMP has the highest coat weight so it gave the lowest roughness and penetration. The carboxymethylated sheets have also high coat weight because of their water uptake rates.

As previously discussed Huang and LePoutre (1998), coating holdout and mass distribution was significantly poorer on all porous sheets on CLC application. LePoutre *et.al.* (1986)'s surface treatment (chapter 2) plugged some of the pores and reduce

pressure migration, provide a hydrophobic surface that would reduce capillary migration, and reinforce interfiber bonding at the surface to improve pick resistance. They examined the papers under the ESEM.

Figure **4.20** compares the dry and wet sheet roughness and backside of the coating roughness. For he original softwood paper, there is a flow into the sheet for clay coating. The CMC reduced this flow, but the blade pressure increases it.

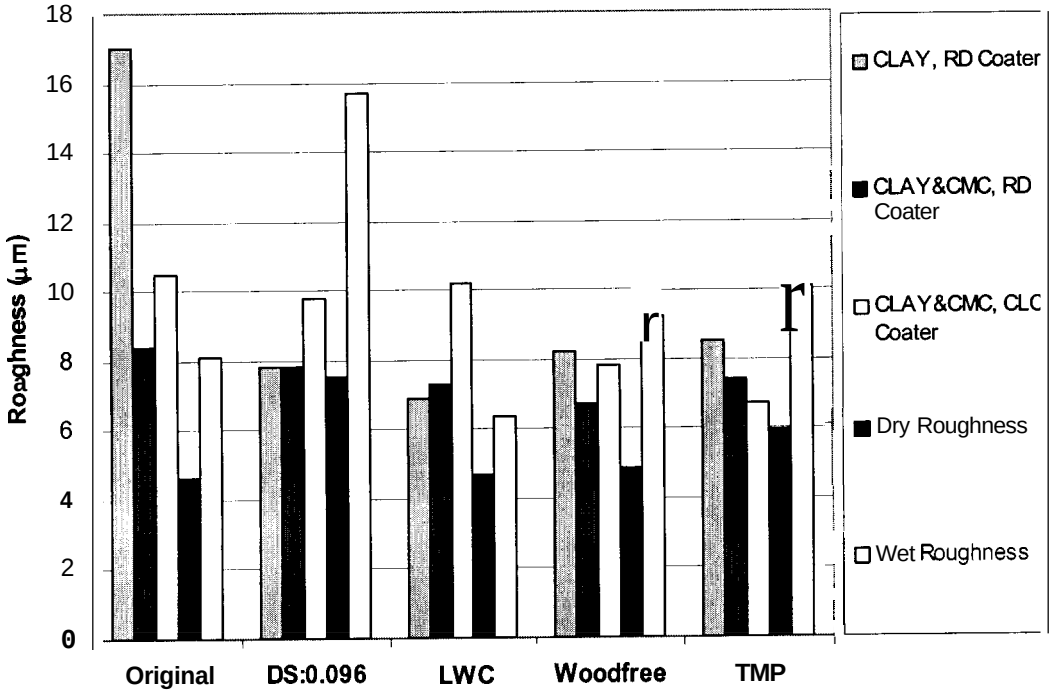

Figure 4.20: **A** comparison between dry and wet roughness of the sheets and backside of the coating

Wet sheet roughness is almost the same as the CMC coating roughness. In Paper DS:0.096, swelling slows down the inflow and CMC doesn't effect the roughness value. Wet sheet roughness is twice the coating back roughness. Therefore swelling is high.

There is some penetration in LWC paper, but the is noticeable higher roughness in CLC coated paper. The CMC affect the woodfree and TMP paper roughness.

Only kaolin clay applied by row draw down coater coated paper backside samples were examined on LSCM. Figure 4.2 1 shows the results taken from LSCM.

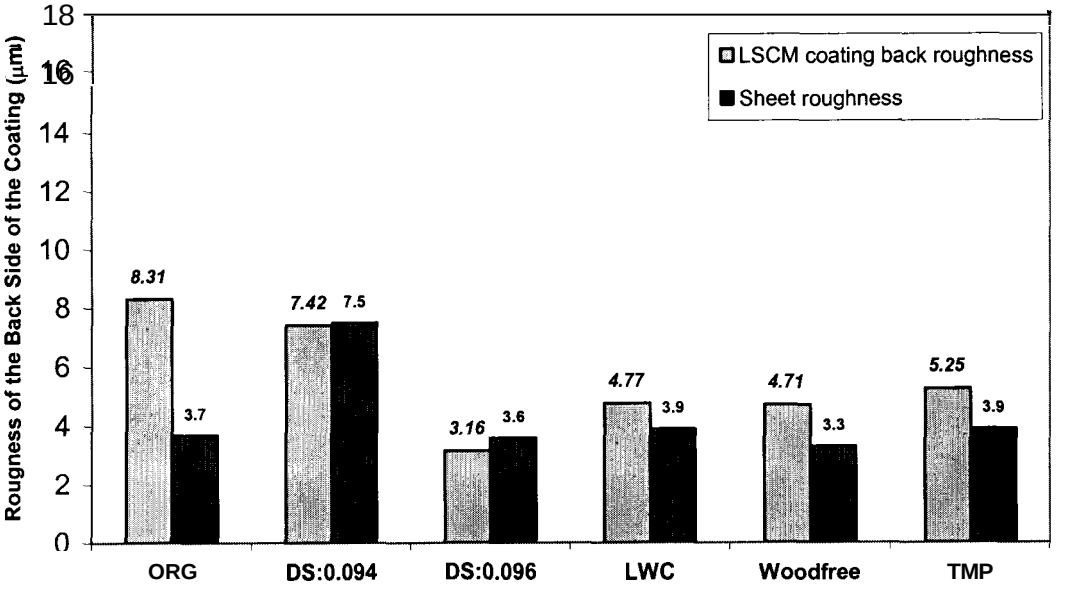

Figure 4.21: Comparison backside of the clay coating applied by rod draw down coater from LSCM with the sheet roughness

It can bee seen that there is significant coating penetration into the original softwood sheet comparing to the other commercial sheets. It is also higher than the carboxymethylated sheets. DS:0.096 has lowest number. Again, the swelling behavior of the treated pulps tend to reduce the backside roughness even though the presence of pinholes has the potential to increase the roughness.

Comparing the two types of roughness measurement method Figure **4.22** is presented.

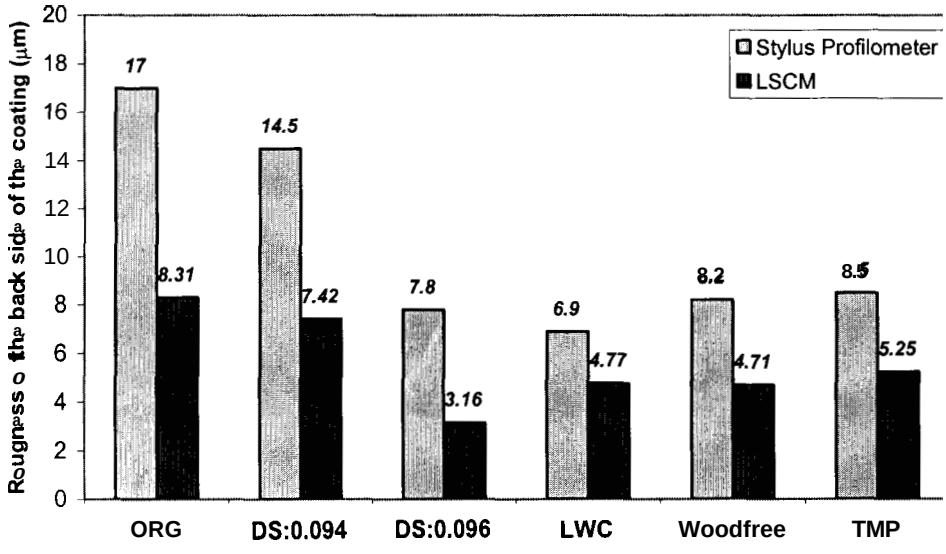

Figure 4.22: **A** comparison between the backside of the coating roughness observed by stylus profilometer and LSCM

The trend in the stylus profilometer roughness is the same as that seen in the LSCM results. Original softwood is the roughest followed by DS:0.094, TMP, Woodfree, LWC and DS:0.096. The carboxymethylated sheets seemed to show the higher inflow than the original sheet but these backside of roughness measurements show that carboxymethylation affected the swelling of the fibers and avoid the coating migration into the fiber pores.

4.2.2. Penetration of Coating

The results for backsides coating roughness indicate that fiber swelling slows down the coating penetration into the pores. Mercury porosimetry results give both base paper and coating pore size distribution and cumulative volume. The cumulative volume is based on

basis weight. For comparison with base sheet volume, it was normalized according to the base paper. Figure 4.23 shows pore diameter distribution and Figure **4.24** shows cumulative volume which is normalized according to the base paper pore volume.

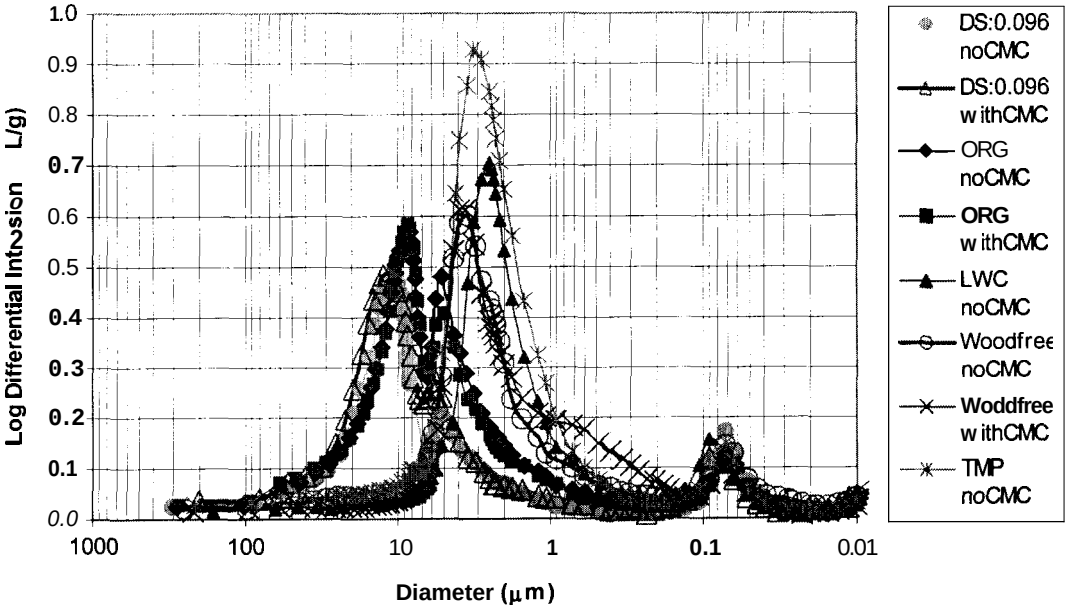

Figure 4.23: Pore size distribution of coated sheets

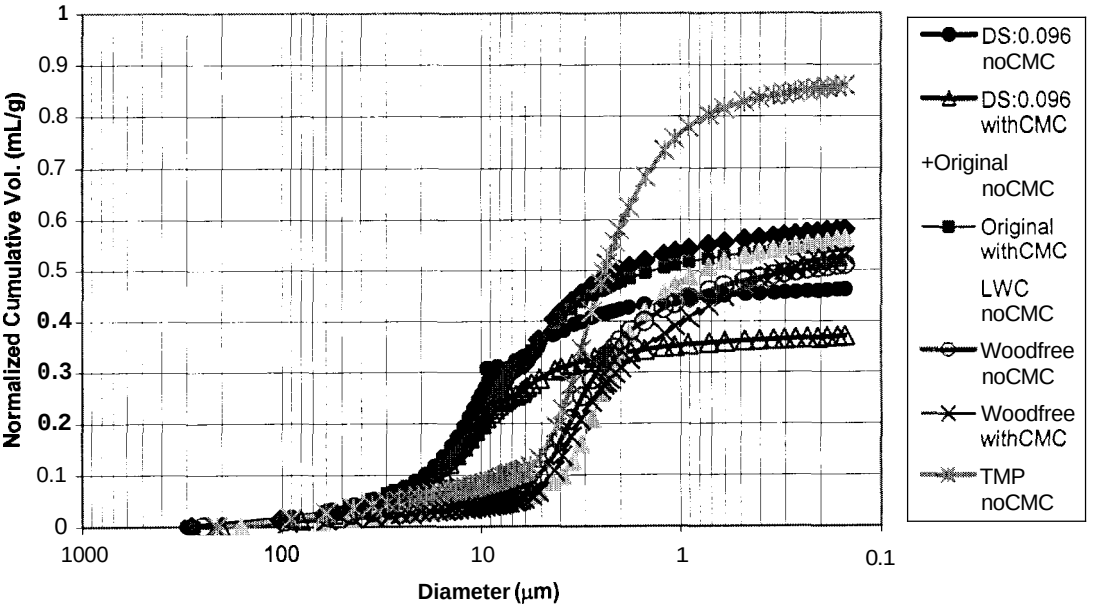

Figure 4.24: Normalized cumulative volume of coated sheets

Comparing the Figures **4.24** and **4.9** (base paper cumulative volume graph), all cumulative volumes are decrease because of penetration into the pore except TMP. Cumulative base paper volume of coated TMP is higher than the uncoated paper. This can be explained by the debonding and fiber raising that may occur when TMP is coated. However, this increase in void volume in the paper shows the weakness of this test: coating wets the base paper causing structural changes that generate changes in paper void volume. These changes cannot be separated from volume changes caused by coating penetration.

Figure **4.25** shows comparison between cumulative base sheet pore volume of uncoated and coated paper. If the volume changes are taken as coating penetration, then there is not much penetration into the original sheet without CMC coating. On the other hand, there is some penetration in coated with CMC. CMC addition did opposite effect for particle

migration. However there is significant inflow for the DS:0.096 sheet especially coating without CMC. In this case CMC addition reduce the particle migration.

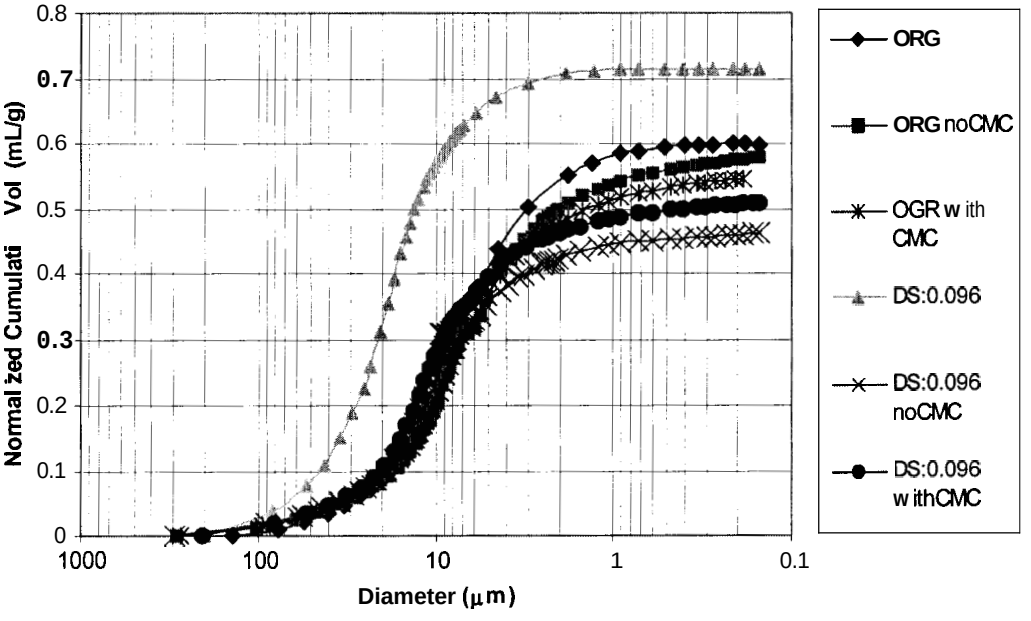

Figure 4.25: **A** comparison between cumulative base sheet volume of uncoated and coated sheet

However, as discussed, these porosity results may be complicated by structural changes.

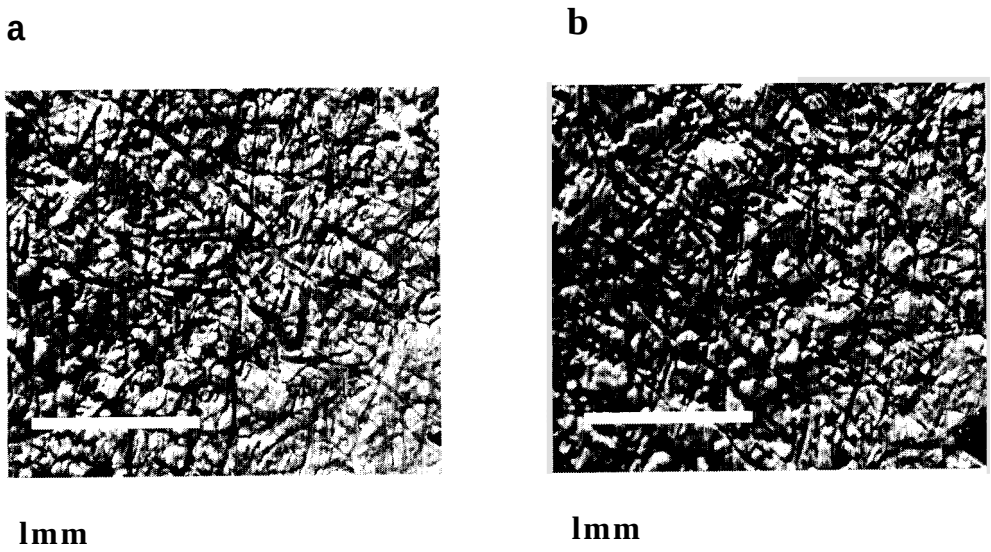

Figure 4.26: Backside of the coating images after removing the fibers a) DS:0.096 (5X) b)original softwood (5X)

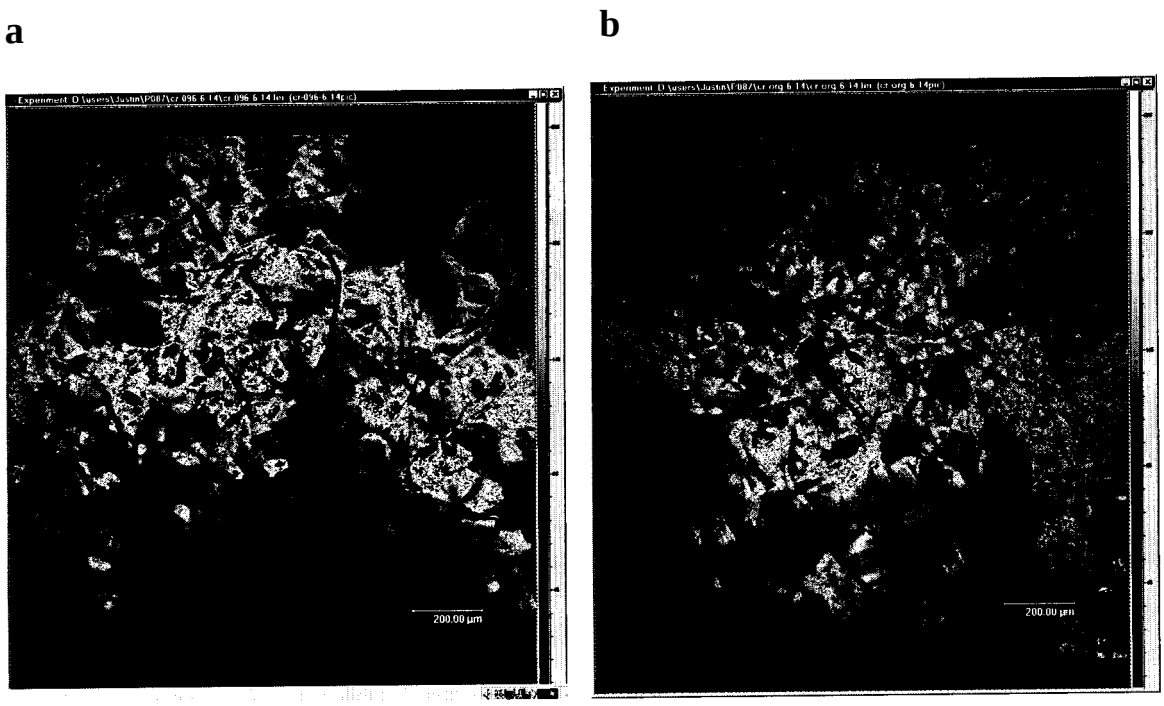

Figure 4.27: High resolution back side of the coating images at a focal dept of interest a) DS:0.096 b) original softwood sheet

Figure 4.27a and 4.27b were taken from the LSCM. Samples were analyzed with a 10X objective lens. Imaging was in 512 **x** 512 format and each sample was "cut" into 400-700 optical sections. The depth of focus for each sample's analysis (z travel) was around 100 μm. It can be seen that the DS:0.096 has some more white areas which can be the coating penetrates thorough to big pinholes. But they did not affect the roughness analysis.

From LSCM 3D graphs were also taken the backside of the coating (Figure 4.28). We can see that there are some inflow for both DS:0.096 and original softwood kraft sheets.

a **b**

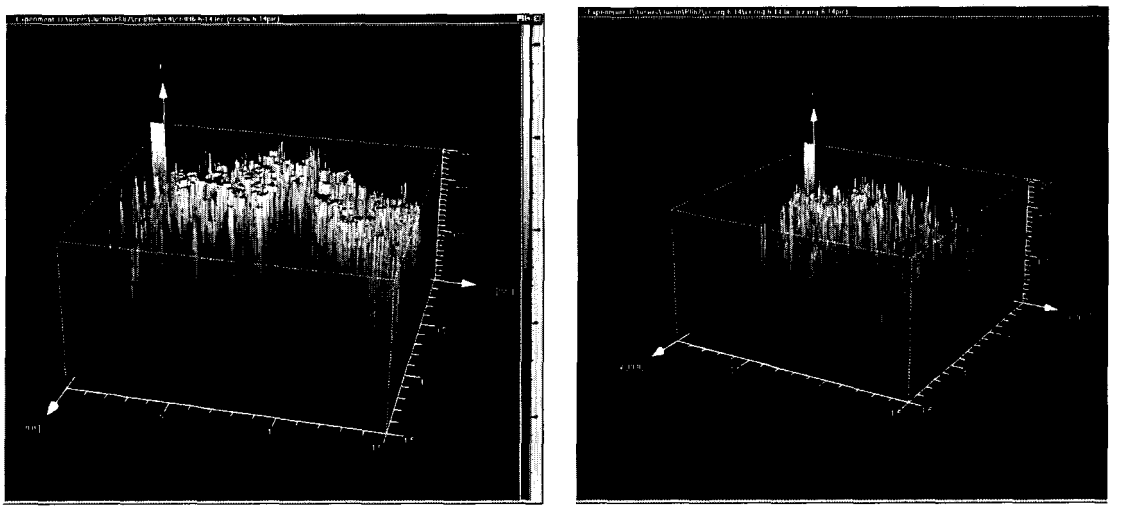

Figure 4.28: 3D graph of the back side of the coating a) DS:0.096 and b) original softwood sheet

4.3. Evaluation of Hypothesis

In this research it was hypothesized that the initial coating cake formation is affected by water uptake of surface fibers and particle bridging in the inter-fiber porous structure. To be able to prove this hypothesis fiber characterization and pore structure of model and original papers are very important parameters that needed to be characterized. The comparison between the commercial and model papers was also important in terms of the real product analysis.

The faster uptake was obtained by carboxymethylation of softwood kraft fibers. Three different degree of substituted model with original and three different commercial papers were examined.

Fiber characterization and dynamic water uptake rate were measured. It was seen that carboxymethylation have small effect on the fiber physical properties but big effect on the fiber swelling which is what we expected. It was also looked at the fiber formation. The carboxymethylated sheets gave the better formation than the original softwood kraft on the sheet formation test. But it was seen that there are many tiny pinholes between the carboxymethylated fibers and they couldn't be removed.

Carboxymethylated fibers have bigger initial contact angle with the water and ethylene glycol and longer wetting time than original softwood kraft. This result can be expected due to the effect of carboxymethylation on swelling and water uptake rate of the model fibers. Characterization of pore structure analysis was effected by the pinholes, which were seen on the fiber formation. Therefore the pore structure of the treated sheets couldn't be characterized accurately.

After produced the carboxymethylated papers which have fast water uptake and more swelling fibers, effect of these parameters on coating penetration were studied. It was expected that the swelling and faster water uptake can be close the pores and gives the better coating cake formation. Two analyses were done for indication. The first one was roughness of the backside of the coating and the second one was the pore volume. It was seemed that due to the pinholes on the fiber formation of the carboxymethylated sheets the roughness of the backside of the coating would be high. But the results showed that the swelling affected the coating penetration and stopped the inflow. It was also examined that if CMC addition makes any differences on the coating inflow. It was seen that it has some effects on the roughness of the backside of the coating and slows down the penetration. On the other hand, the pore volume results showed that there is a significant inflow for the carboxymethylated sheets and penetration of the coating is higher than original softwood kraft. But during the analysis, the high pressure was used and it can affect the sheet formation.

This research tried to increase the understanding of the area covering fiber water interaction and effect of fiber water uptake rate on wetting and final coating structure. Most of the results were important for better understanding of the concept. But it can be also done some further analyses which are recommended in chapter 5.

CHAPTER 5: CONCLUSIONS AND RECOMMENDATIONS

5.1. Conclusions

This work was unique in that an attempt was made to change the fiber water uptake value without changing the fiber size distribution. When handsheets were made with these pulps, pinholes formed regardless of a number of attempts to eliminate them. Even with these pinholes, the treated pulps had less coating penetration.

- Swellability and water uptake amount of fibers can be increased by the carboxymethylation.
- The effect of the carboxymethylation treatment on the fiber length is small.
- Carboxymethylation treatment changed fibers to hydrophobic.
- Fiber swelling of the carboxymethylated sheets, and surface chemical addition of the commercial sheets affect the wetting and initial contact angle results. Swelling increased the contact angle and decreases the wetting time of treated sheets. On the other hand due to the surface chemicals commercial sheets have higher contact angle and wetting time than the original; softwood kraft and treated sheets. The initial contact angle decreases with increasing the fluid viscosity.
- The absorption rate on treated samples cannot be measurement by standard Bristow Wheel apparatus. The technique does not have capability to measure short time absorption of very absorbent sheets.

- Roughness can be analyzed by using laser scanning confocal microscope. The LSCM roughness test results correlate with that obtained with the stylus profilometer.
- Carboxymethylation effects the sheet formation and somewhat brings the pinholes to the sheet, which is hard to avoid. But the sheet formation test is not affected by these pinholes. Carboxymethylated sheets have the better formation.
- The backside coating roughness penetration decreases for swellable fibers indicates that swelling does the close pores and reduces coating penetration. **A** Mercury porosimetry result shows there is significant penetration through the pores of the swellable sheet, but water contact with the sheet during coating causes this test results to be in question.
- CMC addition of the coating reduces coating penetration.
- The final coating structure influenced by fiber and base sheet properties such as water uptake, porosity, roughness, and sheet formation.

5.2. Recommendations

Some other measurements and tests to develop this research may be conducted. The effect of carboxymethylation on fiber swelling and dynamic water uptake rate may be measured by solute exclusion technique. This technique and water retention value by centrifugation may be compared. Drying effects may be examined during the handsheet making process. Drying can affect the pore structure and reduce the pore size and pinholes of the carboxymethylated sheets. Bristow Wheel test seemed to not very helpful for the short time absorption rate because carboxymethylated sheets are more absorbent

than the original and also the commercial sheets. This method can be modified or the new techniques may be investigated. Coating penetration may be examined using different methods and/or different coating structures.

Fiber modification seems to be a hard part of this research because of uniformity and controllability of the treated fibers. Instead of modified the fibers to more absorbent and swellable it may be considered to use a different substrate such as super absorbent polymer which is more controllable and easy to use for closing the pores and stop coating particle migration and gives better cake formation. It can make an artificial sheet out of this type of absorbent polymer with the binder.

The model for the radial and vertical penetration could be improved with a further understanding of the fiber swelling and water uptake rate.

REFERENCES

Adams, A. **A.,** "Effect of Size Press Treatment on Coating Holdout", TAPPI, 66, 5, 87-91, 1983.

Agbezuge, L., Carreira, L. M., Ink/Media Interaction in InkJet Printing, Tutorial Notes, IS&T, Springfield, 1998.

Aspler, J.S., "Interactions of Ink and Water with Paper Surface in Printing", Nordic Pulp and Paper Research Journal, 1, 68-75, 1993.

Baar, A., Kulicke, W. M., Szablikowski, K., Kiesewetter, R., "Nuclear Magnetic Resonance Spectroscopic Characterization of Carboxymethylcellulose", Macromolecular Chemistry and Physics, 195, 1483-1492, 1994.

Baumeister, M., Kraft, K., "Quality Optimization by Control of Coating Structure", 64, 1, 85-89, 1981.

Berg J., Hodgson K., "Effect of Surfactants on Wicking Flow in Fiber Network", Journal of Colloid Interface Science, 121, 1, 22-31, 1988.

Bernié, J. P., Romanetti, J. L., Douglas, W. J. M., "Use of Components of Formation for Predicting Print Quality and Physical Properties of Newsprint", 86th PAPTAC Annual Meeting, Preprint **A,** A285-A291, 2000.

Bernié, J. P., Cheung, P., Douglas, W. J. M., "Components of Formation of Newsprint: CD Variability and Papermachine Parameters", 85th PAPTAC Annual Meeting, Preprint A331-A335, 1999.

Berthold, J., Salmen, L., "Effect of Mechanical and Chemical Treatments on the Pore-Size Distribution in Wood Pulps Examined by Inverse Size-Exclusion Chomotography", Journal of Pulp and Paper Science, 23, 6, J245-J252, 1997.

Bird, R. B., Stewart, W. E., Lightfoot, E. N., Transport Phenomena, John Wiley & Sons, Inc., New York, 1960.

Bletzinger, J. C., "Effect of Acetylation on Water-Binding Properties of Cellulose", Industrial and Engineering Chemistry, 4,474-480, 1943.

Bouchon, M., Drop Spreading on Porous Surface, The University of Maine, MS. Dissertation, June 2000.

Bousfield, D.W., Pellerin, P., Toivakka, M., Nyfors, K., "Modeling of Short Time Penetration into Complex Porous Structures", 2000 TAPPI Coating Conference Proceedings, 2000.

Bristow, J. A., "The Pore Structure and the Sorption of Liquide", Paper Structure and Properties, Edited by J. A. Bristow, P. Kolseth, 183-201, Marcel Dekker Inc., New York, 1986.

Bristow, J. A., "The Swelling of Fiber Building Boars on Immersion in Water", Svensk Papperstidning, 75, 25, 844-852, 1972.

Bristow, J. A., "Liquid Absorption into Paper During Short Time Intervals", Svensk Papperstidning, 70, 19,623-628, 1967.

Casey, J. P., Pulp and Paper- Chemistry and Chemical Technology, Volume 11: Properties of Paper and Converting, Interscience Publishers, Inc., New York, 1952.

Clark, N. O., Windle, W., Beazley, K. M., "Liquid Migration in Blade Coating", TAPPI, 52, 11,2191-2202, 1969.

CLC-6000, "Specifications and Features of the CLC-6000", Simu Tech International Inc., May 2001, Available:
http://www.clc6000.com/facts7.htm , 2001

Corle, T. R., Kino, G. S., Confocal Scanning Optical Microscopy and Related Imaging Systems, Academic Press, San Diego, 1996.

Daul, C. G., Reinhardt, R. M., Reid, J. D., "Studies on the Partial Carboxymethylation of Cotton", Textile Research Journal, 787-792, 1952.

DeRoever, E. W. F., Cosper, D. R., "Fibre Rising and Roughening in Lightweight Coated Paper and Environmental Scanning Electron Microscopy Study", Scanning, 18, 500-507, 1996.

Dickson, R. J., LePoutre, P., "Mechanical Interlocking in Coating Adhesion to Paper", TAPPI Journal, 80, 11, 149-157, 1997.

Dulien, F. **A.** L., Porous Media Fluid Transport and Pore Structure, Academic Press, San Diego, 1992.

Elftonson, J. E., Strom, G., "Penetration of Aqueous Solutions into Models for Coating Layers", 1995 Coating Fundamentals Symposium, 17-25, 1995.

Forseth, T., Helle, T., "Moisture-Induced Roughening During Water Coating of Precalendered Wood-Containing Paper", Journal of Pulp and Paper Science, 24, 10, 301-307,1998.

Fosberg, P., LePoutre, P., "ESEM Examination of the Roughening of Paper in High Moisture Environment", 1994 International Printing and Graphic Art Conference Proceedings, 229-236, 1994.

Gene P. **A.** C., Watters, P., McGenity, P. M., "Factors Influencing the Runnability of Coating Colours at High Speed ", 1992 TAPPI Coating Conference Proceedings, 117-132,1992.

Gurnagul, N., "Sodium Hydroxide Addition During Recycling: Effect on Fiber Swelling and Sheet Strength", TAPPI, 78, 12, 119-124, 1995.

Harisson, J. J., "Effect of Esterification of Pulp Fibers Upon Strength Properties, Hygroexpansivity of Paper", Paper Trade Journal, 119, 5, 28-39, 1944.

Heinze, T., Erler, U., Nehls, I., Klemm, D., "Determination of the Substituent Pattern of Heterogeneously and Homogeneously Synthesized Carboxymethyl Cellulose by Using High-Performance Liquid Chromatography", Die Angewandte Macromolekulare Chemie, 215, 93-106, 1994.

Heinze, T., Pfeiffer, K., "Studies on the Synthesis and Characterization of Carboxymethylcellulose",Die Angewandte Macromolekulare Chemie, 266, 37-45, 1999.

Hoyland, R. W., Howard, P., Field, R., "The Fundamental Properties of Paper Related to Its Uses", Technical Division, BPBIF, 464, 1976.

Hoyland, R. W., Field, R., **"A** Review of the Transudation of Water into Paper-Part 1: Some Structural Aspects", Paper Technology and Industry, 17, 6, 213-214, 1976a.

Hoyland, R. W., Field, R., **"A** Review of the Transudation of Water into Paper-Part 2: The Cellulose-Water Relationship, Wetting and Cutting Angles", Paper Technology and Industry, 17, 6, 216-219, 1976b.

Hoyland, R. W., Field, R., **"A** Review of the Transudation of Water into Paper-Part 3: Some Principles of Flow and Their Application to Paper", Paper Technology and Industry, 17, 8,291-295, 1976c.

Hoyland, R. W., Field, R., "A Review of the Transudation of Water into Paper-Part 4: Liquid Penetration into Paper", Paper Technology and Industry, 17, 8,304-308, 1976d.

Hoyland, R. W., Field, R., "A Review of the Transudation of Water into Paper-Part 5: The Mechanism of Penetration, and Conclusions", Paper Technology and Industry, 18, 1, 7-9, 1977.

Huang, T., LePoutre, P., "Effect of Basestock Surface Structure and Chemistry on Coating Holdout and Coated Paper Properties", TAPPI, 81, 8, 145-152, 1998.

Jayme, G., Froundjian, D., " Uber die Messung der Hydrophilie von Zellstoffen", Cellulosechemie, 18, 1, 9-12, 1940.

Kajaani FS-100 Fiber Length Analyzer, UM Pilot Plant Pulp Test Lab Manual, Maine, 2000.

Katz, S., Beatson, R. P., Scallan, A. M., "The Determination of Strong and Weak Acidic Groups in Sulfite Pulps, Svensk Papperstidning, 6, R48-R52, 1984.

Karnis, A., Shallhorn P. M., "Tear and Tensile Strength of Mechanical Pulps" 0979 International Mechanical Pulping Conference", Transactions of the Technical Section, R92-99, 1979.

Kissa E., "Wetting and Wicking", Textile Research Journal, 66, 10,660-668, 1996.

Klemm, D., Philipp, B., Heinze, T., Heinze, U., Wagenknecht, W., Comprehensive Cellulose Chemistry, Vol 2, Functionalization of Cellulose, WILEY-VCH, Weinheim, 1998.

LEICA-Micrometrics, Leica CLSM Confocal Basics Reference, Leica Microsystems Heidelberg GmbH, Available:
http://www.leica-microsystems.com, 2000a

LEICA-Micrometrics, Leica CLSM Software Reference, Leica Microsystems Heidelberg GmbH, Available:
http://www.leica-microsystems.com, 2000b

LePoutre, P., "Substrate Absorbency and Coating Structure", TAPPI, 61, 5, 51-55, 1978.

LePoutre, P., Hui, H., Robertson, A. A., "The Water Absorbency of Hydrolyzed Polyacrylonitrile-Grafted Cellulose Fibers", Journal of Applied Polymer Science, 17, 3143-3156, 1973.

LePoutre P., Bichard, W., Skowronski, J., "Effect of Pretreatment of LWC Basestock on Coated Paper Properties", TAPPI, 81, 8, 66-70, 1986.

Lindstrom, T., "The Concept and Measurement of Fiber Swelling", Paper Structure and Properties, Edited by J. A. Bristow, P. Kolseth, 75-97, Marcel Dekker Inc., New York, 1986.

Marchhessault, R. H., Dubé, M., St. Pierre, J., Revol, J. F., "New Insights into Fiber Swelling, Interfiber Bonding and Wet Strength", Fiber-Water Interaction in Paper Making V.2, 1977 6th Fundamental Research Symposium, Technical Division, BPBIF, 795-813, 1978.

McLaughlin, R. R., Herbst, J. H. E., "Determination of the Degree of Substitution of Carboxymethylcellulose Over the Entire Substitution Range", Canadian Journal of Research, 28, B, 737-744, 1950a.

McLaughlin, R. R., Herbst, J. H. E., "The Preparation of Sodium Carboxymethylcellulose", Canadian Journal of Research, 28, B, 731-736, 1950b.

Middleman, S., Modeling Axisymmetric Flows, Dynamics of Films, Jets, and Drops, Academic Press, New York, 1995.

Nelson, P. F., Kalkipsakis, C. G., "The Carboxymethylation of a Eucalypt Kraft Pulp", TAPPI, 47, 2, 107-110, 1964a.

Nelson, P. F., Kalkipsakis, C. G., "The Behavior of Salts of a Carboxymethylated Eucalypt Kraft Pulp", TAPPI, 47, 3, 170-176, 1964b.

Nickel J., Olschewski, F., Quentin, I., "The Imaging of Three Dimensional Structures in Confocal Microscopy, Leica Microsystems Heidelberg GmbH, 1-9, Available: http://www.lecia-microsystems.com, 2000.

Olaru, N., Staimberg, S., Bontea, D., Asandei, N., "Research on Optimization of Some Reaction Parameters in Synthesis of Sodium Carboxymethylcellulose", Cellulose Chemistry and Technology, 14, 713-177, 1980.

Ott, E., Spuril, H. M., Graffin, M. W., Cellulose and Cellulose Derivatives, Interscience Publishers, New York, 1954.

Page, D. H., "A Theory for the Tensile Strength of Paper", TAPPI, 52, 4, 674-681, 1969.

Philipp, B., Dautsenberg, H., Lukanoff, B., "Kinetics and Esterification Mechanism of Cellulose According to Physical Structure and Reaction Medium", Polymer Science, 21, 2849-2861, 1980.

Piirainen, R, "Optical Method Provides Quick and Accurate Analysis of Fiber Length", Pulp and Paper, November, 69-71, 1985.

Poresizer 9320 Manual, Micrometrics, Norcross, GA, 30093-1877, USA.

Racz, I., Borsa, J., "Carboxymethylcellulose of Fibrous Character. A Survey", Cellulose Chemistry and Technology, 22,657-663, 1995.

Racz, I., Borsa, J., "Swelling of Carboxymethylated Cellulose Fibres", Cellulose, 4, 293-303,1997.

Reid, J. D., Daul, G. C., "The Partial Carboxymethylation of Cotton to Obtain Swellable Fibers, I", Textile Research Journal, 17, 554-561, 1947.

Reid, J. D., Daul, G. C., "The Partial Carboxymethylation of Cotton to Obtain Swellable Fibers, 11", Textile Research Journal, 18, 551-556, 1948.

Reid, J. D., Daul, G. C., "The Preparation and Properties of Alkali-Soluble Metal Carboxymethylcellulose Fibers", Textile Research Journal, 17,794-801, 1949.

Retulainen, E., "Fiber Properties as Control Variables in Papermaking? Part 1. Fiber Properties of Key Importance in the Network", Paper and Timber, 78, 4, 187-194,1996.

Retulainen, E., Nieminen K., "Fiber Properties as Control Variables in Papermaking? Part 2. Strengthening Interfiber Bonds and Reducing Grammage", 78, 5, 305-313, 1996.

Salminen, P. J., "Water Transport into Paper-The Effect of Some Liquid and Paper Variables", TAPPI Journal, 9, 195-200, 1988.

Sandàs, P. E., Salminen, P. J., "Water Penetration in Coated Papers", 1987 TAPPI Coating Conference Proceedings, 1987.

Scallan, A. M., "The Accommodation of Water within Pulp Fibers", Fiber-Water Interaction in Paper Making V. 1, 1977 6th Fundamental Research Symposium, Technical Division, BPBIF, 9-27, 1978.

Scallan, A. M., Carles, J. E., "The Correlation of the Water Retention Value With the Fiber Saturation Point", Svensk Papperstidning, 17,699-703, 1972.

Scallan, A. M., Kartz, S., Argyropoulos, D. S., "The Conductometric Titration of Cellulosic Fibers", Paprican, 643, 1987.

Scallan, A. M., Grignon, J., "The Effect of Cations on Pulp and Paper Properties", Svensk Papperstidning, 82, 2, 40-47, 1979.

Schuchardt, D. R., Berg, J. C., "Liquid Transport in Composite Cellulose-Superabsorbent Fiber Network", Wood and Fiber Science, 23, 3, 342-357, 1990.

Skowronski, J., LePoutre, P., "Water-Paper Interaction During Paper Coating; Changes in Paper Structure", TAPPI, 68, 11, 98-102, 1985.

Sobue, H., Okuba, M., "Determination of Carboxyl Group in Cellulosic Materials with the Dynamic Ion-Exchange Method", TAPPI, 39, 6, 415-417, 1956.

Stannett, V. T., Williams, J. L., "The Transport of Water in Cellulosic Materials", Fiber-Water Interaction in Paper Making V.1, 1977 6th Fundamental Research Symposium, Technical Division, BPBIF, 497-513, 1978.

Stone, J. E., Scallan, **A.** M., "A Structural Model for the Cell Wall of Water-Swollen Wood Pulp Fibers Based on Their Accessibility to Macromolecules", Cellulose Chemistry and Technology, 2,343-358, 1968.

Stone, J. E., Scallan, **A.** M., "The Effect of Component Removal Upon the Porous Structure of the Cell Wall of Wood II. Swelling in Water and the Fiber Saturation Point", TAPPI, 50, 10,496-501, 1967.

Stone, J. E., Scallan, A. M., "Influence of Drying on the Pore Structures of the Cell Wall", Consolidation of the Paper Web, Edited by F. Bolam, Technical Section, BPBMA, London, 1966.

Taguchi, A., Ohmiya, T., Sodium Carboxymethylcellulose, US Patent & Trademark Office, Patent # 4,525,585, 1985.

Talwar, K. K., "A Study of Improved Strength in Paper Made from Low-Substituted Carboxymethylcellulose Pulps", TAPPI, 41, 5,207-215, 1958.

TAPPI Useful Methods, "Water Retention Value (WRV)", UM-254, 54-56, TAPPI Press, Atlanta, 1991.

TAPPI Test Methods, "Air Resistance of Paper", T 460 om-88, TAPPI Press, Atlanta, 1992-93a.

TAPPI Test Methods, "Fiber Length of Pulp and Paper by Automated Optical Analyzer", T 271 pm-91, TAPPI Press, Atlanta, 1992-93b.

TAPPI Test Methods, "Air Permeability of Paper and Paperboard (Sheffield-Type)", T 547 pm-88, TAPPI Press, Atlanta, 1992-93c.

Tencor Profilometer, Alpha Step 200 Manual, Tencor Instruments, PO Box 3308, Portsmouth, NH 03802, USA.

Toivakka, M., Nyfors, K, "Pore Space Characterization of Coating Layers", 2000 TAPPI Coating Conference Proceedings, 2000.

Toivakka M., Eklund, D., Bousfield, D. W., "Simulation of Pigment Motion During Drying", 1992 TAPPI Coating Conference Proceedings, 403-418, 1992.

Unruh C. C., Kenyon, W. O., "investigationof the properties of Cellulose Oxidized by Nitrogen Dioxide", American Chemical Society Journal, 64, 127-131, 1942.

Verhoeff, J., Hart, J. A., Gallay, W., "Sizing and the Mechanism of Penetration of Water into Paper", Pulp and Paper Magazine of Canada, 64, 12, T509-T516, 1963.

Walecka, J. A., ***"An*** Investigation of Low Degree of Substitution Carboxymethylcellulose", TAPPI, 39, 7,458-463, 1956.

Water Retention Value, UM Pilot Plant Pulp Test Lab Manual, Maine, 2000.

Weise, U., Characterization and Mechanisms of Changes in Wood Pulp Fibers Caused by Water Removal, Helsinki University of Technology, PhD. Dissertation, Acta Polytechnica Scandinavica- Chemical Technology series, No.249, September 1997.

Wenzel, N., R., "Resistance of Solid Surfaces to Wetting by Water", Industrial and Engineering Chemistry, 28, 988-994, 1939.

Windle, W., Beazley, K. M., "Liquid Migration from Coating Colors 11. The Mechanism of Migration", TAPPI, 53, 12,2232-2235, 1970.

Wink, W. **A.,** Van den Akker, J. A., "A New Apparatus and Procedure for Determining the Surface Receptivity and Roughness of Paper as These Relate to Liquid Film Applications", TAPPI, 40, 528-536, 1958.

Winslow, D. A., "Advances in Experimental Techniques for Mercury Intrusion Porosimetry", Edited by E. Matijevic, Surface and Colloid Science, 13, Wiley-Interscience, 259-282, 1969.

Wu, **S.,** Polymer Interface and Adhesion, Marcel Dekker Inc., New York, 1982.

Young, T. **S.,** Weyer, L.G., Pivonka, D. E., Ching, B., "A Study of Coating Water Loss and Immobilization under Dynamic Conditions", 1993 TAPPI Coating Conference Proceedings, 223-233, 1993.

BIOGRAPHY OF THE AUTHOR

Sedef Akinli-Koqak was born in Ankara, Turkey on December 6, 1976. She was raised in Izmir, Turkey until 1993. She graduated with a Bachelor of Science degree from the Chemical Engineering Department at Ankara University in June 1997. She continued at the same university in the Institute of Social Science for her Master of Business Administration degree. In 1998, she received a scholarship from Turkish Pulp and Paper Industry to pursue a Master of Science degree in United States. She joined the Paper Surface Science Program of the Chemical Engineering Department at the University of Maine in the fall of 1999 with the hope of obtaining a Master of Science degree.

Sedef Akinli-Koqak is a candidate for the Master of Science degree in Chemical Engineering from The University of Maine in August, 2001.